UNIVERSITAT ROVIRA i VIRGILI

International Erasmus Mundus Master in
QUATERNARY AND PREHISTORY

Erasmus Mundus

Re-thinking symmetry: Technological and Morphometrical Insights into Shape Variability of Large Shaped Tools from MIS11 in Western Europe

Erica Rosolani

Supervisor Paula García-Medrano PhD
Andreu Ollé PhD

Academic year 2023/2024

Index

Introduction 3

1. Terminology definition 3
2. Symmetry 4
3. Marine Isotope Stage 11 9
4. Galería site 10
5. Guado San Nicola site 13
6. La Noira site 16

Materials and Methods 19

7. Archaeological sample 19
1. Digitalization of the archaeological sample 24
2. Technological Analysis 25
3. Geometric Morphometric Analysis 35

Results 41

1. Technological Analysis 41
2. Geometric Morphometric Analysis 60

Discussions 67

1. Guado San Nicola – USc 71
2. La Noira – *stratum* c 74
3. Galería – GIIa 76
4. Contextualization within MIS11 in Europe 79

Conclusions ____ 84

Bibliography ____ 88

Annex 1 ____ 97
Annex 2 ____ 107
Annex 3 ____ 110

Introduction

In this thesis, large shaped tools coming from three European sites will be analyzed with the aim of analyze morphometrical variations with a focus on bifacial and bilateral symmetry to better understand intra and inter-assemblage variability during Marine Isotope Stage 11 in Soth-western Europe. The sample used for this study is composed by materials coming from three sites (Galería, Atapuerca, Spain; La Noira, Centre, France; Guado San Nicola, Molise, Italy) which are very different between them because of raw materials availability, landscape context and, in the case of Galería and La Noira, also their functionality. The main objective mentioned above has been pursued by combining two types of analyses: 1) Technological analysis on the physical archaeological materials to identify all the features reflecting the knapping process and characterizing the final product; 2) Geometric morphometric analysis on 3D images of the archaeological materials to quantify the variations in shape and symmetry. All information has been statistically processed by applying Principal Component Analysis (PCA) and cluster analysis that allow to recognized similarities and difference between the three assemblages. With this study, unpublished morphometric data are contributed for Guado San Nicola site (which is studied through the application of Geometric Morphometric Analysis for the first time), comparisons between three of the most important sites that testimony the Acheulean technological state after the MIS 12 glaciation are broadened, and a new approach to the symmetry issue in which quantification underlies interpretations to reduce the subjectivity of the researcher and develop an approach that is as scientific as possible.

1. Terminology definition

A controversial debate is still open within the terminology used for Acheulian tool-types and the categories that define their groupings (e.g., Large Cutting Tools, heavy-duty tools, etc.). In the context of this thesis, three types of tools are analyzed (the definitions of which will be later reported in Chapter 2.3.1): handaxe, cleaver, and chopping-tool. According to bibliography, handaxes and cleavers are most commonly included in the Large Cutting Tools (LCTs) category (Bordes, 1961; Isaac, 1977) while chopping-tools are considered as heavy-duty tools (*ibid*). To refer to the totality of all these instrument types still respecting all the characteristics that distinguish them, within the context of this thesis the term *large shaped tools* is used (*sensu* Ollé et al., 2023). The term *shaped* *tool* was first proposed by Kleindienst and Isaac (Isaac, 1977; Kleindienst, 1962) to refers to a "primary class" encompassing all lithic tools resulting from anthropic manufacturing. According to these authors, this primary class can be further divided into "secondary classes," which include large cutting tools (LCTs) and heavy-duty tools. By adding the adjective large to the definition, the latter refers exclusively to large instruments (Ollé et al., 2023) perfectly representing the set studied for this work.

2. Symmetry

Symmetry is a phenomenon constantly present in human life. Examples of symmetry are encountered both in nature and in anthropic environments at different levels of complexity, and this frequency has been noted, documented and reproduced since ancient times. The first who mention symmetry and human's tendency to prefer it to asymmetry was Aristotle in his work 'Metaphysics' and later also Darwin exposed similar observations to explain the sexual selection in humans in his book 'The descent of man'(Giannouli, 2013). Psychological studies, in fact, stand out that symmetry is not only preferred to asymmetry because of its association with harmony and beauty, thus reflecting a well-structured and proportioned system both in its entirety and in its parts, but also because is an organizational agent of human visual perception helping us to understand the world through the recognition of repeated patterns (Giannouli, 2013; Liu et al., 2010) Since symmetry is pervasive in our reality, many disciplines that study it (e.g. biology, maths, physics, chemistry, psychology, sociology, and even philosophy) through different approaches and multiple and variate are also the definitions with which the term symmetry is associated in each one of these (Treder, 2010). Despite the inherent versatility of symmetry and its study, all its expressions can be explained and generalised through its mathematical and geometric conception (Liu et al., 2010; Savriama & Klingenberg, 2011).

2.1 Mathematic and geometric definition of symmetry

The definition of symmetry developed in a mathematical context considers the changes that an object undergoes when a geometric transformation, which in turn is defined as a geometric change that maintains a one-to-one correspondence among all points of the object in a plane or in the space, is applied. So, we can see a transformation as a phenomenon that maps all the points of an object on a plane or in space onto another point in the same plane or space in a reversible way (Savriama & Klingenberg, 2011). Analogously in geometry, symmetry is defined as the invariance of the object to particular transformations (e.g. translation, rotation, reflection, stretch or dilatation) that can be applied to it, meaning that if the object remains unchanged after the transformation it will be symmetric concerning that specific transformation. A singular object can have more than one symmetry if it does not change after its application, and the set of transformations that leave the object unchanged, which are called symmetry transformations, constitutes its identity and characterizes its symmetry (*ibid*).

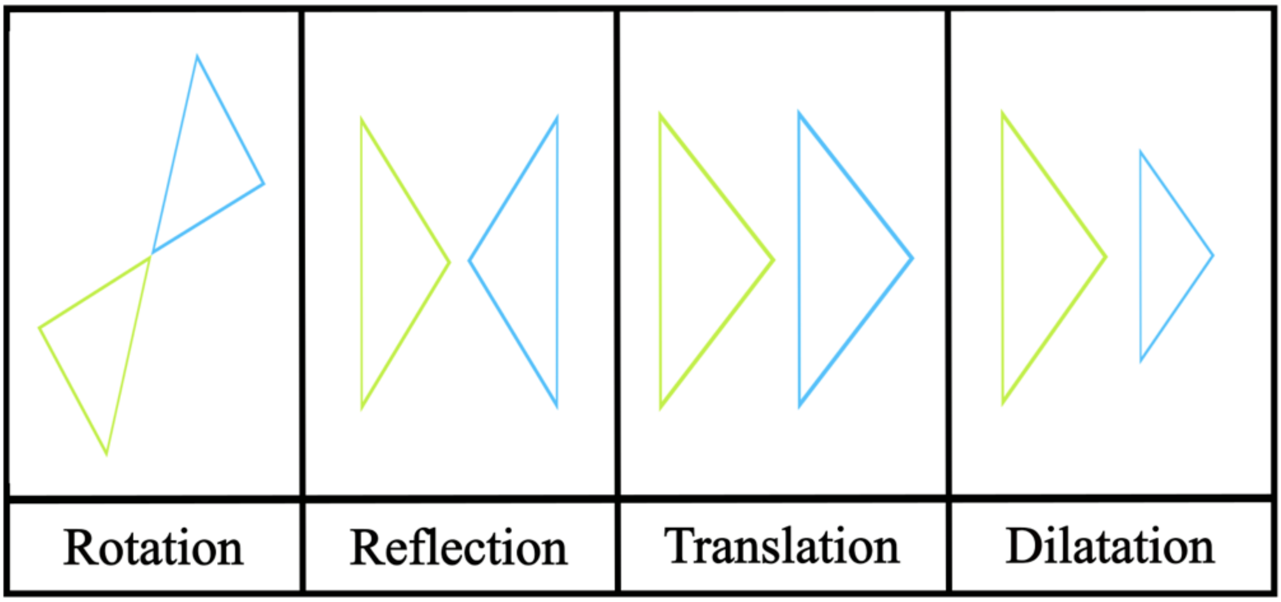

Figure 1: Principal geometric transformations.

One of the most common and easiest symmetries to recognize for humans is bilateral symmetry, also known as mirror symmetry. Bilateral symmetry is the type of symmetry that requires less effort to be recognized and the ability of recognize a bilaterally symmetrical object is already well-developed after the fourth month of life (Tumler et al., 2017). In this specific case the transformation that occurs is the reflection, so the object will present two specular halves to its longitudinal axis. In the archaeological field, this type of symmetry has been recognized mostly in Large Cutting Tools (e.g. handaxes) and the concept of bilateral symmetry has been linked to the one of bifacial symmetry. This is always a reflection according to the longitudinal axis but on a lateral view showing the thickness of the object. Mathematical concepts relating to symmetry can therefore be applied to the study of Large Cutting Tools in combination with other computational tools, such as geometric morphometric analysis. This will limit the personal interpretation through increased methodological standardization.

2.2 Symmetry in the archaeological perception

Since their discovery, Acheulean handaxes have been considered by archaeologists the first hint of symmetry perception in the human lineage (Hodgson, 2011) and have opened a heated debate in which different positions are taken regarding their meaning, functionality and the cultural role they might have played (Machin et al., 2007). Indeed handaxes, which appeared in Africa, Europe, western Asia and in the Indian subcontinent since 1.8-1.6 Mya (Tumler et al., 2017), have been largely studied with several approaches to solve the mystery behind their "standardized" and aesthetically impactful shape. It is precisely the various studies carried out over the last two centuries that have shown how handaxes, even though they are often still regarded as highly standardised tools, are subject to a remarkable degree of variability. This variability lies in the wide range of raw materials used (e.g. basalt, quartz, quartzite, chert, flint, obsidian, calcareous rocks, organic materials etc.), in the differences in size and, mostly, in shape (e.g. triangular, cordiform, oval, etc.). Also, their functionality variate between several activities such as butchery and animal processing (Cassoli et al., 1993; García-Medrano et al., 2014; Ollé et al., 2014; Solodenko et al., 2015; Villa, 1990; Zupancich et al., 2021), vegetable matter processing (Dominguez- Rodrigo et al., 2001; Viallet, 2016), digging (Rots & Van Peer, 2006) and flake dispenser (Iovita & McPherron, 2011). Another element of variability concerns the internal division between Early and Late Acheulean identified by scholars based on a change in the intensity of shaping that occurs around 500 ka (Hodgson, 2009, 2011, 2015; Moncel et al., 2021). Up to this chronological threshold the presence of symmetry is rarely observed in the archaeological records and even when this happen it is considered accidental as there is little concern for the form (Hodgson, 2015), even if there are studies that already attest a preference for symmetry in specific Acheulean assemblages (Saragusti et al., 2005). After 500 ka, in contrast, it is observed what is referred to as the 'over-engineering' or 'over-processing' of handaxes, a phenomenon that results in more proportionate and symmetrical morphologies (Cole, 2015; Machin et al., 2007). A new question then arises within the debate: why is this technological change occurring? There are several hypotheses. One of the most shared theories is based on functional constraints (Cole, 2015), so it takes into consideration the positive relationship between symmetry and efficiency suggesting an increase in shape's symmetry due to opportunistic reasons (Machin et al., 2007; Simão Jorge, 2002). Supporting this theory, also the recognition of early forms of Levallois method in specific Acheulean assemblages points to a better management of convexities which, from a technological point of view, allows a more controlled exploitation of the raw material and the achievement of more aesthetically refined products. Another hypothesis that has been proposed involves the development of an aesthetic sense about sexual selection. Indeed, according to Kohn & Mithen (1999), the manufacture of handaxes had an important social meaning as the production of a symmetric and harmonic tool was an indicator of health and intelligence. A different, but nevertheless interesting view is proposed by Tumler et al. (2017) in a study aimed to understand if a preference for symmetry can be related to the sex and age of the knapper. The experimentation suggests that adult females, juvenile individuals and children display a statistically significant preference for symmetrical handaxes (*ibid*). In this sense, a higher index of symmetry within the record could suggest an increasing participation of these individuals to knapping activities. In addition to these hypotheses that try to explain symmetry as a feature consciously pursued by hominins, it must always be considered that variability is also due to factors that cannot be directly controlled by the knapper (e.g. morphology and size of the blank, type of raw material, flaking strategies). What is certain is that these temporal trends not only dispel the myth of the standardisation of the biface as lithic type, but also allow us to reflect on the significance of these tools from an evolutionary point of view (Beyene et al., 2013; Gamble et al., 2011; Grosman et al., 2011; Hodgson, 2015; Saragusti et al., 2005). Symmetry, however, does not appear exclusively in handaxes, but becomes an important element in the manufacture of a whole series of tools referred to as large shaping tools (Isaac, 1977; Kleindienst, 1962; Ollé et al., 2023). In fact, in all these tools the presence of axis of symmetry (both from a frontal and sagittal view) is often evident already by eye.

2.3 Morphometric approach to symmetry

As mentioned above, symmetry in Acheulean large cutting tools is a topic that has been largely studied in prehistoric archaeology using different approaches. There, a state of arts is presented regarding the main researches aimed at better understanding the symmetry of those *façonnage* products through a morphometric perspective. Archaeologists have been slower than other disciplines (e.g. biology, anthropology, paleoanthropology, etc.) to apply morphological quantification, and in particular the use of software-based techniques, to the study of lithic tools (Hicks, 2023). This type of study only became more widespread in the mid-19th century and was carried out using calipers or micrometers to take linear physical measurements such as length, width and thickness, which were then used to apply multivariate analyses that allowed lithic products to be classified into typological categories based on their morphology (Author et al., 1952; Sackett, 1982).

The first author who published studies where morphometric analyses are applied on Acheulean handaxes was D.A. Roe (Roe, 1964, 1969). Roe took linear metrics on handaxes from 38 Acheulean sites in Southern Britain to document the size and shape variability and refinement. In 1980, A.R. Marathe (Marathe, 1980) add a new variable to the measurements used by Roe (1964, 1969): the weight of each handaxe, which was considered as a dependent variable which, in relation to the independent variables (i.e. length, width and thickness), allowed the identification of a possible correlation. According to the author, a high correlation points to an advanced technological character that allowed to categorize handaxes as symmetrical or asymmetrical (Hicks, 2023). Ten years later the Radial Quantification method is published by Wynn & Tierson (1990): a model based on the superposition of plan view outlines according to radial measurements which are taken both on the vertical axis (tip-to-butt) and the horizontal axis (edge-to-edge). Also in this case, the results of PCAs, performed by combining the different groups of tools, allow to detect differences and categorize handaxes on the basis of the latter. In 1998 Saragusti et al. published the Continuous Symmetry Measure (CSM) represented by the variable S(σ), this method used the 'folding-unfolding' algorithm (borrowed by molecular science) to find the closest symmetrical shape to a general contour line (Hicks, 2023). This work is certainly relevant also within the debate set out in the previous subchapter, as in the same article Saragusti et al. (1998) detect, using precisely the CSM model, a general increase in the symmetry of handaxes across time. Finally, with the dawn of the new millennium, computer-based methodologies are starting to be proposed. In 2005 Hardaker and Dunn developed the Flip Test, a customized computer application to study 2D bilateral symmetry in alternative to the CSM or other manual methods (Hicks, 2023). The program draws the plan contours of both the ventral and dorsal face of an artefact that has been rotated about its long axis (from the tip to the butt). Then it measures the asymmetry index (AI) or area in pixels between the two contours, then divides this value by the squared sum of the length and width of the artefact's pixels, to standardize the scale of the object. The AI value will be expressed by a number between 1 and 6 where 1 represents an ideal level of perfect symmetry and 6 indicates a very low level of symmetry (*ibid*). In the following years, two new indexes have been integrated into the study of symmetry in handaxes: Index of Symmetry (IoS) (Lycett et al., 2006) and Index of Deviation from Symmetry (IDS) (Feizi et al., 2018). Lycett et al. (2006) introduced a new data acquisition device, the cross-coordinate caliper which, in combination with an IoS equation, allows it to be used as an alternative to standard planar measurements to understand morphological variations between assemblages (Hicks, 2023). Feizi et al. (2018), instead, developed the IDS to quantify the relationship between symmetry and cognitive abilities. This method works by enclosing the 3D of an artifact inside a quadrangle which is bifurcated in the middle of his longer axis, to obtain the IDS value the area of each side is measured before the difference between them is divided by the total plan view area of the 3D point cloud model (Hicks, 2023). While all the above-mentioned publications partially represent the multitude of morphological analyses performed on bifaces to understand their symmetrical characterization, only a few projects have focused on a volumetric approach to analyze this problematic. One of the latter is the study realized by Li et al.

(2016) where Avizo Fire 3D imaging software was used to quantify both bilateral and bifacial symmetry of LCTs. Also in this case, bifurcation on the longer side was used and the volume of each side, first bilaterally and then bifacially, was measured and compared (Hicks, 2023).

3. Marin Isotopic Stage 11

The chronological range in which the three sites studied within the context of this work are included is relatable to the Marine Isotopic Stage 11 (425 ka up to 374 ka), which in Europe corresponds to a relatively long interglacial characterized by very warm and humid conditions. MIS 11 in Europe also represent a threshold moment both for human and technological evolution. In fact, recent studies demonstrate that during MIS11 the first Neanderthal traits already started to appear in Europe (Hublin, 2009). In addition, at the end of the glaciations of the MIS12 major innovations happened together with a new diversification in material tradition based on a regionalization that had never been so marked before (Moncel et al., 2016). As mentioned before, the MIS11 is characterized by a sea level higher than the actual one and a climatic warming also in the Northern Hemisphere due to the collapse of ice sheets in Greenland and West Antarctica (Oliveira et al., 2016). Because of its time span, however, palynologists have divided this interglacial stage in three substages characterized by climatic variations:

- MIS11c (460 – 400 ka)
  It's the base of the interglacial and it represents the climatic optimum with the warmest temperatures and the maximum extension of the forest.

- MIS11b (400 – 390 ka)
  The second substage corresponds with an overall cooling of temperatures.

- MIS11a (390 – 367 ka)
  In this final substage a return to warmer conditions occurs, even if with lower temperatures if compared to the substage c. MIS11a is also characterized by significant millennial-scale oscillations expressed as high variability in aridity and temperatures. The latter variability appears to affect to a lesser extent Southwestern Europe, which for that reason could have played an important role in hominin subsistence maintaining ecological niches that fostered both demographic expansion and technological development (Sassoon et al., 2023).

The substages fitting with the chronologies of the sites studied are specifically MIS 11c and MIS 11a, both overall warm moments but characterized by different specific ambiental and climatic conditions as explained just above.

4. Galería

The complex of Galería is located in the Trinchera del Ferrocarril in the Sierra de Atapuerca (Burgos, northern Spain) and it is a karstic system composed of three distinct areas that has been occupied by *Homo heidelbergensis* (García-Medrano et al., 2014, 2015). The central area is the Galería (TG) and it is connected on the north side to the second area, a small chamber called Convacha de los Zarpatos (TZ), and a vertical shaft that rises to the surface to the south constitutes the Tres Simas Boca Norte (TN) (García-Medrano et al., 2015; Ollé et al., 2013). According to García-Medrano et al. (2014) the lower archaeological unit of Galeria complex, together with Sima de los Huesos, documents the first appearance of Acheulean technology in the Sierra de Atapuerca. The stratigraphy of the site shows five main infill phases, named from GI to GV (from bottom to top), and one paleosol (GVI). Within these, only two Units, GII and GIII, present archeopaleontological remains, and both have been divided into two sub-unites (García-Medrano et al., 2015). The earliest occupation in GII is the sub-unit GIIa, which corresponds with a chronological range between 450 and 350 ka. It represents the first exposure of the cave to the outside, while GIIb is separated from the lower sub-unit by a continuous organic layer and it has been dated by ESR-US to 237-269 ka (Falguères et al., 2022; García-Medrano et al., 2014, 2015).

Two different chronologies have been proposed for GIIIa, the lower sub-unit of GIII: a first chronology, obtain using thermoluminescence (TL), of 466 ±39 ka (Berger et al., 2008) and a second one, by ERS-US, of 221-280 ka (Falguères et al., 2013). Different dating methods have been applied also to define the chronology of GIIIb, but for this sub-unit both the thermoluminescence and infrared stimulated luminance approach and ERS-US agreed about an age between 221 and 269 ka (Berger et al., 2008; Falguères et al., 2013).

The lithic assemblage and taphonomic alterations suggest sporadic and repeated low-intensity occupations rather than a home-base settlement (García-Medrano et al., 2014, 2015, 2017; Ollé et al., 2016). In fact, the most likely hypothesis is that the cave was frequented by humans and carnivores, who most probably entered and exited through the TZ area, to catch the animals that fell into the natural trap created by the TN shaft (García-Medrano et al., 2014, 2015, 2017). The abandonment of the cave may be due to a gradual reduction in the meat supply and a consequent loss of interest by humans (*ibid.*). As with other sites in Atapuerca, human remains have also been found in the Galería complex: an adult mandibular fragment with two molars from unit GII (Bermudez de Castro and Rosas,1992), and neurocranial fragment from the lambdatic area of an adult individual from the base of GIII (Arsuaga et al., 1999). Both the human remains were recovered from the Coacha de los Zarpatos (TZ), they have been identified as *H. heidelbergensis* (Arsuaga et al., 1997) or, more recently, generically as pre-Neanderthals as they share features with the fossils from Sima de los Huesos, which have been ascribed to the same clade (Arsuaga et al., 2014; Meyer et al., 2016)

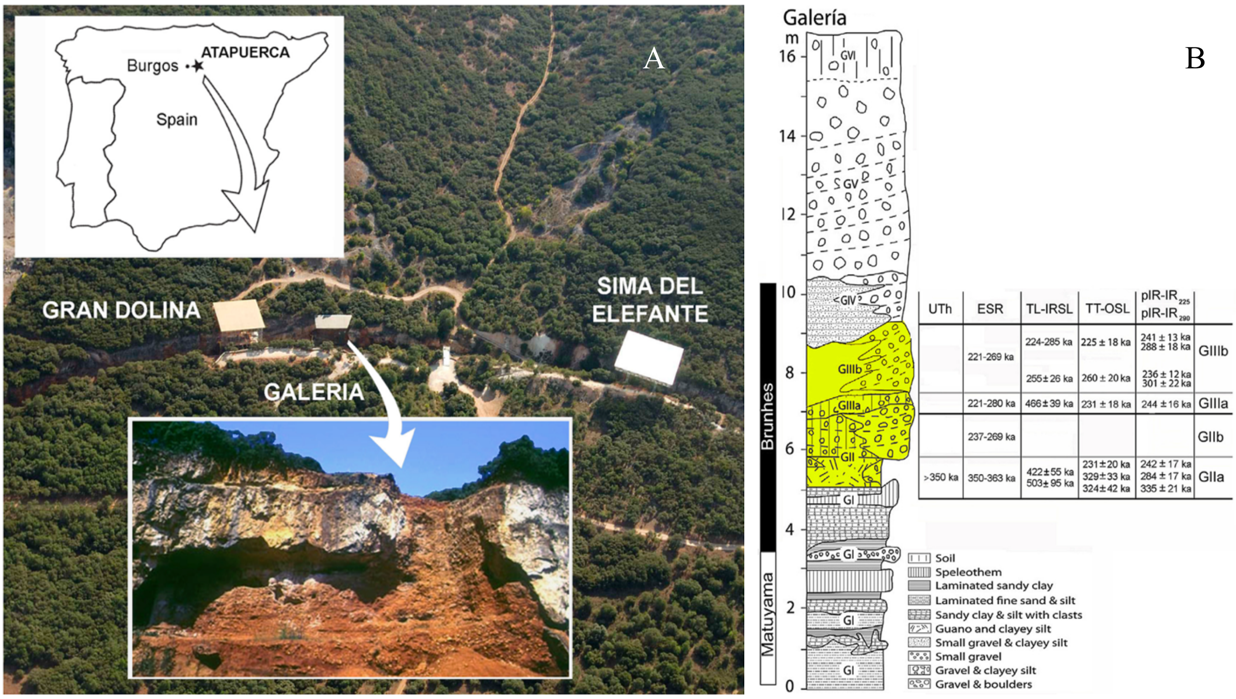

Figure 2: A) Location of the Atapuerca sites, focusing on the Trinchera del Ferrocarril (Railway Trench) and the Galería site (from García-Medrano et al., 2017). B) Chronostratigraphy of La Galería site (from García-Medrano et al., 2015)

The lithic assemblage of La Galería complex belongs to Mode 2 (or Acheulean) and shows a technological stability along all the sequence (García-Medrano et al., 2014; Ollé et al., 2016). The stone tools are made on local raw materials: Neogene chert, Cretaceous chert and limestone were recovered from the heist part of the Sierra (less than 2 km from the site), while quartz, quartzite, sandstone and shist were collected from Vena River and Arlanzón River terraces (García-Medrano et al., 2014; Ollé et al., 2013). The *chaînes opératoires* appear highly fragmented and suggest knapping activities undertaken predominantly outside the cave (García-Medrano et al., 2014, 2015, 2017; Ollé et al., 2013, 2016; Terradillos-Bernal & Rodríguez, 2012). The latter hypothesis is supported by an overrepresentation of functional objects (García-Medrano et al., 2015; Ollé et al., 2013), a low percentage of cores if compared to sharped tools and scarce presence of cortex on the stone tools pointing to an absence of the first stages of knapping sequence inside the cave (Ollé et al., 2013). These technological traits suggest a knapping activity limited to solving immediate problems, while the majority of the tool were brought already-made in the site (García-Medrano et al., 2015). The principal methods used in La Galería complex are centripetal, which covers a dominant role in the assemblage, and unipolar longitudinal methods, while orthogonal and multipolar methods are attested mostly on chert (García-Medrano et al., 2014, 2015, 2017; Ollé et al., 2013; Terradillos-Bernal & Rodríguez, 2012). Use-wear studies have been also performed on the lithic assemblage of La Galería using a Scanning Electron Microscope (SEM) and it results that artifacts of all size were used, but there is a clear predominance of small-size retouched flakes showing functional traces (Márquez et al., 2001; Ollé et al., 2005; Ollé Cañellas, 2005). Two different types of activities have been identified: the main represented is the butchery activity, while woodworking is attested but in low percentages (*ibid.*). The Galería lithic assemblage is also characterized by a high number of Large Cutting Tools (LCTs) including both handaxes and cleavers (García-Medrano et al., 2015, 2017). Along the archaeological sequence a gradual standardization of shapes is denoted, as well as a gradual decrease of their presence from GII to GIII (*ibid*). The faunal assemblage sees a significance predominance of herbivores, both infant and adult individuals, of which all the skeletal elements are represented in the sample and usually not disturbed by any fossildiagenetic processes (García-Medrano et al., 2017). The low degree of hominin impact combined with the scarcity of trampling marks (Cáceres, 2002) on the faunal remains suggest once again the complementary nature of the site over a home-base one (Cáceres et al., 2010; García-Medrano et al., 2014, 2015, 2017; Ollé et al., 2005). The taphonomic study detected an abundant presence of manganese (Mn) on bones, which indicates humidity and waterlogged condition in the site, while the low percentage of fossils altered by atmospheric agents or by plant actions suggest the poor natural lighting of the cave (García-Medrano et al., 2017).

4.1 Sub-unit GIIa

The sub-unit GIIa represents the first cave exposure to the outside and the earliest human occupation in the Galería complex and it includes the following levels: GIId-TZ; TG7, TG8, TG9; TN2A, TN2B, TN3, TN4 (García-Medrano et al., 2014). The lithic artifacts are made on six types of raw materials, all of which available within a distance of 2-5 km from the Galería site, that appear selected and adapted to different uses (García-Medrano et al., 2015; Ollé et al., 2013). The two most frequently exploited raw materials for this sub-unit are Neogene chert (~50%) and quartzite (33.57%), from which the majority of retouched tools were generally made (García-Medrano et al., 2015). The LCTs assemblage from sub-unit GIIa is made up of both handaxes, mostly belonging to the shaping phase and made from quartzite, sandstone and Neogene chert, and cleavers, made exclusively from quartzite (García-Medrano et al., 2014). Both the tool-types present two different kinds of blank: cobbles or big flakes (*ibid*). Aside to cutting tools (24%) the lithic assemblage is characterized by an 18% of non-modified cobbles and a 54.51% made up of simple flakes, retouched flakes, broken flakes and flake fragments (García-Medrano et al., 2015). Five refits have been identified in this sub-unit for a total of 15 refitted pieces, and they all show flake production (García-Medrano et al., 2017). These also include one fragmented hammerstone (GIIa-R04) with several marks on the cortical part which attest an intensive use for percussion activities probably both outside and inside the cave. The faunal remains from sub-unit GIIa have yielded only partial information due to their poor preservation state result of the acidity of the organic layer in TN and TG areas from which most of the remains come. As for the other sub-units of the Galería complex, also in the GIIa there is a predominance of herbivorous and, additionally, axial and cranial remains are more abundant than appendicular elements (*ibid*).

5. Guado San Nicola

Guado San Nicola (GSN1) is a Middle Pleistocene site located near to Monteroduni in the south-west of Molise region (Central Italy), and it was systematically excavated between 2008 and 2013 from the University of Ferrara under the direction of prof. Carlo Peretto (Muttillo, Lembo, et al., 2014; Peretto et al., 2016). The open-air site of Guado San Nicola was situated on the left bank of the Volturno river, on the top of the oldest fluvial terrace, at ~250 meters above the sea level (Peretto et al., 2016). The latter terrace belongs to the Main Filling Unit which corresponds to the main filling of the nearby Isernia basin, and it mainly consist of polygenic gravelly, silty and clayey deposits that contained interstratified tephra levels (Peretto et al., 2016). The excavated area covers 98 m^2 and four archeological levels have been identified: SU A*B, SU B, SU B*C, and SU C. According to the radio-isotopic analyses, the Guado San Nicola sequence was deposited during the transition from the Marine Isotope Stage 11 to the Marine Isotope Stage 10 and also the Electron Spin Resonance and Uranium series (ESR/U-series) lead on 6 teeth of horse and rhinoceros from three different stratigraphic units confirmed an average age of 364 ± 36 ka (Peretto et al., 2016). The archaeological record is as interesting for the lithic industry as for the fauna assemblages. The site of Guado San Nicola (GSN1) represents one of the oldest chronologies in Europe for the appearance of the Levallois method and, moreover, the coexistence of the latter methodology and handaxe production has been considered as an evolutionary behavior in technological terms that would considers Levallois *chaînes opératoires* as a “natural consequence of the exploitation of two separate convex surfaces from a peripheral striking platform” (Muttillo et al., 2014). The lithic assemblage of GSN1 is composed by a total of 4,142 flint elements made on stabs and pebbles mainly collected from secondary position (Muttillo et al., 2014) and 365 elements made on limestone cobbles (Rufo, 2014). More specifically four raw materials, all locally available, have been identified: aphanitic flint, micro-brecciated flint, macro-brecciated flint, and silicified limestone (Peretto et al., 2016).

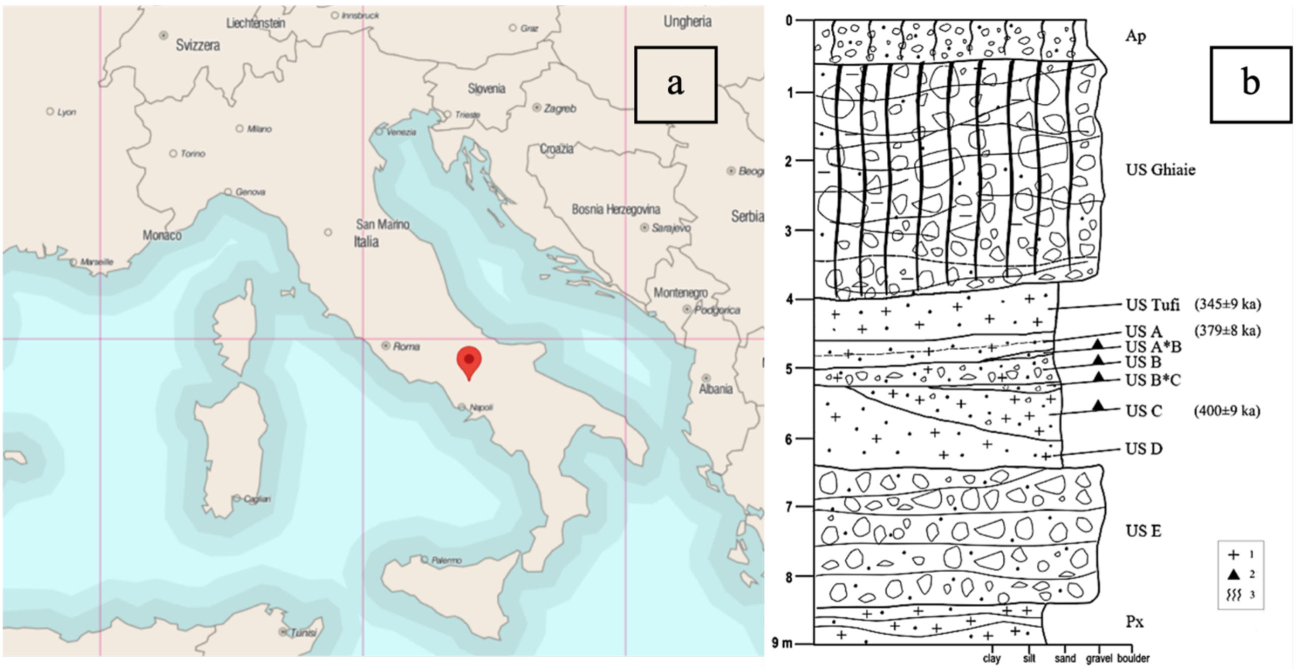

Figure 3: a) Location of Guado San Nicola site (Monteroduni, Central Italy) (modified from geamap.com). b) Stratigraphy and chronologies of Guado San Nicola site from Peretto et al. (2015).

According to Muttillo et al. (2014), the composition of lithic assemblages is broadly stable along the stratigraphy for both *débitage* and *façonnage* production. Predominant is the opportunistic production of flakes through the S.S.D.A. method (Système par Surface de Débitage Alternée; Forestier, 1993) alongside to handaxe manufacturing, but centripetal and Levallois *débitage* are also attested. The *débitage* activity is highly productive, the cores are usually exploited until the exhaustion of the raw material and secondary reduction sequences are poorly attested (Peretto et al., 2016). The percentage of retouched instruments is not elevated, usually is limited to the retouch of simple flakes, but a gradual increase has been observed in the most recent levels (Muttillo et al., 2014; Peretto et al., 2016). In terms of bifacial production, the Guado San Nicola complex shows a rare diversity of the bifacial reduction sequence that is reflected in significant intra-site variability (Peretto et al., 2016). The faunal assemblage of GSN1 is composed by Cervus elaphus acoronatus, Cervidae, Equus ferus ssp., Palaeoloxodon sp., Bos primigenius, Stephanorhinus kirchbergensis, Ursus sp. and Dama sp. Megacerini. The diversity within the assemblage reflects the diversified environment characterized by woodland and shrubby areas alongside open lands (Peretto et al., 2016). Furthermore, the absence of cold indicators in association with the presence of Merck's rhinoceros and aurochs suggests one or more warm-temperate phases (Sala et al., 2014b). Zooarchaeological analyses identified intentional fractures for marrow extraction and cut-marks on horse and rhinoceros bones, but also peculiar marks on shed antlers that have been linked to knapping activities (*ibid*).

5.1 Stratigraphic Unit C

Stratigraphic Unit C, dated at 400±9 ka by $^{40}Ar/^{39}Ar$ (Nomade & Pereira, 2014a), is characterized by a conoid depositional environment and it consists of a series of decimetric levels of weakly silty gravelly sands and weakly silty gravel sands whose origin is mostly volcanic (Turrini et al., 2014a). In this level, which represents the oldest human occupation in the site, lithic industry and fauna have been recollected (Fig.4).

The lithic assemblage of SU C is composed by 1417 artifacts mainly made on aphanitic and brecciated flint. Reflecting the general trend of the site, flakes are predominant in the complex while cores and retouched elements are poorly represented (Muttillo et al., 2014). Handaxes constitute the 3% of the lithic assemblage from this level, which is a meaningful representation especially when put in relation to the totality of lithic tools, and the preferential blanks are flint slabs (*ibid*). They don't show any morphological standardization and they appear heterogenic also when considering their dimensions. During the *chaîne opératoire* of handaxes the major technical investment is concentrated on tip and margins rather than in the base. The typical *débitage chaîne opératoire* of the SU C foresees an initialization phase where unipolar detachments prepare the core to its maximum exploitation, then the production phase is led by using direct percussion with hard stone as tallon morphologies and well pronounced bulbs suggest (*ibid*). Four *débitage* methods are present in the assemblage in different proportions: S.S.D.A. (58%), centripetal (25%), discoid (11%), and Levallois (6%). The transformation phase is poorly represented, covering the 4,7% of SU C lithic complex, and it is characterized by denticulates, scrapers, notches (*ibid*).

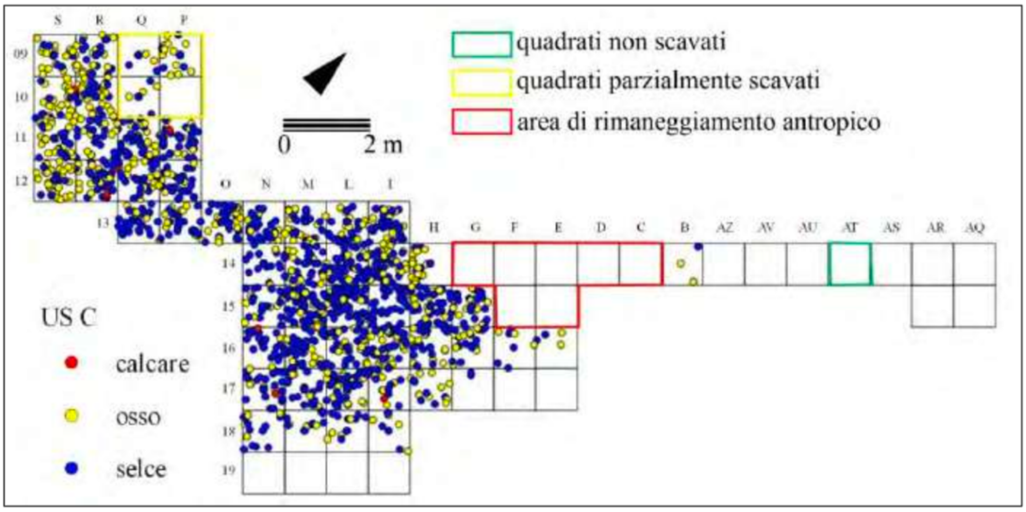

Figure 4: Plan of the excavation area of SU C and spacial distribution of founded materials. (Red dot = limestone; Yellow dot = bone; Blue dot = flint; Green square = not excavated squares; Yellow square = partially excavated squares; Red square = area of anthropic remnants). (from Muttillo et al. 2014)

6. La Noira

The open-air site of La Noira is located in the Middle Loire Basin (Center region, France) on the western slope of the Cher River valley (García-Medrano et al., 2022; Hardy et al., 2018). The site was discovered during a sand and gravel extraction in the fluviatile formation in 1972 by Jean Déport and archaeological excavations were carried out between 2011 and 2018 (Despriee et al., 2016a; M.-H. Moncel et al., 2020).The sedimentary sequence of the site was deposited in an alluvial plane context and it contains four units corresponding to five successive sediment strata (Despriee et al., 2016b; García-Medrano et al., 2022; Moncel et al., 2020): the first unit (*stratum* a) is a coarse slope deposit which has been covered by two sequences of sandy alluvial layers (*stratum* b); above it a layer of diamictons of pebbles with frost-shattered debris and coarse colluvial (*stratum* c), and finally a washed sandy-silty soil (*stratum* d) (García-Medrano et al., 2022). Within this stratigraphy, only *stratum a* (LN.a) and *stratum c* (LN.c) have returned archaeological remains, attesting correspondently a first early Acheulean occupation dated around 700 ka and a second one, which actually does not attests only one occupation but several recurrent ones, dated by ERS to 449±45 ka at his top (Iovita et al., 2017). According to these chronologies, the occupation of *stratum a* would have taken place between the end of river incision and the fluvial deposits suggesting that were present at the beginning of MIS 16 glacial stage, while the occupation of *stratum c* would have started at the end of MIS 12 and developed largely during MIS 11 (García-Medrano et al., 2022; Moncel et al., 2021; Shen et al., 2012). For this reason, La Noira is one of the few sites in Western Europe that can provide us information about human settlements between the end of MIS 17-16 and the end of MIS 12, that is a timeframe within the early Acheulean about which there is still a consistent information gap.

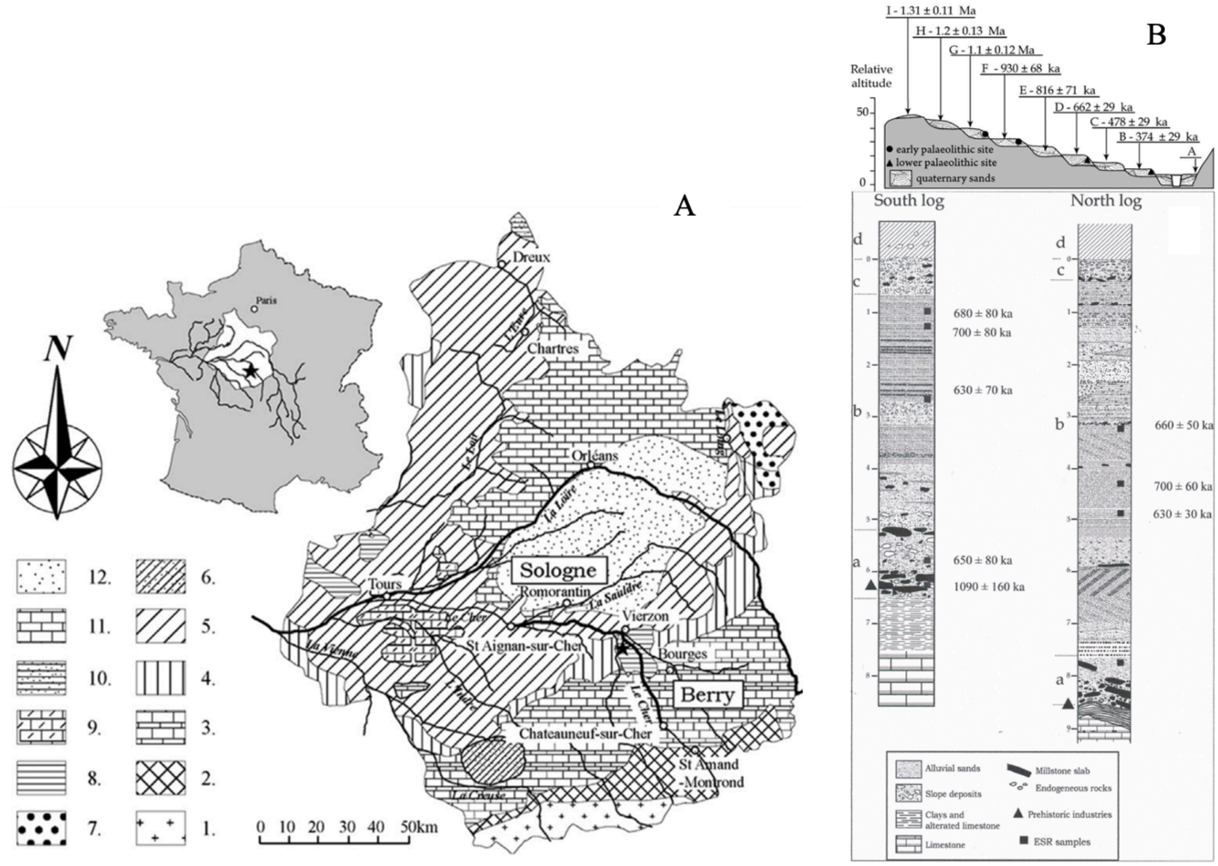

Figure 5: A) Location of La Noira (from Despriee et al. 2016) and B) chronostratigraphy of the site (from Moncel et al. 2020).

Within the archaeological evidences of la Noira, bones are not represented due to a lack of conservation while the lithic assemblage is very rich both in *stratum a* and *c* representing an example of well-developed Acheulean technology (Hardy et al., 2018). A total of 918 lithic elements have been recollected from *stratum a1* including cortical and knapped slab fragments, cores, retouched and unretouched flakes, handaxes, bifacial tools and cleavers (Moncel et al., 2020). The lithics from this *stratum* are made on lacustrine millstone (which was recovered *in situ* in form of slabs) or Jurassic silification (Despriee et al., 2016a; Hardy et al., 2018; Iovita et al., 2017; Moncel et al., 2020) and there would not appear to be a selection of raw material on the basis of quality, but rather on the basis of the shape and thickness of the slabs (Moncel et al., 2020). Core technology seems to be the predominate activity in the site aiming to the production of both small and big flakes, even if the *chaînes opératoires* devote to the production of small flakes are more structured and productive than the ones devote to the production of the big ones (*ibid*). Retouched products include scrapers, denticulates, notches and points on flakes which are also showing traces due to their use (Hardy et al., 2018). Functional analyses were conducted also on unretouched flakes and Large Shaped Tools and made it possible to revise the function of the site by integrating domestic activities into the workshop function, which had already been recognized (*ibid*).

6.1 *Stratum* c

The *stratum c*, dated on his top at 449±45 ka through ERS (Iovita et al., 2017), attests the second human occupation of la Noira site. This *stratum* records an important change in terms of human behaviors under several aspects as: land-use, core technology, and intensity of shaping activity (Moncel et al., 2021). A change in land-use is indicated by the use of a wider range of raw material, some obtained from distances between 30 and 100 kilometers, if compared to the few locally available materials used in *stratum a*. Lithic elements from *stratum c*, in fact, are made on Eocene/Oligocene millstone (72%), Jurassic oolitic (18%), Cretaceous flint (8%), and in some rare case also on quartz or quartzite. Core technology shows important innovations as centripetal and generally deep scars with impact points located away from the core edge and the removal of large and invasive flakes from flat surfaces that seem to indicate a transition towards the Levallois technique or an early form of it. 85 *façonnage* products have been found in *stratum c*. As in the case of *stratum a* there is no evidence of raw material selection, even if variation in blank types according to the raw material used to produce these shaped tools has been observed, while shaping activity is more intense than in the previous occupation and is characterized by an increase in handaxes' proportions. Another difference from *stratum a* is a decrease in the production of retouched flakes, although within this there is evidence of an increasing realization of composite tools mainly made in Cretaceous flint and Jurassic "chailles" (*ibid*).

Materials and Methods

1. Archaeological sample

The archaeological sample analysed for this thesis was composed by three different assemblages: sub-unit GIIa of Galería (Atapuerca, Burgos, Spain), *stratum* C of La Noira (Centre Region, France), and stratigraphic unit C of Guado San Nicola (Molise, Italy). The materials coming from the three European sites have been collected during archaeological excavations, well documented and with accessible information. The general state of preservation is good enough to allow technological analysis and digital data acquisition. In the following subchapters, number, typology and generical features of the materials coming from each assemblage will be presented.

1.1 Galería – Subunit GIIa (Atapuerca, Spain)

Galería is a cave site located in Galería complex, one of the sites situated in the Sierra de Atapuerca (Burgos, Spain). The site has a total chronology ranging from 466 ka to 221 ka (Falguères et al., 2013) attesting several human occupations in the two units of GII and GIII.

The sample from Galería studied for this thesis comes from the subunit GIIa and is composed by 9 handaxes and 4 cleavers, for a total of 13 integral tools, stored between the Centro Nacional de Investigación sobre la Evolución Humana (CENIEH, Burgos, Spain) and the Museo de Burgos (Spain). The artefacts have been made on sandstone (which is the most used raw material), quartzite, and Neogene chert. All of the three raw materials are available in the surroundings of the Sierra de Atapuerca (in the heist parts of the Sierra or in the River Arlanzón terraces), within 2 and 5 kilometers of distance (García-Medrano et al., 2015; Ollé et al., 2013).

The materials that constitute the sample have been recovered from sub-level GIIa whose composition is predominantly fine, highlighting how the sub-unit bears witness to the first opening of the cave (Núñez-Lahuerta et al., 2022), with presence of bioturbated lutites, stalagmitic crusts and detrital breccias originated by the mother rock of the cave itself (Rosas et al., 1998).

Lithic products from this subunit, aside to the large cutting tools composing the studied sample, are describing a typical Acheulean core technology (cores and flakes). Six raw materials are used for the lithic products of subunit GIIa: Neogene chert and quartzite are the most used ones followed by sandstone, limestone, cretaceous flint, and quartz. The lithic assemblage, which is predominantly concentrated in TN area, is characterized by a significant predominance of flakes (simple, retouched and broken flakes together with flake fragments and angular fragments) and unmodified cobbles (García-Medrano et al., 2014, 2017). Regarding the retouch activity, a selection of small to medium Neogene chert and quartzite flakes can be noted and the retouch is aimed to the creation of marginal scrapers and denticulated edges (García-Medrano et al., 2017). Only few cores, mainly knapped on Neogene chert by longitudinal and orthogonal methods, have been recollected from this subunit (*ibid*). Generally, the operational sequences are fragmented supporting the theory that knapping activities were most often performed outside the cave (Ollé et al., 2013, 2016). Within the whole assemblage, the preferred type of support is the quartzite cobble. The latter is a unique feature of Galería-GIIa, as it is the only site from Atapuerca complex that shows a predominant use of this type of blank (García-Medrano et al., 2014, 2017; Ollé et al., 2013, 2016). Galería-GIIa is the only assemblage within the sample studied for this thesis that provided refits. In fact, five refits made up by a total of 15 refitted pieces have been reconstructed for this subunit. All of them are relate to flake production but one exception. The latter refers to the fragmentation of a cobble used as a hammerstone that probably get broken due to the intense use (García-Medrano et al., 2014, 2017).

Aside to lithic artefacts, numerous faunal remains have been recovered from the sub-unit GIIa. The faunal assemblage is mainly composed by herbivores and the most frequently found skeletal parts are axial and cranial elements (Cáceres, 2002; Cáceres et al., 2010). The taphonomic analysis of the faunal materials leaded to the reconstruction of a very humid context marked by the strong presence of concretions (caused by the water-carbonate combination) and manganese oxide (the formation of which requires an aerobic environment with stagnant water). All the latter information supports the main hypothesis concerning the nature of human occupation of the cave: the Galería site was a natural trap for animals that fell into the complex with no way out, and both humans and carnivores took advantage of the primary access to prey (Cáceres, 2002).

Based on the occupational pattern of the site, the handaxes and cleavers found in GIIa are interpreted as part of a butchery-tool assemblage preserved within a reliable stratigraphic context. The chronology of this subunit has been correlated with Oxygen Isotope Stage 11 (OIS11)(Aguirre, 2001). However, thermoluminescence (TL) dating provides even older estimates: 503 ± 95 ka for a sample just below Levels TG7-TN2, and 422 ± 55 ka for TG9 (Berger et al., 2008). More recent Electron Spin Resonance-Uranium Series (ESR-US) dating has produced new age estimates of 350-363 ka

(Falguères et al., 2013). Thus, a mean chronology ranging between 450 and 350 ka can be stated for this subunit.

1.2 Guado San Nicola – Unit C (Central Italy)

Guado San Nicola is an open-air site located in Molise region (Central Italy) with a total chronology ranging from 400 ± 9 ka to 345 ± 9 ka (Pereira et al., 2016) during which two different human occupations have occurred.

The sample from Guado San Nicola analyzed for this work comes from stratigraphic unit c (USc) and is composed by 26 integral handaxes stored in the Museo Nazionale del Paleolitico of Isernia (Molise, Italy). The artefacts have been made mainly on flint and only few items on limestone. Within the type of flint used to knap the tools, a predominance of aphanitic lithotypes can be noticed but also the brecciated ones have been widely exploited (Muttillo, Arzarello, et al., 2014). Both lithotypes are from secondary positions, probably from detrital deposits, while the limestone comes from the alluvial areas of the Volturno River (*ibid*).

The materials that constitute the sample have been recovered from the Unit C, a level made of slightly silty gravelly sands (mainly volcanic sediment from Roccamorfina's activity) that were deposited in an input channel to the ancient conoid of T. Lorda (Turrini et al., 2014b). Within the level, taphonomic alterations (e.g. surface wear identified on lithic artifacts) indicate events of reworking by water, a phenomenon that is coherent with the characterization of the deposit in a conoid context (*ibid*).

Lithic products from this stratigraphic unit, aside to the handaxes composing the studied sample, are describing a typical Acheulean core technology (cores and flakes) made up by a total of 1417 lithic remains realized on aphanitic and microbrecciated flint well distributed on all the excavated surface (Muttillo, Arzarello, et al., 2014). More than half of the assembly is composed of flakes which were obtained by different *debitage* methods: SSDA ((Système par Surface de Débitage Alterné), centripetal, discoid, and few cases of centripetal recurring Levallois (Muttillo, Arzarello, et al., 2014; Peretto et al., 2016). Within flake category, also some configuration flakes (n.14) produced while shaping handaxes are present and support the use of soft organic hammer by direct percussion technique. A high percentage (>50%) of *debitage* products exhibit fractures that mostly occurred during the knapping process (e.g. simple fractures, Siret fractures, and *languette* fractures). Cores cover a discrete percentage of the total assemblage and are intensively exploited until every knapping surface is unusable (Muttillo, Arzarello, et al., 2014). The retouched elements are underrepresented and consist principally of simple scrapers and denticulates (Muttillo, Arzarello, et al., 2014; Peretto et al., 2016). Both typologies are most commonly made on flakes obtained by the SSDA method. Regardless of the method, all operational chains are described as fragmented (*ibid*). Of interest is the presence of a significant number of unworked flint slabs with no signs of use characterized by partial cortical covering on opposite surfaces ("sandwich" type). The latter, characterized by natural edges and a pronounced degree of fracturing, would appear to be a natural and random accumulation of raw material (Muttillo, Arzarello, et al., 2014).

Aside to lithic materials, numerous faunal remains have been recovered from unit C. The most represented family types are deer, elephant, aurochs and horses, which suggest a woodland environment alternated with slightly more open bushland areas. In agreement with the latter, this stratigraphic unit should correspond to temperate and warm-temperate climatic events that occurred during MIS11 (Sala et al., 2014a).

The chronology of Unit C has been confirmed also by $^{40}Ar/^{39}Ar$ analysis (which gave back a chronology of 400 ±9 ka) and further supported by the high presence of *Cervus elaphus acoronatus* (Nomade & Pereira, 2014b; Sala et al., 2014a). For the site of Guado San Nicola and, consequentially also of Unit C, the nature of the human occupation has not been defined due to the lack of elements enabling the formulation of concrete hypotheses. Notwithstanding, the abundance of archaeological finds and the stratigraphic sequence render the deposit reliable evidence of the final phase of MIS11.

1.3 La Noira – *Stratum* c (Centre, France)

La Noira is an open-air site located in Centre region (France) that covers a total chronology ranging from the end of MIS 17-16 (~700 ka), which is attested by the lower layer of *stratum* a, to the very beginning of MIS 11, evidenced in *stratum* c. During this time span, two main occupations occurred leaving as testimony a vastly lithic assemblage.

The sample from La Noira is composed by 48 handaxes and 1 chopping-tool, for a total of 49 integral tools, stored in the Institut de Paléontologie Humaine (Paris, France). All of the artefacts have been made on flint and within the latter three different types of silicious rocks can be identified: Eocene-Oligocene milestone coming from other valleys of the Middle Lorain basin (from a maximum distance of 50 km from the site), Jurassic oolitic or encrinic silicifications (also defined as *chailles*) which is the only locally available raw material, and Cretaceous flint available within a range of 30-100 km from the site (M. H. Moncel et al., 2021b).

The materials that constitute the sample have been recovered from the *Stratum* c, a level made of sand and quartz gravels with few or totally absent clay within which endogenous pebbles and sedimentary siliceous rocks as limestone and milestone are present (*ibid*).

Lithic products from this *stratum*, aside to the large shaped tools that are composing the studied sample, are describing a typical Acheulean core technology (cores and flakes). Numerous local raw materials are present within the assemblage – Millstone and "Chaille" Jurassic flint are the most used while quartz, quartzite, and sandstone are less frequent – but a type of Cretaceous flint that was available at a distance of 30 to 100 km from the site is also well represented (M. H. Moncel et al., 2021b). As for the two previous assemblages, also for the *stratum* c of La Noira the higher percentage within the sample is those for flakes. The latter are characterized by quite standardized dimensions (small flakes) while quantities of cortex is highly variable (*ibid*). The percentage of retouched flakes, instead, is not so elevate and is primarily composed of products with bifacial retouching, denticulates, convergent scrapers and tips. Overall, flint products – both simple and retouched – are smaller, thinner and noncortical while for the other raw materials no significant difference can be noticed. Cores are mainly bifacial worked by partial discoidal method and are characterized by a number of negatives ranging from 2 to 9 (*ibid*). Some of the cores from *stratum* c show features relatable to Levallois method as well as two of the flakes from this subunit. This seems to point out the presence of an early Levallois core technology that evolved just after the end of MIS 12. Finally, no refits have been found in *stratum* c from La Noira but the presence of complete operational chains indicates *in situ* knapping activity by supporting the hypothesis that La Noira was a lithic workshop. According to the taphonomical studies, the lithic products from *Stratum* c do not present any form of mechanical alteration (e.g. traces of crushing or micro-denticulation) which suggests that the artefacts have not undergone any kind of post-depositional displacement (García-Medrano et al., 2022). Due to the sedimentary conditions of the site, no faunal remains have been preserved in La Noira (Hardy et al., 2018). On the opposite, the high number of lithic artefacts suggests that La Noira was a knapping workshop and, furthermore, recent studies show that the hominids who occupied the site also carried out a number of other activities as woodworking, plant processing, and butchery (Hardy et al., 2018).

The chronology for the occupation of *Stratum* c has been placed between 449±45 ka through ERS (Iovita et al., 2017). That means that this sample attests the transition between MIS12 and MIS11.

The latter transition is confirmed also by the environmental reconstruction which, in that moment, describes the surrounding of La Noira as open landscapes with slope solifluction depositions that predate the gradual development of forest areas (Limondin-Lozouet et al., 2015).

2. Digitalization of the archaeological sample

As part of this work involves a morphometric study using software for geometric morphometric analysis, it was necessary to generate an archive with the 3D models of each artefact of the sample. In addition, as the archaeological collections are located in different European cities and it was not possible to transport the same equipment to the various institutions where the materials are stored, the digitization has been done using two different methods: using a laser scanner and with photogrammetry. The handaxes from Guado San Nicola have been digitalized using photogrammetry. Large Cutting Tools from Galería have been scanned using Breuckmann SmartScan, which is a structured light scanner, in combination with Optocat software v. 2012 R2-2206 (AICON 3D Systems GmbH, Surrey). In the case of La Noira, it was used a DLP projector Laser Scanner together with the Flexscan software v.3.3.5 (García-Medrano, 2021). The protocol followed to digitalize the materials by photogrammetry is explained step by step in the Annex 1.

After obtaining the 3D models of the sample materials, these were processed and modified on the MeshLab software (v. 2023.12) to store the files in accordance with the system requirements of the Artifact Geo-Morph Toolbox 3D (AGMT3-D) software, which was then used to perform the geometric morphometric analyses. Below is a list of the requirements of the AGMT3-D software and the changes that need to be made to 3D models in order to fulfil them:

- <u>N° of faces</u>
  Each 3D model is made up of faces (or triangles) that recreate the surface and the morphology of the object. The number of these faces can be very variable, and it determines the quality of the model itself. Within the context of this study, the 3D models of Guado San Nicola realized by photogrammetry have a mean number of faces of 41.977; while the 3D models of La Noira and Galería realized by scanner have a mean number of faces of 3.150.577. The AGMT3-D software does not support as many faces as the 3Ds made with the scanner, so the number of faces in the La Noira and Galería 3Ds was reduced to 360.000. The number of faces of the Guado San Nicola 3Ds was not reduced as it was already below the maximum supported by the AGTM3-D software. Reducing the number of faces of a 3D inevitably leads to a loss of

quality, but the latter is not invalidating when analyzing the same 3Ds within geometric morphometric analysis.

- File format

  Each 3D model of the sample has been exported as VRLM file. This is a necessary step because the AGMT3-D software is only able to process VRLM files in the *Process Folder* phase to generate the archive needed to proceed with analysis.

3. Technological Analysis

A technological analysis was carried out valuating the same parameters for each single archaeological material from the three assemblages. I personally carried out the technological analysis on the tools of La Noira *stratum* c and Guado San Nicola stratigraphic unit c, while the data for Galería sub-unit GIIa were kindly provided by Paula García-Medrano (García-Medrano et al., 2014, 2015). The observations have been collected in a database realized on Microsoft Excel (v. 16.86) where each technological feature was coded in order to describe how the blanks were modified leading to the final product. All the parameters considered during the technological analysis are described below in order to show the different categories used to define the archaeological materials and explain their apport to the study.

3.1 Tool-type

The identification of the tool-type has been included in order to compare the degree of symmetry in relation to the typology of the items. Whitin the context of this study, the definitions of handaxe and cleaver are based on the ones proposed by Bordes (Bordes, 1961) and Kleindienst (Kleindienst, 1962), the latter author was also used as reference to define the terms chopping-tool and spheroid (ibid). The tool-type categories used to define the large shaped tools are explained in Table 1.

All materials identified as fragments were excluded from the study as they can provide only limited information related to the section of the object that has been preserved and it is not possible to trace the original morphology that the intact tool would have had.

Category	Definition
Handaxe	Two faces worked with a convergence of the margins in the distal section
Cleaver	One or two faces worked with a transversal distal margin
Chopping-tool	Rounded morphology core with one or more negatives localized in the distal section and that do not cover more than 50% of the total surface
Fragment	Broken tool, it is characterized by a missing section of tool itself

Table 1: Definitions of Tool-type categories used as used in the database of the study.

3.2 Blank type

The influence of blank morphology on the final shape of the product is an issue that is widely discussed in the literature and still leaves room for contrasting opinions. Defining the existence of a direct relationship between the morphology of the support and the one of the final products is not one of the objectives of this thesis, and for this reason the identification of the blank type, where possible, was mainly considered in order to better understand the shaping strategies and the intensity of transformation to which the tool was subjected. Within the archaeological sample analysed, six categories have been identified (Table 2). The definition of the categories used is based on the ones proposed by García-Medrano and colleagues (García-Medrano et al., 2020).

Category	Definition
Flake	Support detached from a previous core during debitage production
Cobble	Rounded support collected from river gravels
Nodule	Support naturally eroded from bedrocks
Slab	Angular support
Block	Support broken from bedrocks
Unknown	Not identified support due to an intense knapping activity which completely modified the original blank

Table 2: Definition of Blank type categories as used in the database of the study.

3.3 Raw material

The type of raw material has been recorded to observe if it is possible to detect a trend leading the choice of specific type for different tools and to verify if it can be a relevant variable to explain variability in the symmetry. Four different raw materials have been identified within the sample: flint, quartzite, limestone, and sandstone. Below, a brief description of the four general (Table 3) raw materials based on the definitions of Peresani (Peresani, 2011).

Category	Definition
Flint/chert	Chemical sedimentary rock commonly composed of silicate microfossils and spherical quartz aggregates of varying sizes. It forms as a result of silica concentration during diagenesis or marine sedimentation.
Quartzite	Metamorphic rock formed from metamorphosed or silicified sandstones with a high percentage of quartz. It forms under conditions of high temperature and pressure.
Limestone	Carbonate chemical sedimentary rock that may contain varying percentages of silica. The admixture of silica and carbonate can be primary or secondary and affects the texture of the raw material.
Sandstone	Detrital sedimentary rock composed of sandy granules of varying mineral nature bonded by a cement that is formed by chemical precipitation of the minerals. The size and type of grains and cement influence the functional properties of the artefacts.

Table 3: Definition of Raw material categories as used in the database of the study.

Site	**Category**	**Definition**
La Noira	**Cretaceous flint**	Fine-grained groundmass flint in blond or grey colour available within a distance of 30-100 km from the site. As suggested by the name, it originates from Cretaceous formations.
	“Chaille” flint	Allochthonous flint available in local tertiary detrital remains above the site. It can be partially lateritize and it originates from Jurassic formations.
	Millstone	Fine-grained and homogeneous groundmass, sometimes lateritize. It is a lacustrine flint available both on site and within a distance of 50 km from the site.
Guado San Nicola	**Aphanitic flint**	Flint of various shades of brown colour, with presence of dark and light micritic elements, and with a high degree of lustre and transparency.
	Micro-brecciated flint	Homogeneously textured flint with brown to white chromatic variations and sporadic presence of dark micritic.
Galería	**Neogene chert**	It originates from Late Miocene formations, and it is available in the Arlanzón River basin (little distance from the site) under the form of large blocks.

Table 4: Definition of flint types as used in the database of the study.

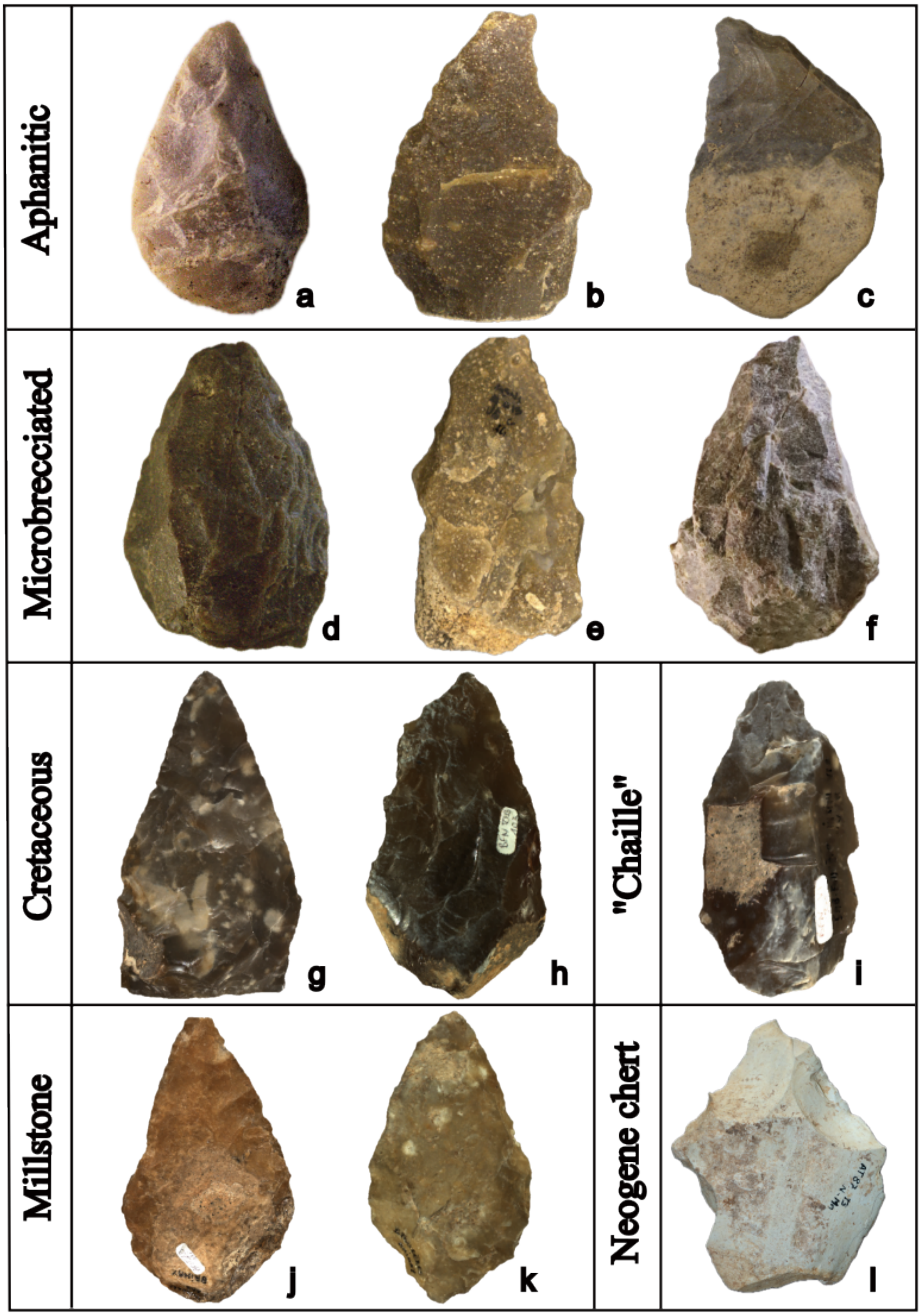

Figure 6: Photos of the different type of flint and chert present within the sample studied. Aphanitic flint (*a*: white; *b*: blond; *c*: gay) and microbrecciated flint (*d*, *e*, and *f*) from the sample of Guado San Nicola – Usc. Cretaceous flint (*g*: blonde; *h*: gary), “Chaille” Jurassic flint (*i*), and millstone (*j*: lateritize; *k*: *gîte*) from the sample of La Noira – *stratum* c. Neogene chert (*l*) from Galería – GIIa.

As the three sites are located in different geographical regions, and consequently the specific type of flint or chert used differ according to the geological resources of each area, in the database it has been included also the specific category in order to have a more precise description of the three assemblages. Descriptions of the latter are presented in the Table 4. The descriptions provided for La Noira are based on the ones gave by Moncel et al. (M. H. Moncel et al., 2021b), the description provided for Guado San Nicola are based on the ones gave by Muttillo et al. (Muttillo, Arzarello, et al., 2014), and the description provided for Galería are based on the one gave by (Ollé et al., 2013). Photos of each specific raw material is showed in Figure 6.

3.4 Number of faces

This parameter indicates how many faces of the tool have been show detachments due to knapping activity. The categories used to define this variable are unifacial (only one shaped face) and bifacial (two shaped faces) (García-Medrano et al., 2020). Hence, non-anthropic detachments or the presence of natural surfaces that have not been modified by the knapper are not considered in the counting of number of faces. This variable is useful to define the typology of tool but also to detect the management of the blank during the knapping process and identify possible errors occurred during it.

3.5 Type of hammer

The identification of the knapping technique is mainly reflected in the features of the negatives present on the shaped faces of the tool. The use of a hard hammer usually generates deep detachments on the edge, a marked concavity in correspondence of bulb of the flake detached and the scar is not very invasive on the surface. By contrast, the use of soft organic hammer is generally indicated by flat, invasive negatives which do not significantly alter the morphology of the margins. A third category, defined as combined hammer, has been used to indicate those cases where both hard and soft hammer is used during different removal series (Inizan et al., 1999).

3.6 Location and percentage of cortex

The presence or absence of cortex and, when it is present, his localization on tools' surface is a data often strictly related to the invasiveness of the scars on the tool's surfaces and the degree of supports' transformation.

Category	Definition
0%	No cortex present on the tool
<50%	The cortex covers less than the half of the tool
>50%	The cortex covers more than the half of the tool
100%	Totally cortical – i.e. All the surface is covered by cortex

Table 5: Definition of the Percentage of cortex categories as used in the database of the study.

The amount of cortex present on the surface of a tool is an indicator of the intensity of transformation of the original support. To quantify the amount of cortex present on the materials studied, three categories expressed in percentage have been used (Tab. 5)(García-Medrano et al., 2020). The location of the cortex on a tool's surface denotes in which areas the knapping activity was concentrated, modifying the initial support the most. As for the percentage, also the location of the cortex has been registered through a classification in five categories showed in the Table 6.

Category	Definition
Mid	Cortex present only in the medial section of the tool
Butt	Cortex present only on the butt of the tool
Mid-distal	Cortex present in the medial and distal section of the tool
Mid-proximal	Cortex present in the medial and basal section of the tool

Table 6: Definition of Location of cortex categories as used in the database of the study.

3.7 Removal series

The number of removal series visible on a tool is a key feature to reconstruct its knapping process. The categories for this variable indicate the identification of one, two or more removal series, even if it is not so common to see more than two removal series on large shaped tools (García-Medrano et al., 2020). The presence of more than one single removal series indicates higher processing of the original blank and it often leads to more refined final products. The final retouching, if any, was also considered as a stand-alone removal series. When present, it can be defined as: invasive, if the removals affect at least 50% of the surface; non-invasive, when the removals affect less than 50% of the surface; specific, when the modality of detachment is related to specific type of retouch (i.e. *tranchet*).

The invasiveness of the scars on the tool's surface has been also classified for each removal series according to two categories: invasive, when the removals are covering at least 50% of the piece's surface; non-invasive, when the removals are covering less than 50% of the piece's surface and their location is close to the margin (*ibid*). Often the invasiveness of removals is directly linked to the use of soft hammer, so this variable can be also useful to define the type of hammer used during the knapping process.

Also, the number of scars has been documented to assess knapping intensity. In order to limit the subjectiveness factor, only scars with a length of more than 1 cm have been considered. The number of scars has been used together with the surface area (in^2) of each artefact to determine the Scar Density Index (SDI)(Shipton & Clarkson, 2015). The Scar Density Index (SDI) has been obtained by dividing the total number of scars of each item per surface area of the same (tot. number of scars/surface area). Additionally, to explore the potential correlation between SDI and volume, which may indicate a relationship between the number of scars and tool size, a one-way analysis of variance (ANOVA) has been conducted to assess the relationship between SDI and volume at each site.

3.8 Depth scars on edge

The depth of scars on the edge of the tool is a variable most commonly related to the type of hammer used by the knapper. As mentioned before, hard hammers tend to characterize denticulate edges due to deep removals while soft hammers enhance the creation of continuous edges through the detachment of marginal removals. Scars on edge have been considered *deep* when they cause denticulate edges and *marginal* when they generate continuous edges (García-Medrano et al., 2020).

3.9 Edge-profile and Cross-section

The delineation of edge-profile, which can be observed in profile view, and the shape of the tool viewed in cross-section are two variables which significantly influence the morphology of the tool and its bifacial symmetry. The edge-profile can be categorized as straight, sinuous or curved while according to the cross-section a tool can be symmetrical, non-symmetrical or plano-convex (Fig. 7).

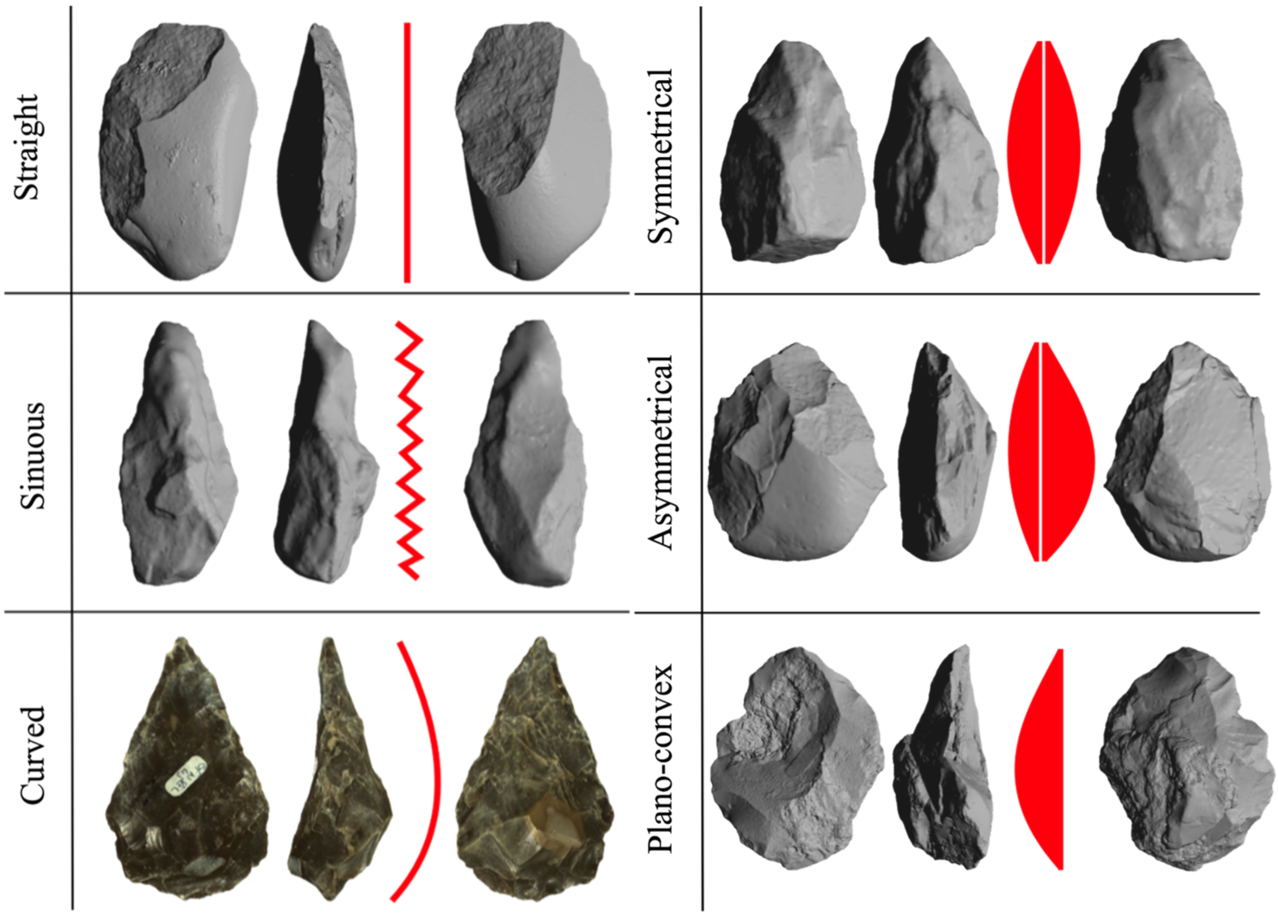

Figure 7: Typologies of edge-profile (left) and cross-section (right) used in the database for this study.

3.10 Dimensions

Using the AGMT-3D software, several measurements were recorded for each large shaped tool:

- Maximum length
- Maximum width
- Maximum thickness
- Width at middle length
- Distal width
- Proximal width
- Base length
- Distal thickness

- Elongation index (which is the ratio of maximum length to maximum width)
- Refinement index (which is the ratio of maximum width to maximum thickness)
- Distal refinement index (which is the ratio of distal width to distal thickness)

All these measurements can be very useful to better understand the morphological variability of the tolls composing the three assemblages and, by reflection, in which areas of the tool the knapper focalized the most.

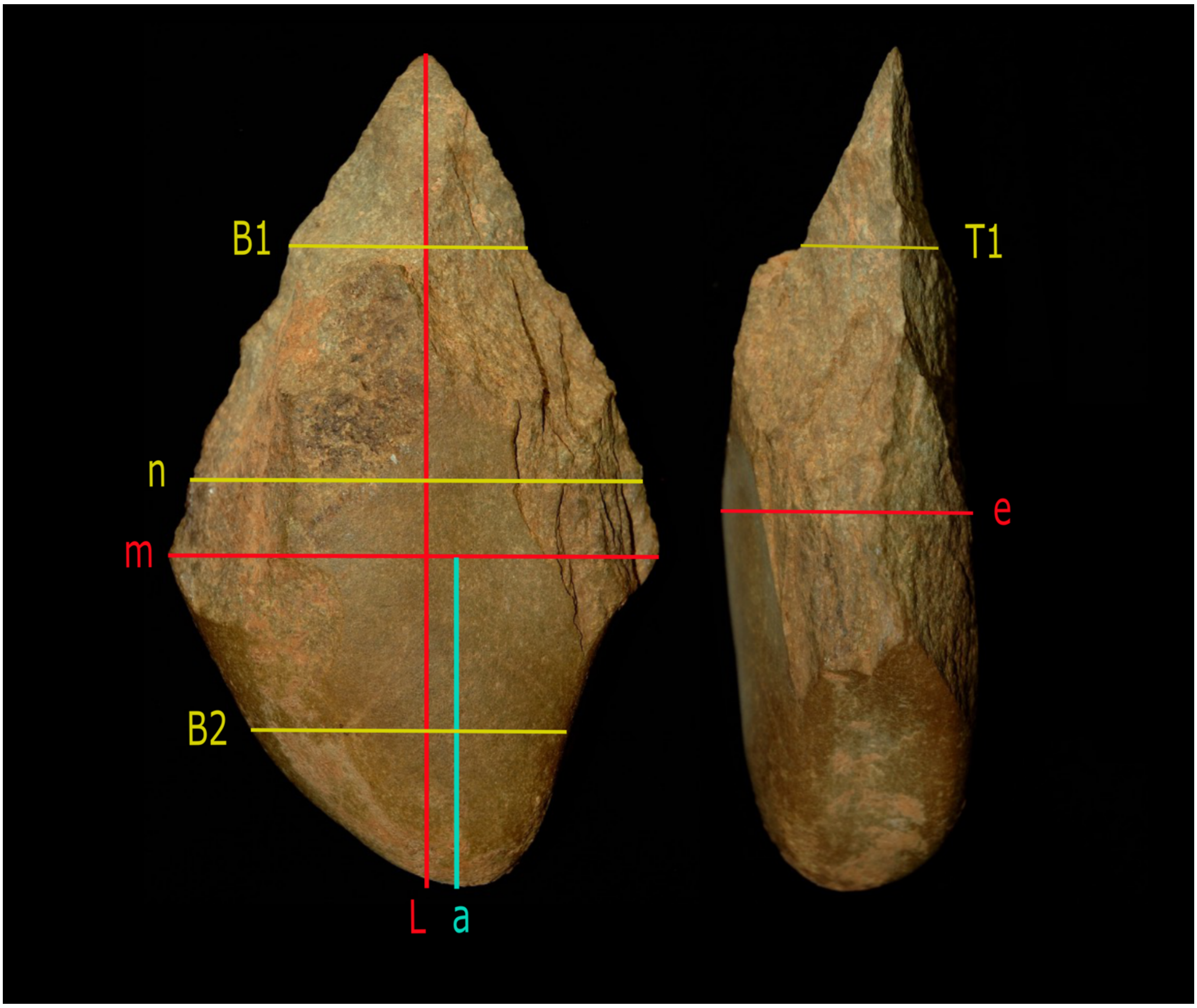

Figure 8: Measurements recorded for each large shaped tool from the sample | L: maximum length; m: maximum width; e: maximum thickness; n: width at middle length; B1: distal width; B2: proximal width; T1: distal thickness. Photo: Handaxe (ATA94_TG7_F20_4) from subunit GIIa of Galería (by P. García-Medrano).

3.11 Statistical treatment of technological data

The technological analysis involved statistical data processing, more specifically descriptive statistical analysis and a principal component analysis (PCA) which allowed to determine the main technological features of the sample. The latter determination is fundamental in order to understand the technological features characterizing the sample and to contextualize the information resulting from geometric morphometric analysis.

The descriptive statistic applied on the sample was aimed to describe each site according to its technological features. Under this premise, histograms showing absolute and percentiles values of each site and raw material has been realized using the opensource software PAST v.4.15 (Hammer et al., 2001).

Principal Component Analysis have been performed to identify the main differences and similarities between the three assemblages. In order to do that, all the nominal variables of the database have been transformed in percentage (%) to obtain absolute values for each group (García-Medrano et al., 2023). The latter percentage values have been then uploaded on the opensource software PAST v.4.15 (Hammer et al., 2001), as the software provide a number of multivariate analyses like Principal Component Analysis. Within the results obtained from PCA analysis, particular attention has been lead on:

- <u>Scatter plot</u>
  It is the visual representation of the position of each group inside the Cartesian system and the distance between one group and the other. In the plot, the two axis (x and y) correspond to the two most representative PCs. For this specific study, the scatterplot shows the different raw materials and the color-coding by which these are represented indicate the site where they are present.

- <u>Scores</u>
  Numerical values of each PC (PC1 and PC2) for each group.
- <u>Loadings plot</u>
  Histogram showing the load of each variable and its positioning on the negative or positive section of the scatter plot.

- Loadings

  Numerical values of each PC (PC1 and PC2) for each variable included in the analysis.

The PCA results were subjected to the following non-parametric tests to understand their statistical significance:

- Kruskal-Wallis (K-W)

  It was applied to check the equality of the medians of the different groups.

- Mann-Whitney U test

  It was used to test pairwise differences in group median values.

Additionally, to show the distances and patterns of relationships among the various raw materials, a cluster analysis was conducted.

4. Geometric Morphometric Analysis

Geometric Morphometric Analysis have been performed using Artifact Geo-Morph Toolbox 3D (AGMT3-D). The latter is an opensource software designed to provide an easy-to-use tool to study the shape of archaeological artifacts by applying landmark-based geometric morphometric analysis (Herzlinger & Grosman, 2018). As many other methods used to perform geometric morphometric analysis, also the AGMT3-D software bases the comparison between the different artifacts of the sample on a mesh of points located on the surface of each item and which position is expressed by three Cartesian coordinates. These points are more commonly defined as *landmarks* and they should be placed according to homology principle, which it means that each point should have the same position across all the specimens of the sample. However, the latter criteria cannot be applied so easily on lithic industries and to overcome that issue the concept of *semi-landmarks*, points which base their homology on the geometrical positioning, has been introduced (*ibid*). Afterward, the user can select a number of multivariate statistical analysis to enhance the quantification of shape variability within the sample. The protocol used to perform GMA on the sample is described below.

As a first step, the semi-landmarks have been placed on the surface of each item. This can be done by selecting the button *Process folder* in the project panel. The software will ask to select a folder containing the 3D models of the archaeological artifacts in VRML format (.wrl files). Once that each file has been read and upload, a review of the orientation of each object according to Y (which should correspond to the ventral face and can be modified by rotating the item of 180°) and Z (which correspond with the orientation of the basal and distal sections and can be modified by rotating the item of 90° per time) will be required. In order to proceed with the generation of the semi-landmarks grid, it is also necessary to indicate the density of the latter in terms of number of latitudes and number of landmarks per latitude. In the context of this thesis, the software was asked to generate a 50x50 grid for a total number of 5000 landmarks for each item. Then, it is possible to proceed with the process of all the files according to the information previously provided, and at the end of the process each VRML file contained in the original folder will be integrated by two other new files: a 3dl file containing all the information regarding the 3D model (faces, vertices, vertex color, etc.); a Microsoft Excel file containing the landmarks' coordinates. Having all these three files for each artefact of the sample, it is possible to start a new project that will enhance the statistical treatment of the information.

Once that a new project has been created and named, the software will process the data file and it will require to apply two mandatory procedures. The first one is a Generalized Procrustes Analysis (GPA) which superimpose the landmarks coordinates of all the objects to eliminate all the non-shape-related variabilities and modifies the landmarks' coordinates to filter out variations caused by different spatial locations (translation), positioning (rotation), and scale (scaling to centroid size 1). The second one is a Principal Component Analysis applied on the superimposed coordinate data which enables the identification of the major axes of shape variability in the data itself. In the latter analysis each PC component represents a specific variation trend in shape and the first two PCs (PC01 on X axis and PC02 on Y axis) will be visually showed by the software as a scatter plot.

Although the AGMT3-D software provides a significance tester, a multivariate analysis of variance (MANOVA) was applied on the raw results of the PCA to assess whether the differences between the groups were statistically significant (García-Medrano et al., 2023).

Below are presented the tools on the Artifact GeoMorph Toolbox 3D software that were used during the analyzes in this thesis.

Items Attribute – Software allows you to define a maximum of two attributes to each object of the sample to visualize categories both in the scatter plot and in the results of multivariate statistical analysis. For this study, Attribute1 was indicating the tool-type, while Attribute2 was explaining the specific raw material of each item (Tab. 7a). According to the attributes' assignation, the items will be color-coded in the scatterplot and 90% confidence ellipses and their centroids may be applied for each group enhancing the understanding of group distribution (Herzlinger & Grosman, 2018). As the discussions of this thesis are based on a comparison between the three sites, a secondary scatterplot has been realized defining only one attribute corresponding to the archaeological site of provenience (Tab. 7b).

a

	Categories
Attribute 1	Handaxe
	Cleaver
	Chopping-tool
Attribute 2	Aphanitic flint
	"Chaille" Jurassic flint
	Cretaceous flint
	Limestone
	Microbrecciated flint
	Neogene chert
	Quartzite
	Sandstone

b

	Categories
Attribute 1	Galería
	Guado San Nicola
	La Noira

Table 7: Categories used to define Attribute 1 and 2 on AGMT3-D.

Warp Tool – The *warp tool* visualise the nature of shape variability over shape trends expressed by any of the principal components. That means through the Warp Tool it is possible to visualise as much the mean shape (corresponding to principal component score of 0) as the ideal positive and negative extremes of the assemblage variability. This tool is also very useful to identifies which landmarks, according to the specific shape trend showed by the selected PC, variate the most along the sample thanks to a color-coding system. The images of the models generated through the Warp Tool have been used to visualize the ideal morphologies in the extremes of the PCA scatters.

Raw results – In the raw result section numerical values for principal component scores, inherent attribute, and metrics are given. These can be exported to 3rd party software and be used to proceed with different statistical analysis. Raw results can be used to export the data of all the PCs and apply test of reliability on them and they also allow to have measurements of the tools calculated directly on the 3Ds reducing possible errors or subjectivity of the person who is measuring.

PC Var Report – The principal component variability report shows general statistic of each PC and the corresponding cumulative variability chart. Thanks to this tool is possible to verify how representative are the two PCs used to generate the PCA scatters.

Assemblage var – The Assemblage Variability panel shows a general report with date, name of the project, sample size, analysis resolution, and total shape variability (which is automatically calculated by the software as the mean multidimensional Euclidean distance of all the items from the sample centroid) along with three tables (one for each Attribute and one where the two attributes are combined). Additionally, a number of analytical tools allow to better investigate inter- and intra-groups variability. The *group mean distance calculator* has been used to calculate multidimensional Euclidian distance between different groups' centroids. The *inherent attributes summary statistic*, as suggested by the name, provides the summary statistic of an inherent attribute (e.g. median, mean, standard deviation, etc.) that have been used to compare specific features between the different groups.

Group details and Main shape – The *mean shape* has been used to calculate the group's centroid showing the mean shape of the group and their distance from the latter under form of phylogenetic tree.

Significance tester – It has been used to test the statistical significance of different features within the groups.

Compare group means – This tool was used to directly compare two different groups based on one of the attributes and to understand the effect of each of the three main dimensions (maximum length, width and thickness) on the mean morphology of the group itself.

4.1 Symmetry analysis

The study of symmetry has been conducted using the results of Geometric Morphometric Analysis. The open-source software AGMT3-D, as previously mentioned, provides several tools to statistically analyze groups of archaeological artifacts (Herzlinger & Grosman, 2018). In the Assemblage

Variability Report, it is possible to obtain summary statistics for each inherent attribute, offering a statistical analysis of the sample's deviation from perfect 3D bilateral or bifacial symmetry. The software, with the support of third-party software MatLab R2017b, which facilitates the statistical calculations presented by the main software, constructs a hypothetical perfect symmetry through a mechanism based on the reflection of the landmarks of one side onto the other one in both frontal (for bilateral symmetry) and sagittal (for bifacial symmetry) views (Herzlinger & Goren-Inbar, 2020). According to this mechanism, the closer the value is to 0 the further from perfect symmetry the group is, while a value greater than zero indicates a more symmetrical assemblage, directly proportional as the value increases.

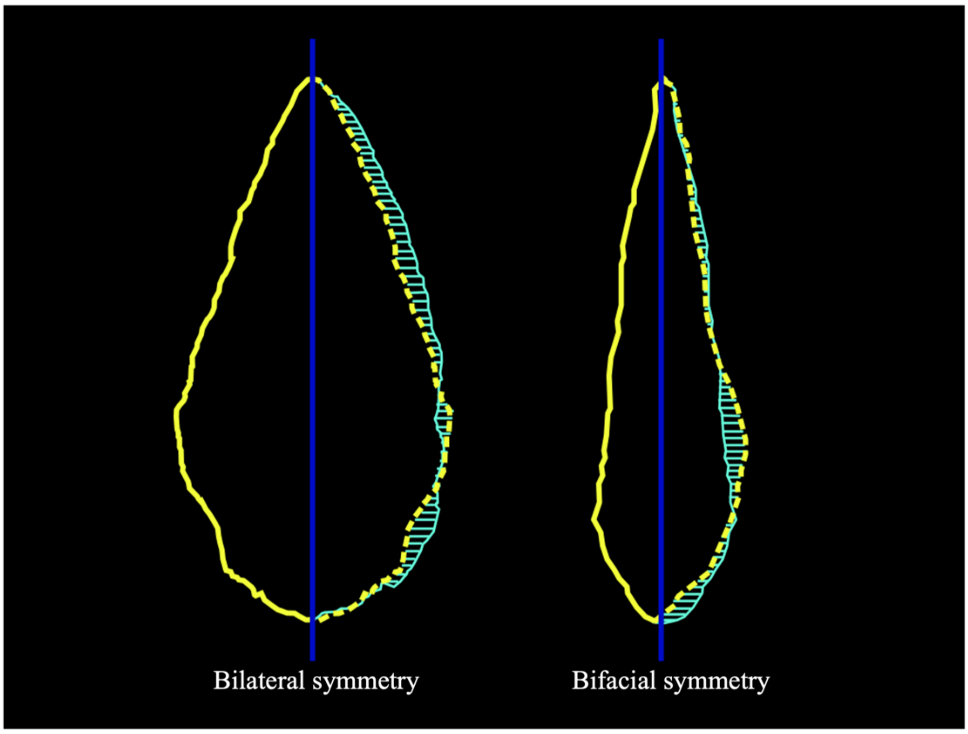

Figure 9: Visual representation of perfect bilateral and bifacial symmetry and deviation from it. The yellow continuous line indicates the left edge profile from which the landmarks are mirrored on the opposite side (yellow dashed line). The light blue continuous line indicates the real right edge profile while the horizontal lines represent the distance from the perfect symmetry. Blue vertical lines are indicating the symmetry axis.

Additionally, the Significance Tester tool automatically performs a Wilcoxon Rank Sum Test on Group Centroid Sizes, determining whether the attribute shows statistical significance when comparing it between two different groups. The significance level has been set at 0.5 as suggested in the work by Herzlinger and Goren-Inbar (ibid).

Results

1. Technological Analysis

The technological analysis was conducted on all the 88 large shaped tools composing the sample: 13 tools from Galería-GIIa, 26 from Guado San Nicola-USc, and 49 from La Noira-*stratum* c. Absolute values for archaeological site, tool-type, type of blank, and raw material are displayed in Table 8. Based on these results, the technological characterization of each assemblage will be presented below.

		Galería-GIIa		**Guado San Nicola-Usc**		**La Noira-*stratum* c**	
		n.	%	n.	%	n.	%
Tool-type	Handaxe	9	69,2	26	100	48	98
	Cleaver	4	30,8	0	0	0	0
	Chopping-tool	0	0	0	0	1	2
Type of blank	Flake	6	46,2	0	0	12	24,5
	Pebble/Cobble	6	46,2	0	0	5	10,2
	Nodule	1	7,7	0	0	1	2
	Slab	0	0	16	61,5	16	32,7
	Unknown	0	0	10	38,5	15	30,6
Raw material	Flint/Chert	3	23,1	23	88,5	49	100
	Quartzite	7	53,8	0	0	0	0
	Limestone	0	0	3	11,5	0	0
	Sandstone	3	23,1	0	0	0	0

Table 8: Absolute and percentage values of each archaeological site for all the variables used for the technological analysis.

1.1 Galería – GIIa

The sample from Galería-GIIa consist of handaxes (69,2%) and cleavers (30,8%). These LCTs are shaped on three different raw materials: Neogene chert (23,1%), quartzite (53,8%), and sandstone (23,1%). The preferred types of support are flake and cobble (~46,2% each), while only one tool has been made on a chert nodule. All the tools from the assemblage are bifacially worked but one, which is unifacial. The hard hammer (84,6%) is the most used, one handaxe attest the use of combined hard and soft hammer, and for another tool it wasn't possible to identify the type of hammer used. The most common category for cortex's localization is *mid-distal* (46,1%) followed by *totally cortical* (30,8%), while *non cortical* (15,4%) and *butt* (7,7%) are scarcely represented. Regarding the number of reduction sequences, the majority of the sample results from two sequences (46,1%) or just one reduction phase (38,5%), only two tools have been shaped by two reduction sequences combined with final retouch (15,4%). The edge-profile is very heterogeneous as all of the three categories (sinuous, straight, and curved) are well attested. The cross-section is prevalently asymmetrical (76,9%) without any presence of plano-convex tools. The linear measurements indicates that tools from Galería-GIIa have mean metrics equal to 106,09 mm for the maximum length, 69,02 mm for the maximum width, and 34,30 mm for the maximum thickness.

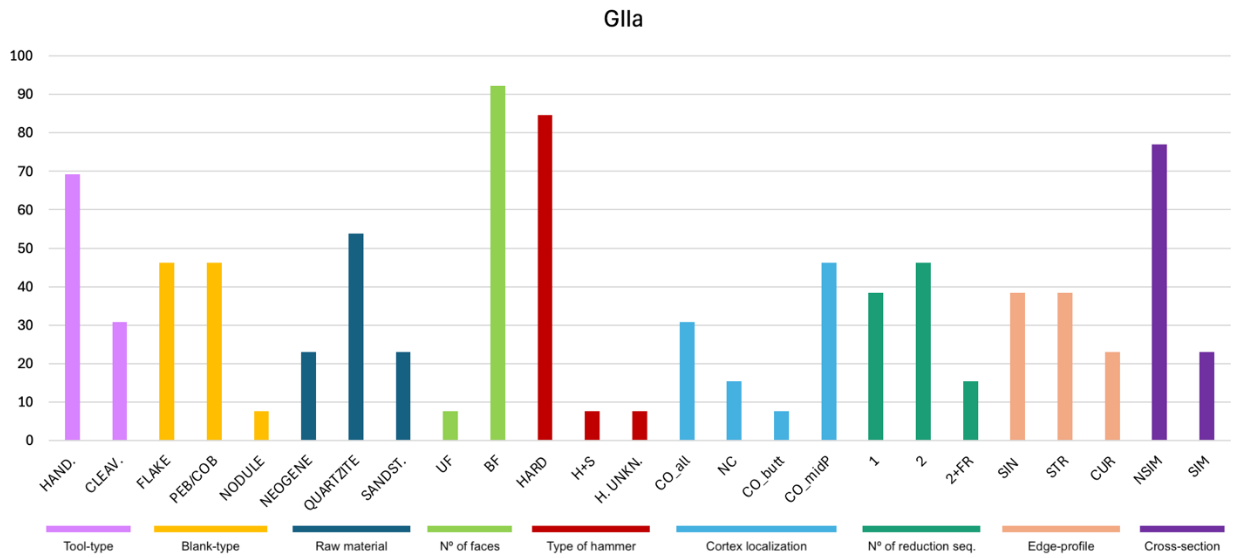

Figure 10: Histogram describing the sample of Galería-GIIa. The x-axis indicates the variables for each technological feature present in the sample, while the y-axis indicates the percentage of each variable. (HAND.: Handaxes; CLEAV.: Cleaver; PEB/COB: Pebble or Cobble; SANDST.: Sandstone; UF: Unifacial; BF Bifacial; H+S: Combined hammer; H.UNKN.: Hammer unknown; CO_all: Totally cortical; NC: Non-cortical; CO_butt: Cortex on butt; CO_midP: Cortex in the mid-proximal section; 1: One reduction sequence; 2: Two reduction sequences; 1+FR: One reduction sequence plus final retouch; 2+FR: Two reduction sequences plus final retouch; SIN: Sinuous; STR: Straight; CUR: Curved; NSIM: Asymmetrical; SIM: Symmetrical).

The mean elongation index for Galería-GIIa is 1.54, i.e. the tools from the assemblage are considered as elongated. The refinement index, instead, is below the threshold value of 2.35 (with a mean value of 2.07) thereby defining the assemblage as non-refined. However, when considering the distal refinement index of the instruments, an average value of 2.53 is obtained, indicating that the distal section of Galería-GIIa LCTs is generally refined.

1.1.1 Neogene chert

Tools made on Neogene flint, which represent 23,1% of Galería-GIIa sample, are all handaxes bifacially worked and shaped on flake (66,7%), with the exception of one single case where the blank-type is a nodule (33,3%). The only type of hammer identified is hard hammer (66,7%) but for one of the handaxes it wasn't possible to determine it and for that reason has been considered as unknown (33,3%). The amount of cortex and its location is very variable, in fact, one of the three handaxe does not present cortex at all (~33,3%), another one has cortex residuals only on the butt (~33,3%), and the last one has cortex only in the mid-section (~33,3%). The shaping activity is mainly developed in two reduction sequences (66,7%) while only one handaxe combines two sequences with final retouch (33,3%). The final products are characterized by sinuous (66,7%) or straight (33,3%) edge-profiles and the totality of the sample has an asymmetrical cross-section.

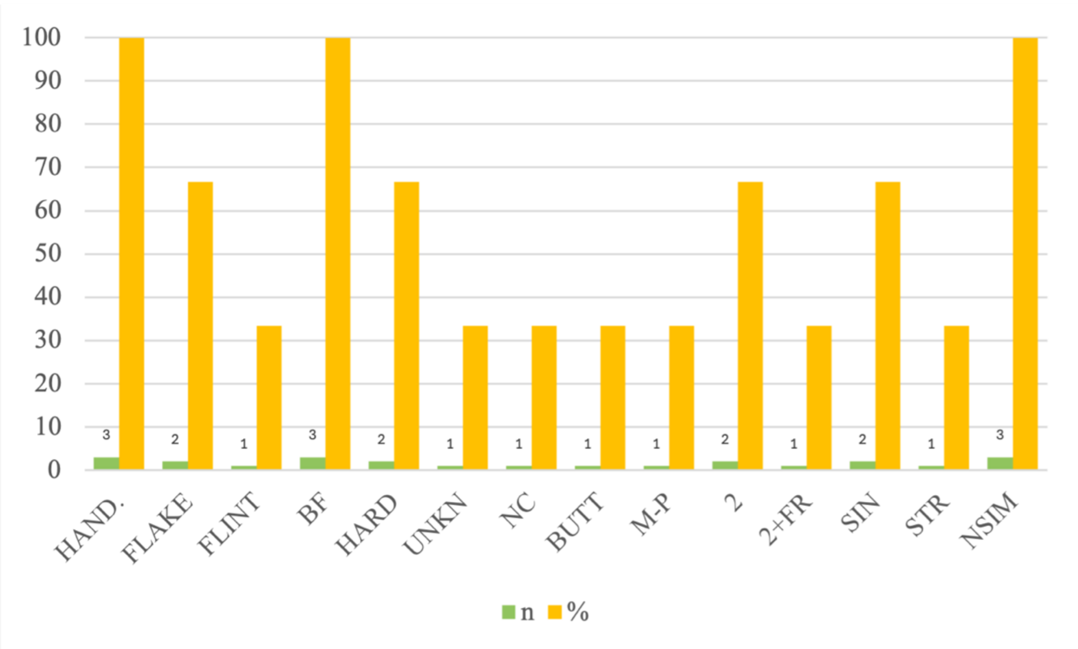

Figure 11: Histogram describing the sample of Neogene chert from Galería-GIIa. The x-axis indicates the variables for each technological feature present in the sample, while the y-axis indicates the absolute number and the percentage of each variable. (HAND.: Handaxes; COB: Cobble; BF Bifacial; H. UNKN.: Hammer unknown; NC: Non-cortical; BUTT: Cortex on butt; M-P: Cortex in the mid-proximal section; 2: Two reduction sequences; 2+FR: Two reduction sequences plus final retouch; SIN: Sinuous; STR: Straight; NSIM: Asymmetrical).

1.1.2 Quartzite

Tools made on quartzite, that represent 53,8% of Galería-GIIa sample, are handaxes (42,9%) and cleavers (57,1%). Two types of blanks have been attested with a quite equal significance: flake (57,1%) and pebble (42,9%). All the tools have been worked bifacially (85,7%) but one tool that has only one face shaped (14,3%). The use of hard hammer (85,7%) is prevalent, even if for one tool has been attested a combination of both hard and soft hammer (14,3%). The mid-proximal section is the most common location for cortex residues (57,1%) followed by total presence of cortex on the surface of the tool (28,6%) and total absence of cortex, which is attested only in one cleaver (14,3%). The shaping strategies most employed involve one or two reduction sequences (~42,9% each) with an exception where two reduction sequences have been combined with final retouch (14,3%). Straight (57,1%) edge-profile is the most recurrent within the sample followed by sinuous (28,6%) and one only case of curved edge (14,3%). The final products are asymmetrical (57,1%) or symmetrical (42,9%) and this duality appears to be related to the toll-type as all the symmetrical tools are cleavers.

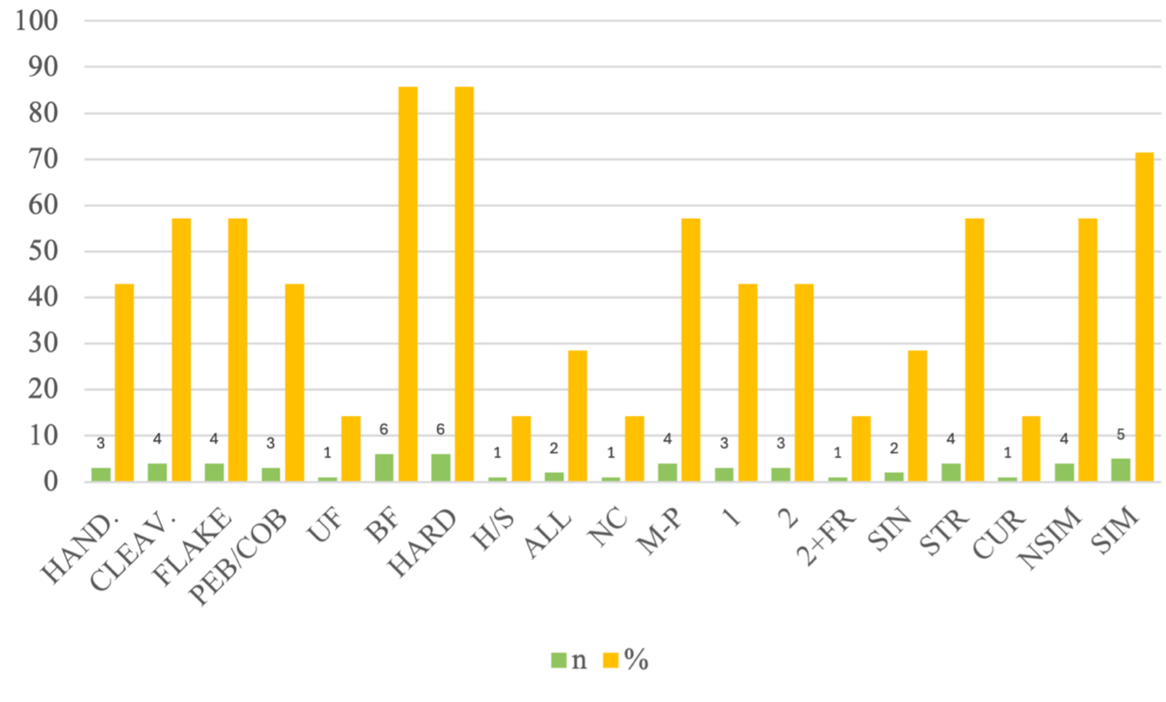

Figure 12: Histogram describing the sample of quartzite from Galería-GIIa. The x-axis indicates the variables for each technological feature present in the sample, while the y-axis indicates the absolute number and the percentage of each variable. (HAND.: Handaxes; CLEAV.: Cleaver; COB: Cobble; UF: Unifacial; BF Bifacial; H/S: Combined hammer; ALL: Totally cortical; NC: Non-cortical; M-P: Cortex in the mid-proximal section; 1: One reduction sequence; 2: Two reduction sequences; 2+FR: Two reduction sequences plus final retouch; SIN: Sinuous; STR: Straight; CUR: Curved; NSIM: Asymmetrical; SIM: Symmetrical).

1.1.3 Sandstone

Tools made on sandstone, which represent 23,1% of Galería-GIIa sample, are all handaxes bifacially worked and made on pebble by using hard hammer. All the tools are totally cortical (66,7%) but one preserves cortex only in the mid-section of the tool (33,3%). For exception of one only handaxe realized through two reduction sequences (33,3%), the preferred shaping strategy consists of a single reduction sequence without any final retouching (66,7%). The most common edge-profile is curved (66,7%) but also one handaxe with sinuous edge is present in the sample (33,3%). All the final products have an asymmetrical cross-section.

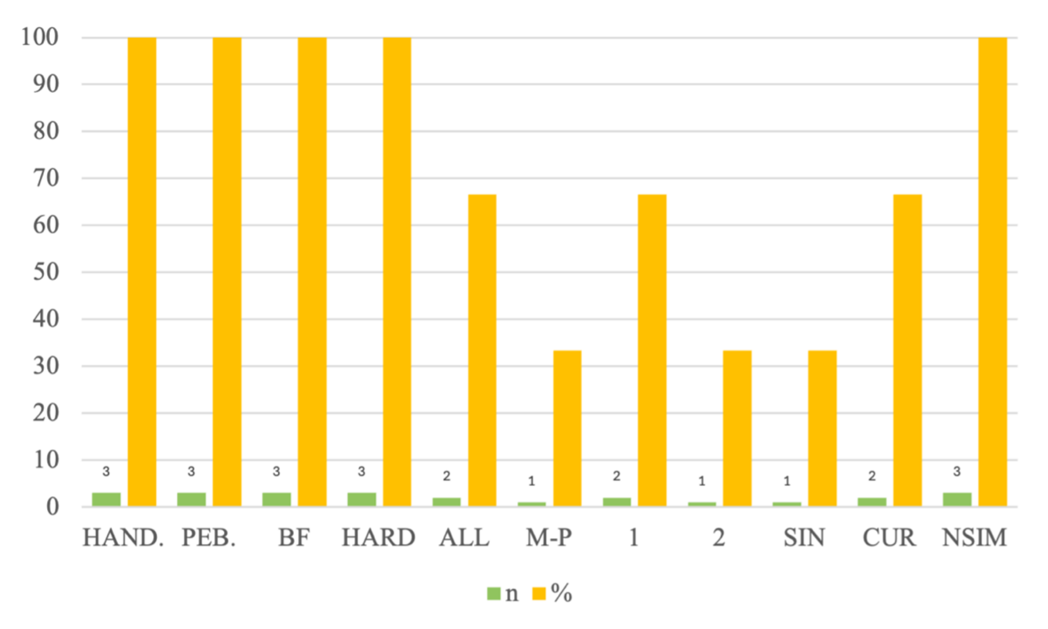

Figure 13: Histogram describing the sample of sandstone from Galería-GIIa. The x-axis indicates the variables for each technological feature present in the sample, while the y-axis indicates the absolute number and the percentage of each variable. (HAND.: Handaxes; COB: Cobble; BF Bifacial; ALL: Totally cortical; M-P: Cortex in the mid-proximal section; 1: One reduction sequence; 2: Two reduction sequences; SIN: Sinuous; CUR: Curved; NSIM: Asymmetrical).

1.2 Guado San Nicola – US c

The sample from Guado San Nicola-USc is composed only by handaxes bifacially worked that have been shaped on three different materials: Aphanitic flint (~61,5%), Microbrecciated flint (~26,9%), and limestone (~11,5%). Only the 61,5% of the sample allowed the identification of the starting blank, which in the same percentage corresponds to slabs, while the remaining 38,5% was defined as unknown. The preferred type of hammer is the soft organic one (~92,3%) but there is also attestation of hard hammer (3,8%) and combined use of both the latter (3,8%). The presence and localization of the cortex, when it is present, is very variable within the sample. The 34,6% of the tools don't show any trace of cortex on their surface, while the remaining 65,4% is distributed between the following location categories: totally cortical (3,8%), mid (3,8), butt (15,4%), mid-proximal (30,8%), and mid-distal (11,5%). Regarding the number of reduction sequences, the majority of the sample results from one (26,9%) or two (65,4%) sequences combined with final retouch while only handaxes have been made through only one reduction sequence without final retouch (7,7%). The edge-profile is mainly sinuous (50%) or straight (38,5%), but also curved type is attested (11,5%). The most frequent cross-section is asymmetrical (57,7%) followed by plano-convex (34,6%) and very few symmetrical tools (7,7%).

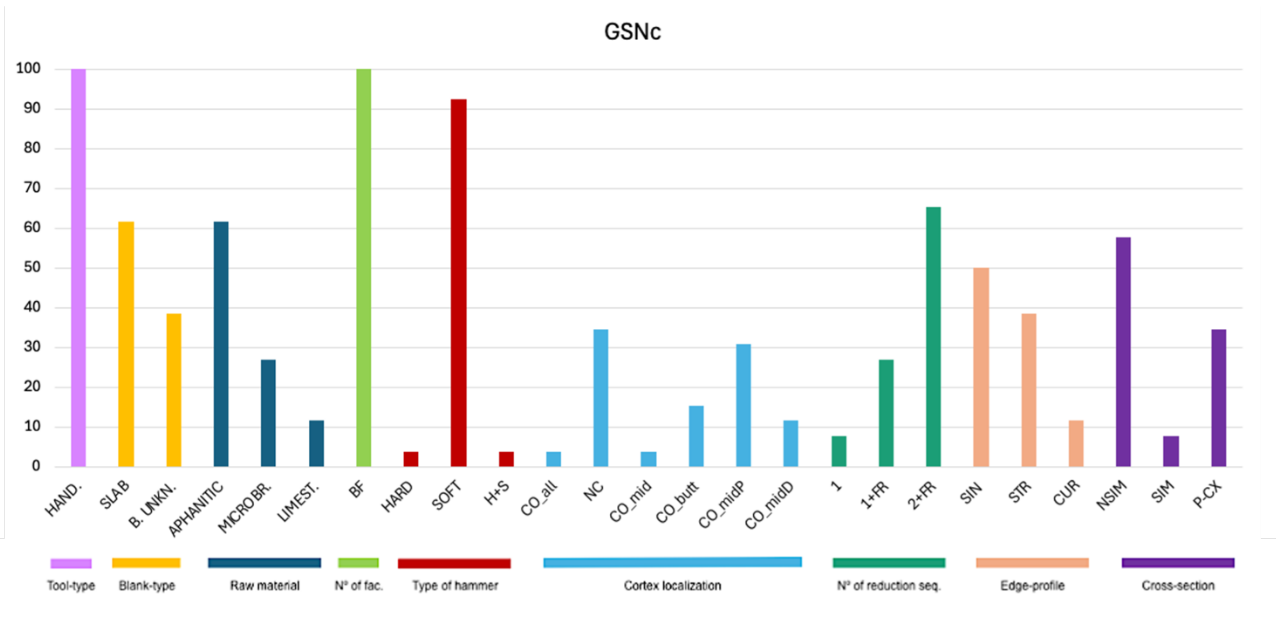

Figure 14: Histogram describing the sample of Guado San Nicola-USc. The x-axis indicates the variables for each technological feature present in the sample, while the y-axis indicates the percentage of each variable. (HAND.: Handaxes; B.UNKN.: Blank unknown; MICROBR.: Microbrecciated; LIMEST.: Limestone; BF Bifacial; H+S: Combined hammer; CO_all: Totally cortical; NC: Non-cortical; CO_mid: Cortex in the mid-section; CO_butt: Cortex on butt; CO_midP: Cortex in the mid-proximal section; CO_midD: Cortex in the mid-distal section 1: One reduction sequence; 1+FR: One reduction sequence plus final retouch; 2+FR: Two reduction sequences plus final retouch; SIN: Sinuous; STR: Straight; CUR: Curved; NSIM: Asymmetrical; SIM: Symmetrical; P-CX: Plano-convex).

The mean elongation index for Guado San Nicola-USc is equal to 1.66, so the handaxes from that assemblage are defined as elongated and are also representing the major elongation index across the whole sample studied. The refinement index, instead, has a mean value of 1.55, which is below the threshold value of 2.35, thereby defining the assemblage as non-refined. The same happens for the mean distal refinement index of Guado San Nicola-USc as the mean value is equal to 1.62 and it does not state any refinement in the distal part of the tools.

1.2.1 Aphanitic flint

Tools made on Aphanitic flint, that represent ~61,5% of Guado San Nicola-USc sample, are handaxes bifacially worked. The 50% of the tools have been realized on slabs while the remaining 50% didn't allow the identification of the starting support. The preferred hammer is the soft organic one (87,5%), while hard hammer and combined use of both are less attested (~6,2% each) due to the intense shaping activity that, most probably, erased the traces of hard hammer use. The 31,3% of the sample do not have any cortex residuals, while the remaining 68,7% is distributed between the following location categories: mid-proximal (37,5%), mid-distal (~12,5%), butt (~12,5%), and mid (~6,2%). The preferred shaping strategy consists of one (~18,8%) or two (75%) reduction sequences combined with final retouch, while only one handaxe has been shaped through one only sequence without final retouch (~6,2%). The most frequent edge-profile is sinuous (50%) followed by straight (37,5%) and curved (12,5%), while the cross-section is mainly asymmetrical (62,5%) or plano-convex (~31,3%).

1.2.2 Microbrecciated flint

Tools made on Microbrecciated flint, that represent ~26,9% of Guado San Nicola-USc sample, are handaxes bifacially worked with soft organic hammer. The 14,3% of the tools composing the sample are totally cortical, the ~28,6% do not preserve cortex, and the remaining ~57,1% is distributed between cortex on the butt and cortex in the mid-section of the tool (~28,6 each). The majority of the handaxes from this sample are the result two reduction sequences plus final retouch (57,1%) while only two handaxes have been shaped through one sequence combined with final retouch (28,6%) and only one through one sequence without any final retouch (14,3%). The most common edge-profile is the sinuous one (57,1%) followed by the straight one (28,6%) and the curved one (14,3%). Asymmetrical cross-edge is the most frequent, but also plano-convex (28,6%) and symmetrical (14,3%) are attested.

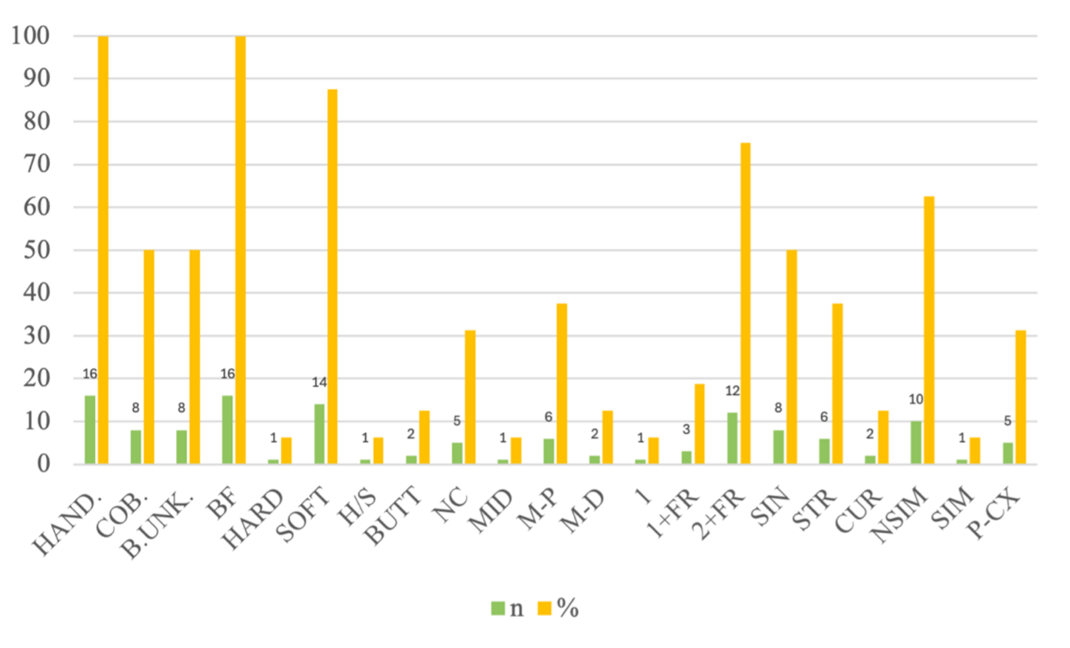

Figure 15: Histogram describing the sample of aphanitic flint from Guado San Nicola-USc. The x-axis indicates the variables for each technological feature present in the sample, while the y-axis indicates the percentage of each variable. (HAND.: Handaxes; B.UNKN.: Blank unknown; BF Bifacial; H/S: Combined hammer; NC: Non-cortical; MID: Cortex in the mid-section; BUTT: Cortex on butt; M-P: Cortex in the mid-proximal section; M-D: Cortex in the mid-distal section 1: One reduction sequence; 1+FR: One reduction sequence plus final retouch; 2+FR: Two reduction sequences plus final retouch; SIN: Sinuous; STR: Straight; CUR: Curved; NSIM: Asymmetrical; SIM: Symmetrical; P-CX: Plano-convex).

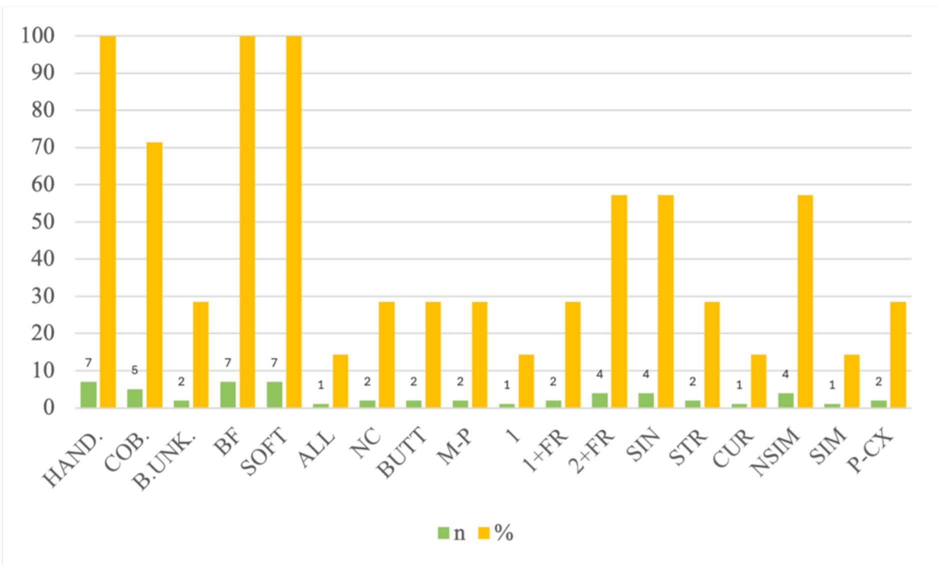

Figure 16: Histogram describing the sample of microbrecciated flint from Guado San Nicola-USc. The x-axis indicates the variables for each technological feature present in the sample, while the y-axis indicates the percentage of each variable. (HAND.: Handaxes; COB.: Cobble; BF Bifacial; ALL: Totally cortical; NC: Non-cortical; BUTT: Cortex on butt; M-P: Cortex in the mid-proximal section; 1: One reduction sequence; 1+FR: One reduction sequence plus final retouch; 2+FR: Two reduction sequences plus final retouch; SIN: Sinuous; STR: Straight; CUR: Curved; NSIM: Asymmetrical; SIM: Symmetrical; P-CX: Plano-convex).

1.2.3 Limestone

Tools made on limestone, that represent ~11,5% of Guado San Nicola-USc sample, are handaxes bifacially worked on slab by using soft organic hammer. Most of the tools from that sample do not present any trace of cortex (66,7%) and only 33,3% has cortex in the mid-distal section. The preferred shaping strategy involve one reduction sequence combined with final retouch (66,7%), but also two reduction sequences plus final retouch has been identified (33,3%). The edge-profile is straight (66,7%) or sinuous (33,3%) and the final products have plano-convex (66,7%) or asymmetrical (33,3%) cross-section.

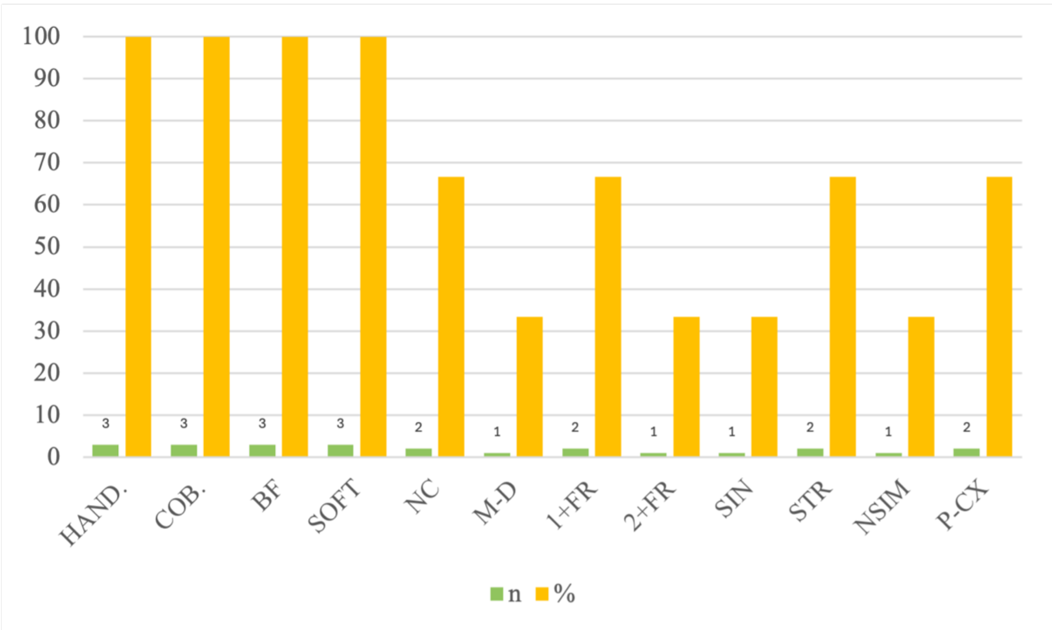

Figure 17: Histogram describing the sample of limestone from Guado San Nicola-USc. The x-axis indicates the variables for each technological feature present in the sample, while the y-axis indicates the percentage of each variable. (HAND.: Handaxes; COB.: Cobble; BF Bifacial; NC: Non-cortical; CO_mid: Cortex in the mid-section; 1+FR: One reduction sequence plus final retouch; 2+FR: Two reduction sequences plus final retouch; SIN: Sinuous; STR: Straight; NSIM: Asymmetrical; P-CX: Plano-convex).

1.3 La Noira – *stratum* c

The sample from La Noira-*stratum* c, is composed only by handaxes but one chopping-tool. These large shaped tools, all bifacially worked, have been realized on three different types of flint: Millstone (74%), Cretaceous flint (8%), and "Chaille" Jurassic flint (18%). The blank-type is quite variable. The majority if the items within this assemblage are made on slabs (23,7%) or have been modified too much to identify the original support. Tools on flake are well represented (24,5%), while those on cobble (10,2%) and nodule (2%) are very few. Soft organic hammer is the preferred type of hammer (85,7%), but also hard hammer (4,1%) and a combination of both the latter types (10,2%) are attested. The 20,4% of the sample is totally devoid of cortex and the remaining tools present cortex mainly localized in the mid-proximal (62%). Shaping strategies consisting of one or two reduction sequences are few represented with respectively a percentage of 6% and 5%. On the contrary, one or two reduction sequences combined with final retouches (respectively 36% and 46%) are more frequent. The large shaped tools from the sample present sinuous (44%), straight (34%), and curved (22%) edge-profile; while the cross-sections are mainly asymmetrical (48%) or symmetrical (34%) with a good percentage of plano-convex final products (18%).

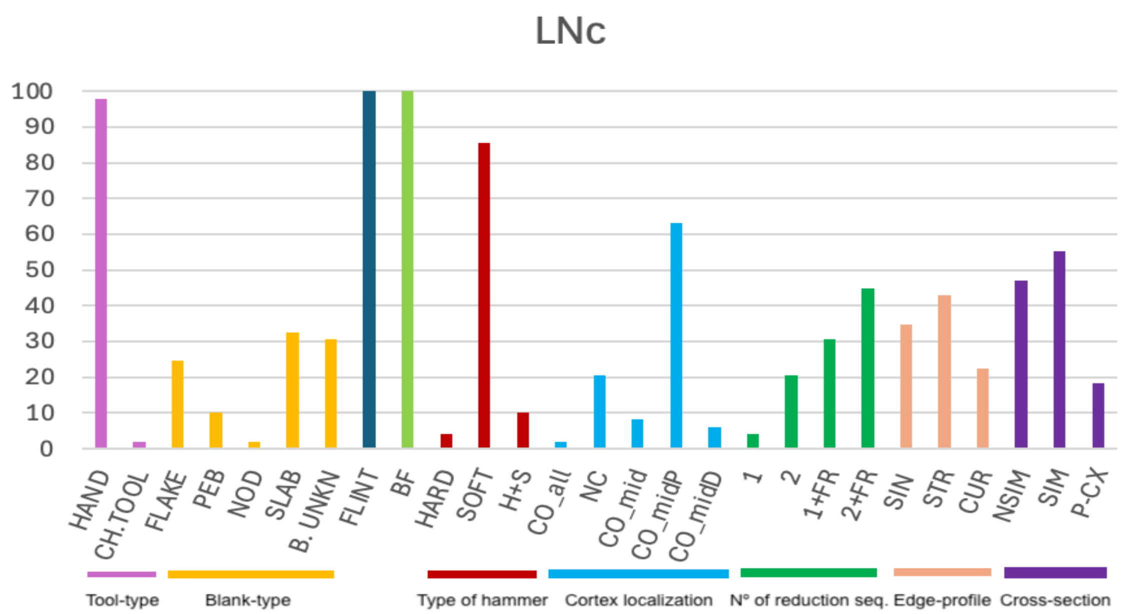

Figure 18: Histogram describing the sample of La Noira-*stratum* c. The x-axis indicates the variables for each technological feature present in the sample, while the y-axis indicates the percentage of each variable. (HAND: Handaxe; CH.TOOL: Chopping-tool; PEB: Pebble; NOD: Nodule; B.UNKN: Unknown blank; BF: Bifacial; H+S: Combined hammer; CO_all: Totally cortical; NC: Non-cortical; CO_mid: Cortex in the mid-section; CO_midP: Cortex in the mid-proximal section; CO_midD: Cortex in the mid-distal section; 1: One reduction sequence; 2: Two reduction sequences; 1+FR: One reduction sequence plus final retouch; 2+FR: Two reduction sequences plus final retouch; SIN: Sinuous; STR: Straight; CUR: Curved; NSIM: Asymmetrical; SIM: Symmetrical; P-CX: Plano-convex)

The mean elongation index for La Noira-*stratum* c is equal to 1.56, i.e. the tools from the assemblage are considered as elongated. By contrast, the mean value for refinement index is 1.97, which is below the threshold of 2.35, and it defines the assemblage as non-refined. However, when considering the distal refinement index of the instruments, the resulting value is equal to 2.57, indicating that the distal section of La Noira-*stratum* c tools is not only generally refined but also represent the major distal refinement across the whole sample studied.

1.3.1 Millstone

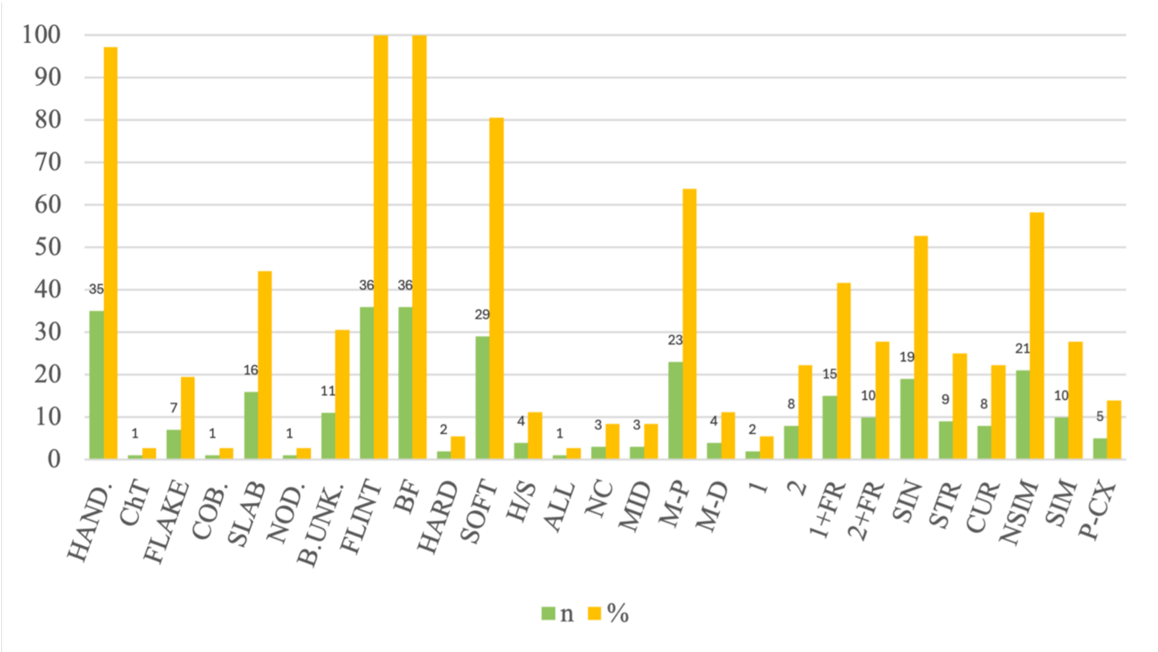

Figure 19: Histogram describing the sample of millstone flint from La Noira-*stratum* c. The x-axis indicates the variables for each technological feature present in the sample, while the y-axis indicates the percentage of each variable. (HAND.: Handaxe; ChT: Chopping-tool; COB.: Cobble; NOD.: Nodule; B. UNKN.: Unknown blank; BF: Bifacial; H/S: Combined hammer; ALL: Totally cortical; NC: Non-cortical; MID: Cortex in the mid-section; M-P: Cortex in the mid-proximal section; M-D: Cortex in the mid-distal section; 1: One reduction sequence; 2: Two reduction sequences; 1+FR: One reduction sequence plus final retouch; 2+FR: Two reduction sequences plus final retouch; SIN: Sinuous; STR: Straight; CUR: Curved; NSIM: Asymmetrical; SIM: Symmetrical; P-CX: Plano-convex).

Tools made on millstone, which represent ~74% of La Noira-*stratum* c sample, are all handaxes (%) but one only chopping-tool (2%). The sample is composed by handaxes and one chopping-tool bifacially worked on flint, most commonly by using soft organic hammer (~80%). For the 30,6% of the large shaped tools made on millstone it was not possible to identify the type of blank due to the intense shaping activity, while for the remaining 69,4% a high variability can be noticed. In fact, the preferred blank-type is the slab (~44,4%) followed by the flake (19,4%), while cobbles and nodules of flint have been used just in two cases (one cobble and one flint nodule). A strong use of soft organic hammer (~80%) can be noticed, but also the combined use of both hard and soft hammer (11,1%) and the use of only hard percussor (~5,6%) are attested. The cortex is totally absent in the 8,3% of the sample while only one instrument is completely cortical. The remaining ~89% of tools mainly preserve cortex in the mid-proximal (63,9%), but also in the mid-distal (11,1%), and mid section (8,3%) of the final product. Also, the reduction strategies are quite variate; a major part of the sample is the result of one reduction sequence combined with final retouch (~41,7%) but also two (~22,2%) or just one (~5,6%) sequences without any final retouch and two sequences plus final retouch (~27,8%) have been identified. The edge-profile mainly represented in the assemblage is the sinuous one (52,8%), followed by straight edges (25%) and curved ones (22,2%) with lower values. The final products are mainly asymmetrical (~58,3%) and in few cases symmetrical (~27,8%) or plano-convex (~13,9%).

1.3.2 Cretaceous flint

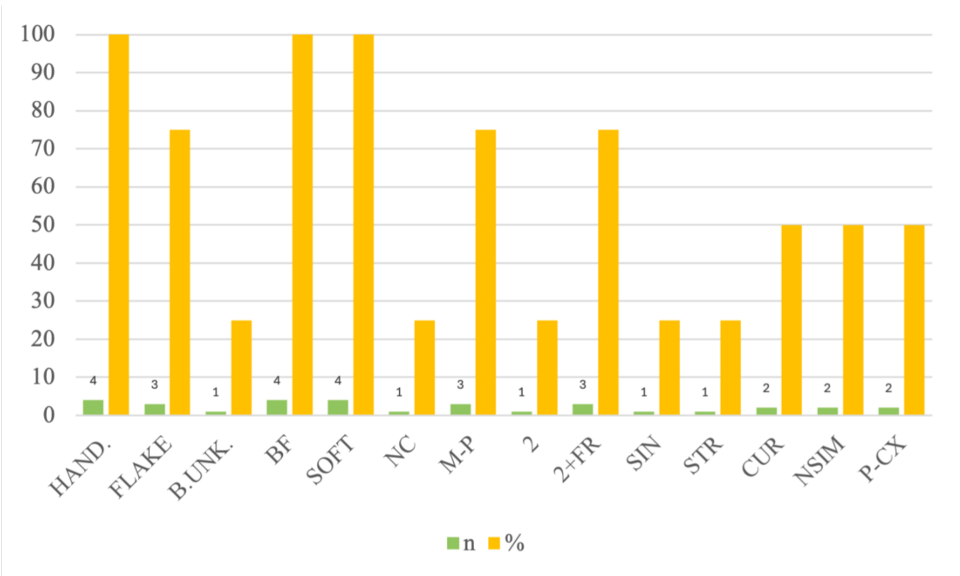

Figure 20: Histogram describing the sample of cretaceous flint from La Noira-*stratum* c. The x-axis indicates the variables for each technological feature present in the sample, while the y-axis indicates the percentage of each variable.(HAND.: Handaxe; B. UNKN.: Unknown blank; BF: Bifacial; NC: Non-cortical; M-P: Cortex in the mid-proximal section; 2: Two reduction sequences; 2+FR: Two reduction sequences plus final retouch; SIN: Sinuous; STR: Straight; CUR: Curved; SIM: Symmetrical; P-CX: Plano-convex).

Tools made on Cretaceous flint, which represent ~8% of La Noira-*stratum* c sample, are handaxes bifacially worked by using soft organic hammer. For the 25% of the sample it was not possible to identify the blank-type, while the remaining 75% is made on flake. The cortex, present in the 75% of the handaxes on Cretaceous flint, is located in the mid-proximal section. The final products are the result of two reduction sequences (25%), most of the time combined with final retouch (75%). The most frequent edge-profile is the curved one (50%), but also sinuous (25%) and straight (25%) types are well attested. The cross-section is symmetrical (50%) or plano-convex (50%).

1.3.3 "Chaille" Jurassic flint

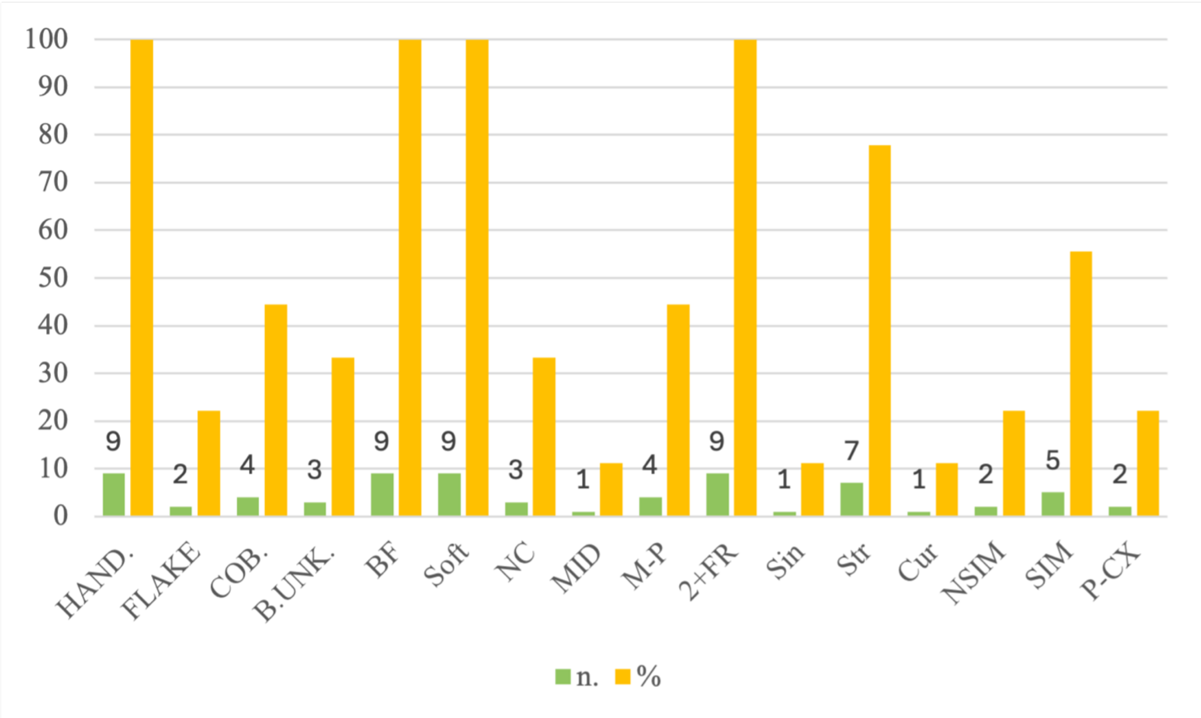

Figure 21: Histogram describing the sample of "Chaille" Jurassic flint from La Noira-*stratum* c. The x-axis indicates the variables for each technological feature present in the sample, while the y-axis indicates the percentage of each variable.(HAND.: Handaxe; COB,: Cobble; B. UNKN.: Unknown blank; BF: Bifacial; NC: Non-cortical; MID: Cortex in the mid section M-P: Cortex in the mid-proximal section; 2+FR: Two reduction sequences plus final retouch; SIN: Sinuous; STR: Straight; CUR: Curved; NSIM: Non-symmetrical; SIM: Symmetrical; P-CX: Plano-convex).

Tools made on "Chaille" Jurassic flint, that represent ~18% of La Noira-*stratum* c sample, are handaxes bifacially worked by using soft organic hammer and obtained as the result of two reduction sequences combined with final retouch. For the ~33,3% of the sample it was not possible to identify the blank-type, while the remaining ~67,7% is made on flake (~22,2%) or cobble

(~44,4%). The most common localization for the cortex is the mid-proximal section (~44,4%), only one handaxe has cortex in the mid-section (11,1%), and the remaining ~33,3% do not have any trace of cortex. The straight edge-profile (77,8%) is the most frequent, while sinuous (11,1%) and curved (11,1%) have been noticed only in one tool each. The final products are mainly symmetrical (55,6%) as the asymmetrical and plano-convex ones are only the 22,2% each.

1.4 Scars Density Index (SDI)

The Scars Density Index is a value representing the number of negatives present in 1 in^2 of item surface area which can be a hint of shaping intensity. Within the context of this study, it has been calculated by dividing the number (no.) of total negatives per the total surface area (in^2) of the tools. Galería-GIIa is the assemblage that includes the tools with the highest number of detachments, followed by La Noira-*stratum* c, and finally Guado San Nicola-USc that is shows the lowest mean number of detachments. Similarly, Guado San Nicola shows smaller surface areas than the ones of Galería and La Noira, which is a data coherent with those obtained by linear measurements. The mean Scars Density Index (SDI), consequently, suggest a more intense shaping activity for the large shaped tools of Galería-GIIa (~0,005) and La Noira-*stratum* c (~0,004) while Guado San Nicola-USc has a lower density suggested by an SDI equal to ~0,007.

	n. scars	**surface area (in^2)**	**SDI**
GIIa	24	5432,51	0,0051
GSN	18	2870,36	0,0071
LN	20,8	5627,69	0,0043

Table 9: Comparison between mean number of scars, mean surface area and mean Scar Density Index for each of the three sites.

The ANOVA test to verify the relationship between the number of scars and volume gives the values shown in Table 10. According to these results, Guado San Nicola-USc has the highest level of scar intensity based on the volume/SDI ratio.

	n.	Sars | n. (mean)	Volume | mm^2 (mean)	SDI (mean)	F	p-value
GIIa	13	24	106735,7	0,0051	29,99	<0.01
GSN-Usc	26	18	48713,7	0,0071	50,23	<0.01
LN-stratum c	49	20,7755102	110.502	0,0043	69,72	<0.01

Table 10: Relationships between volume and scar density index (SDI) values based on ANOVA analysis applied for each site.

1.4 Multivariate Analysis

Principal Component Analysis applied on groups ordered according to the raw material gave as result the scatter slot depicted in Figure 22. In the scatter plot, PC1 explains 49% of the variance while PC2 explains more than the 21%. Thereby, the PCA can explain more than 70% of the variance of the sample. More than the 99% of the variance is explained by the first eight PCs (Tab.11).

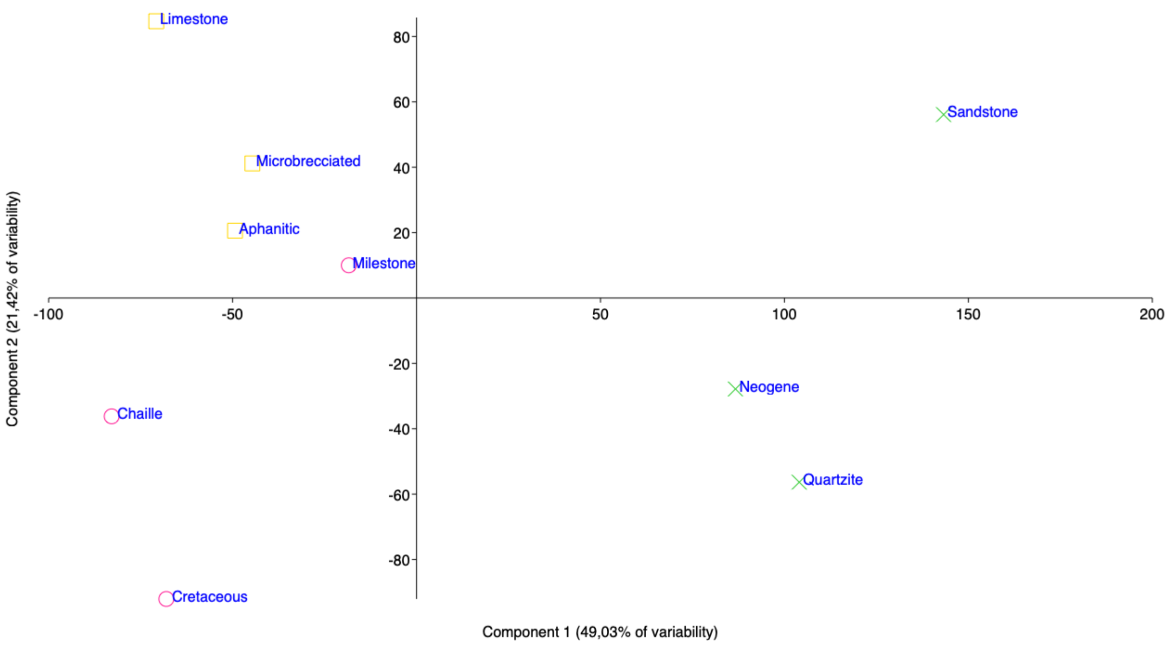

Figure 22: PCA with all the technological features considered according to the different raw materials (Sandstone, Limestone, Microbrecciated flint, Aphanitic flint, Millstone, Neogene chert, Quartzite, Chaille flint, and Cretaceous flint). Yellow squares are indicating raw materials from Guado San Nicola-USc, pink circles are indicating raw materials from La Noira-*stratum* c, and green crosses are indicating raw materials from Galería-GIIa.

PC	Eigenvalue	% variance	Cumulative %
1	7515,6	49,031	**49,031**
2	3283,54	21,421	**70,452**
3	1575,29	10,277	**80,729**
4	1342,56	8,7587	**89,4877**
5	738,124	4,8154	**94,3031**
6	571,165	3,7262	**98,0293**
7	184,514	1,2037	**99,233**
8	117,485	0,76646	**99,99946**

Table 11: Eigenvalue, percentage of variance, and cumulative percentage of variance of the eight PCs.

PC1 describes the variation from more intensive shaping, characterized by final retouching carried out with soft organic hammer, low presence of cortex and symmetrical or plano-convex cross-sections (negative values), to shorter shaping realized with a hard hammer and characterized by a higher presence of cortex and asymmetrical final products (positive values). (Fig.23-24). According to the loadings of PC1, the groups with positive values (sandstone, neogene chert, and quartzite) are mainly characterized by the use of hard hammer during the knapping activity, which mostly involved one or two removal sequences without a final retouch and resulting in final products with asymmetrical plano-convex cross-sections. Variables with less influence that mainly characterize the same groups are: cleaver as type-tool variable, flake or cobble as blank-type, presence of cortex all over the tool, and sinuous edge profile. The groups with negative values (limestone, microbrecciated flint, aphanitic flint, millstone, "Chaille" flint, and cretaceous flint) are mainly characterized by the use of organic soft hammer during the knapping activity, which mostly involved one or two removal sequences combined with final retouch and resulting in final products with symmetrical or, more often, plano-convex cross-sections. Variables with less influence that mainly characterize the same groups are: handaxe as type-tool variable, unknown blank, absence of cortex, and straight edge profile.

PC22 shows the variation from tools on cobbles that have been shaped during one only reduction sequence plus final retouch and presenting asymmetrical or plano-convex cross-section (positive values), to tools on flake, shaped through two reduction sequences plus final retouch and showing more symmetrical cross-sections.(Fig.23-24). According to the loadings of PC2, the groups with positive values (sandstone, limestone, microbrecciated flint, aphanitic flint, and millstone) are mainly characterized by cobbles as blank, which were worked through one removal series which was often combined with final retouch. The final products have mainly asymmetrical or plano-convex cross-sections. Variables with less influence that mainly characterize the same groups are: handaxe as type-tool variable, use of soft organic hammer, presence of cortex all over the tool, in the mid-distal section or not present at all, and sinuous edge profile. The groups with negative values (neogene chert, quartzite, “chaille” flint and cretaceous flint) are mainly characterized by flakes as blank or unknown blanks, which were worked through two removal series which were often combined with final retouch. The final products have symmetrical cross-sections and with presence of cortex in the mid-proximal section of the tool. Variables with less influence that mainly characterize the same groups are: cleaver as type-tool variable, use of hard or combined hammer when identified, and sinuous edge profile.

The Kruskal-Wallis test for equal medians applied on the PCA results for raw materials established that there are no significant differences between the medians of the groups, as the p-value is higher than 0.05 and the same happens for the results obtained for archaeological site. The Mann-Whitney U test has been realized to verify if the pairwise groups show statistically significant differences between them. According to the results of the test (Tab. 12-13) we conclude that no statistical significance exists between any of the pairwise of groups, excluding the possibility of different distributions of data within the three groups.

	Nº of sites	**z**	**p-value**
Group 1/2	3/4	0,44721	0,65472
Group 2/3	4/2	0,44721	0,65472
Group 1/3	3/2	1,3416	0,17971

Table 12: Results of Mann-Whitney U test on PC1.

	Nº of sites	**z**	**p-value**
Group 1/2	3/4	0,44721	0,65472
Group 2/3	4/2	1,3416	0,17971
Group 1/3	3/2	0,44721	0,65472

Table 13: Results of Mann-Whitney U test on PC2.

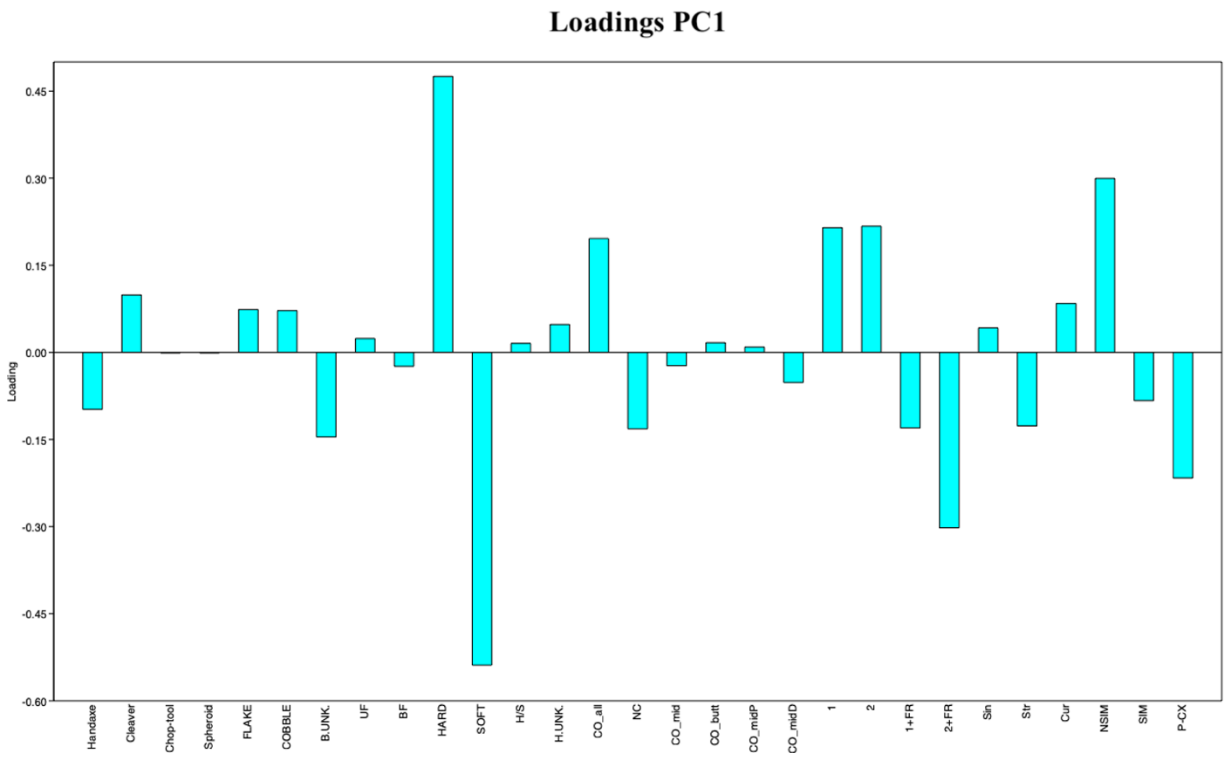

Figure 23: Loadings for PC1.

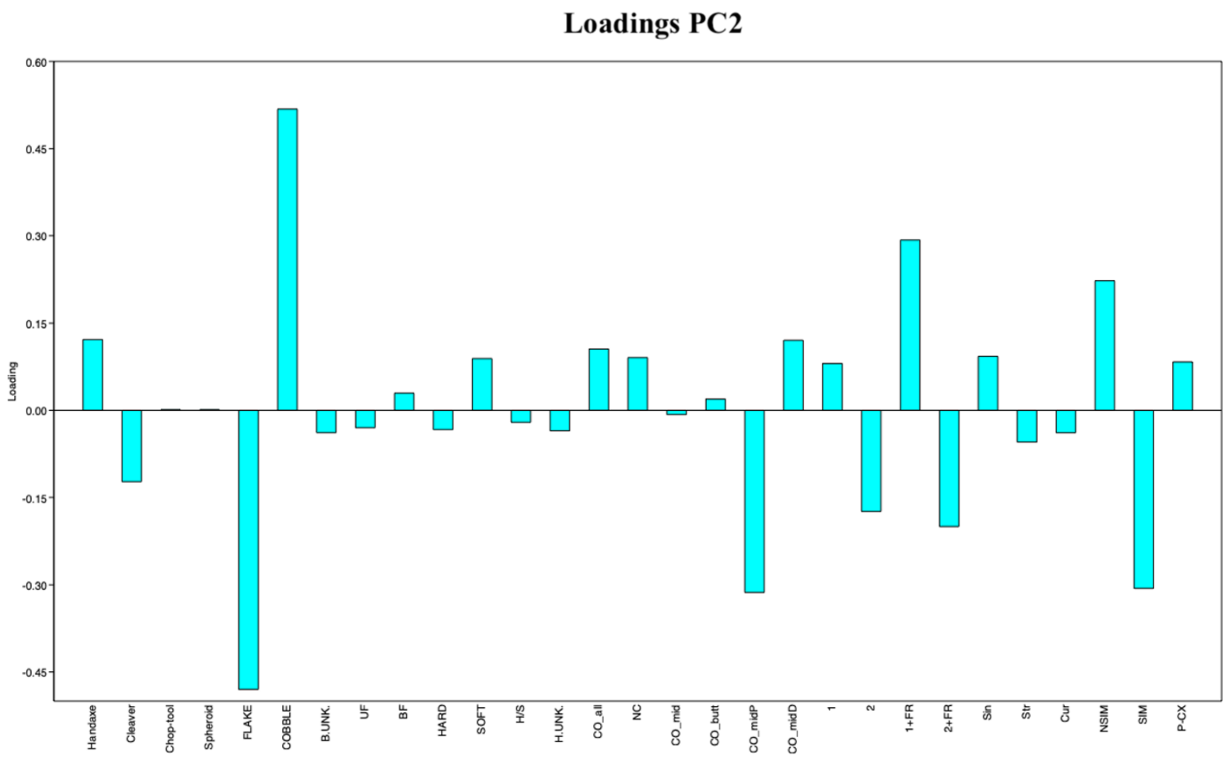

Figure 24: Loadings for PC2.

In the dendrogram showing the results of cluster analysis (Fig. 25) each color corresponds to an archaeological site: green for Galería-GIIa, pink for La Noira-*stratum* c, and orange for Guado San Nicola-USc. The dendrogram highlights the existence of two main groups. A first group is composed by Neogene chert (3 handaxes), quartzite (3 handaxes and 4 cleavers), and sandstone (3 handaxes), i.e. all the categories from Galería-GIIa. The second group includes the tools from the raw materials of Guado San Nicola-USc and La Noira-*stratum* c: aphanitic flint (16 handaxes), microbrecciated flint (7 handaxes), limestone (3 handaxes), millstone (35 handaxes and 1 chopping-tool), "Chaille" Jurassic flint (4 handaxes), and cretaceous flint (9 handaxes).

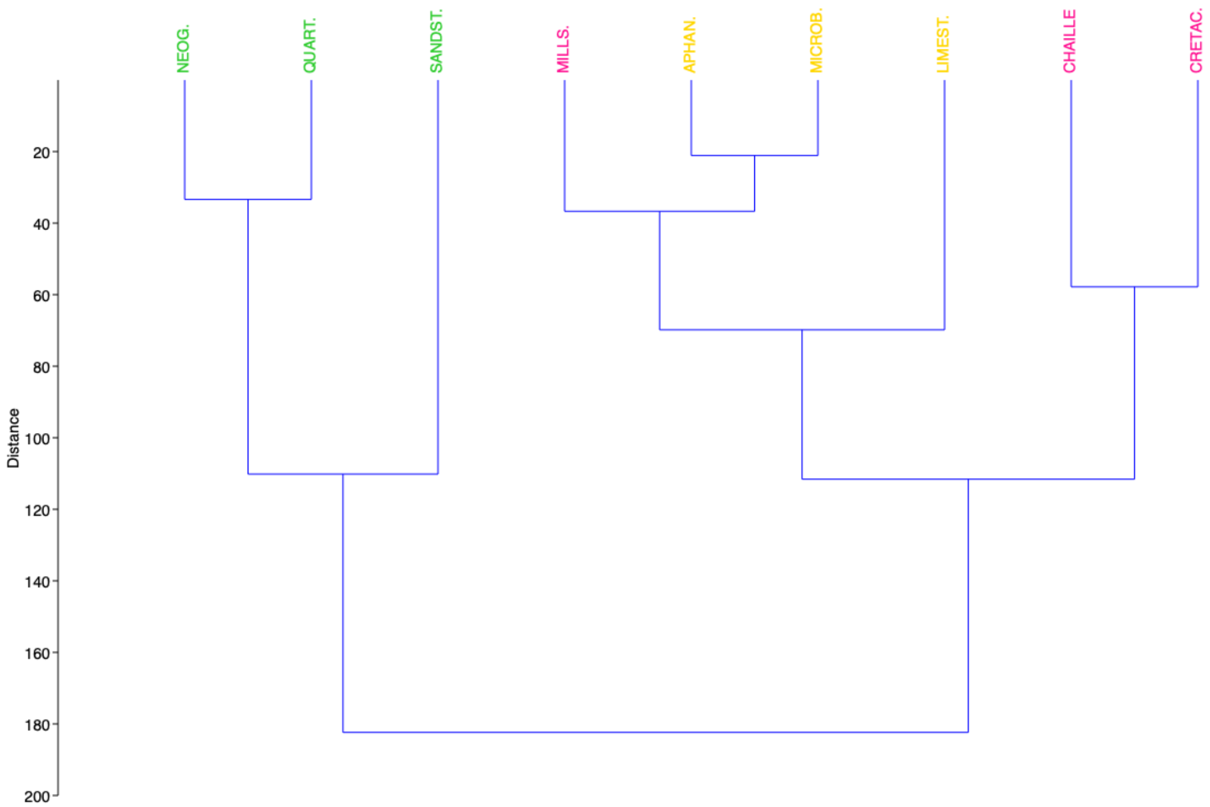

Figure 25: Dendrogram resulting from cluster analysis. The archeological site of each raw material (NEOG: Neogene chert; QUART: quartzite; SANDST: sandstone; MILLS: millstone; APHAN: aphanitic flint; MICROB: microbrecciated flint; LIMEST: limestone; CHAILLE: "Chaille" Jurassic flint; CRETAC: cretaceous flint) is indicated by the color code: green for Galería-GIIa, pink for La Noira-*stratum* c, and orange for Guado San Nicola-USc.

2. Geometric Morphometric Analysis

Geometric morphometric analysis has been used on the same sample analyzed during the technological analysis (n.88) with the aim of better understand the variation of shape and symmetry and the linkage of it with the technological features. As for the previous analysis, the whole sample has been sub-divided according to the typology of tool (handaxe, cleaver, or chopping-tool) and the raw material used. Hence, in this sub-chapter the results obtained by applying geometric morphometric analysis on Artifact GeoMorph Toolbox 3-D will be presented.

After the application of the General Procrustes Analysis (GPA) and the Principal Component Analysis (PCA), it was possible to visualize the results according to the different attributes.

Using the warp tool a model representing the mean morphology of the sample is generated and in the case of this study the model has a teardrop shape with rounded butt and curved edges. Additionally, it was possible to identify the areas more susceptible to morphometric variation. According to PC1 the mid section and the edges of the distal part are the most variable (Fig. 26a), while according to PC2 the main variations are localized on the left distal edge and on the right proximal edge (Fig.26b).

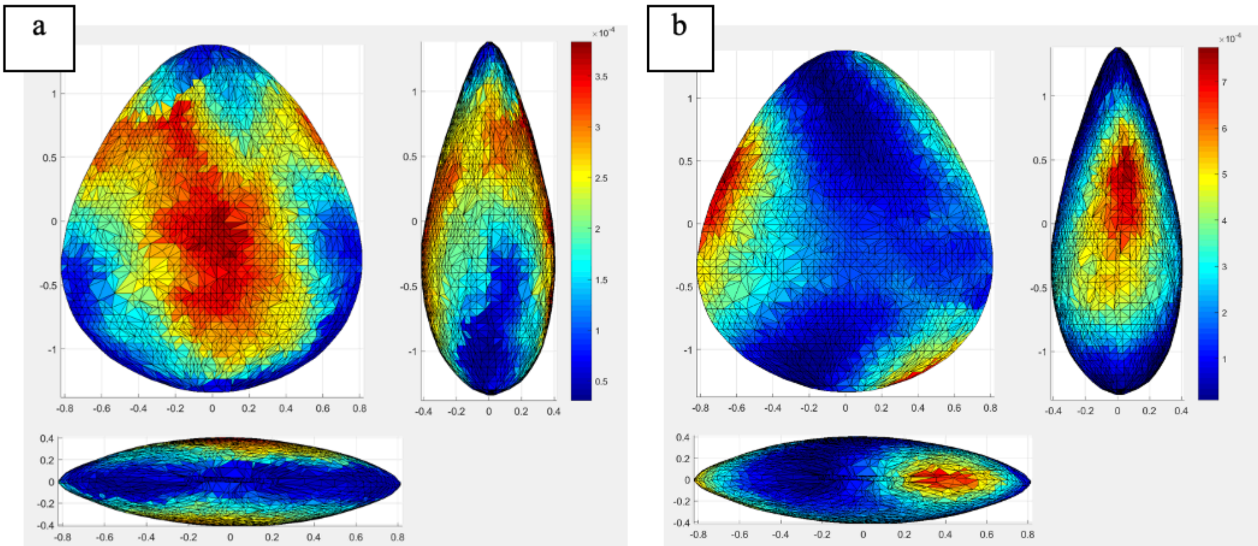

Figure 26: Warp tool showing the degree of variance in an ideal mean shape of the sample: a) Warp tool model according to PC1; b) Warp tool model according to PC2.

2.1 Geometric morphometric by tool-type

The scatterplot obtained by organizing the groups by tool-types is depicted in Figure 27. According to the plot, the cleavers and the chopping-tool are characterized by a major maximum wideness and from oval to rounded shapes. On the other hand, handaxes have very heterogeneous (Table 14) shapes as their distribution covers all the plot.

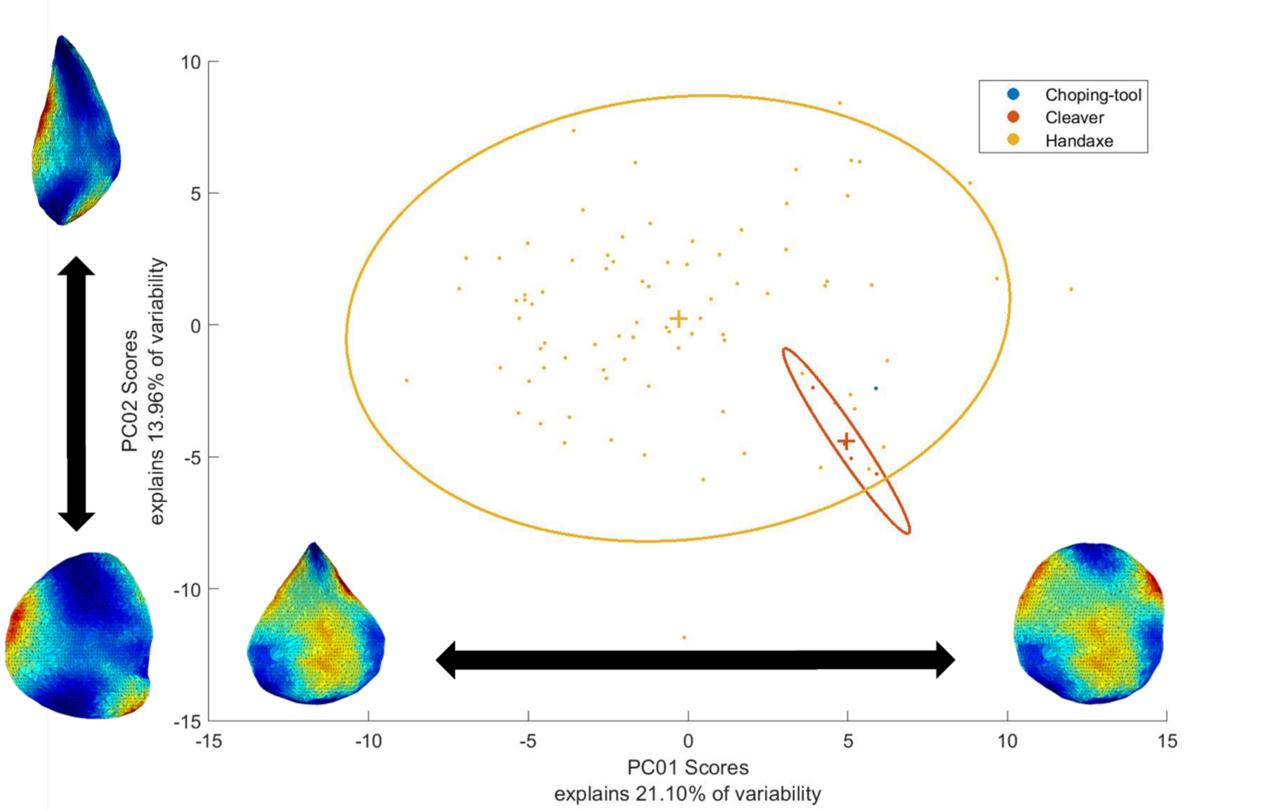

Figure 27: PC scatterplot according to tool-type.

Summary statistics applied on Attribute 2 values, which refers to the sub-division in tool-type, indicate variability, deviation from bilateral and bifacial symmetry, left and right edge curvature, left and right planform irregularity, and left and right section irregularity. As the assemblages for the chopper-tool is composed only by one item, the variability was not calculated (as non-existent), while for handaxe and cleaver, respectively composed by 83 and 4 LCTs, the software calculated a variability of ~8,97 for the first and ~6,12 for the second one. Accordingly, handaxes have a major variance than cleavers.

Group name	Items	Variability	Deviation from bilateral symmetry	Deviation from bifacial symmetry	Left edge curvature	Right edge curvature
Chopping-tool	1	0	10,85678	10,40526	1,036693	0,97073
Cleaver	4	6,118581	5,790988	4,336349	0,953093	0,841208
Handaxe	83	8,966309	7,358119	6,68443	0,87579	0,916511

Table 14: Results from summary statistic for Attribute 2.

The shape variability of handaxes and cleavers resulted significantly different by applying the Wilcoxon Rank-Sum Test as the Rank-Sum is equal to 3788 and the p-value is < 0,01.

The group with higher deviation from bilateral symmetry would be Chopping-tool (~10,41) but this data cannot be reliable as the group is composed by only one item. Consequently, Handaxe group shows a higher deviation (~7,36) than Cleaver group (~5,79). Comparable results are obtained for the deviation from bifacial symmetry Handaxe has a value equal to ~6,68 while Cleaver only reach a mean of ~4,34. Hence, handaxes appear to be more symmetrical than cleavers for both bifacial and bilateral symmetry. The deviation from a perfect 3D symmetry, neither bilateral or bifacial, is not statistically significant according to the Wilcoxon Rank-Sum Test, as the p-values are respectively equal to 0,51 and 0,72.

The edge curvature is more enhanced in Chopping-tool than Handaxe and Cleaver groups. Chopping-tool group has a value of ~1,04 for the left edge and ~0,98 for the right one. On the other side, Handaxe group has a value of ~0,88 for the left edge and ~0,92 for the right one while Cleaver group has a value of ~0,95 for the left edge curvature and ~0,84 for the right one.

According to the tool-type it was possible to define the mean shape of handaxes and cleavers (Fig.28), as well as the Euclidean distance of individual tools from it. Handaxes (n.83) have a distance from the mean shape ranging from ~5,05 and ~15,15 with a median of ~8,53 and a mean value equal to ~8,97. Furthermore, the distance range from the mean shape of cleavers (n.4) is between ~5,06 and ~7,07; the median is ~6,17 and the mean ~6,12. Verifying the statistical significance of mean shapes differences between Cleaver group and Handaxe group by applying the Wilcoxon Rank-Sum Test, it is possible to stand that the two groups are significantly different (Rank-Sum = 4870; p-value = < 0,01).

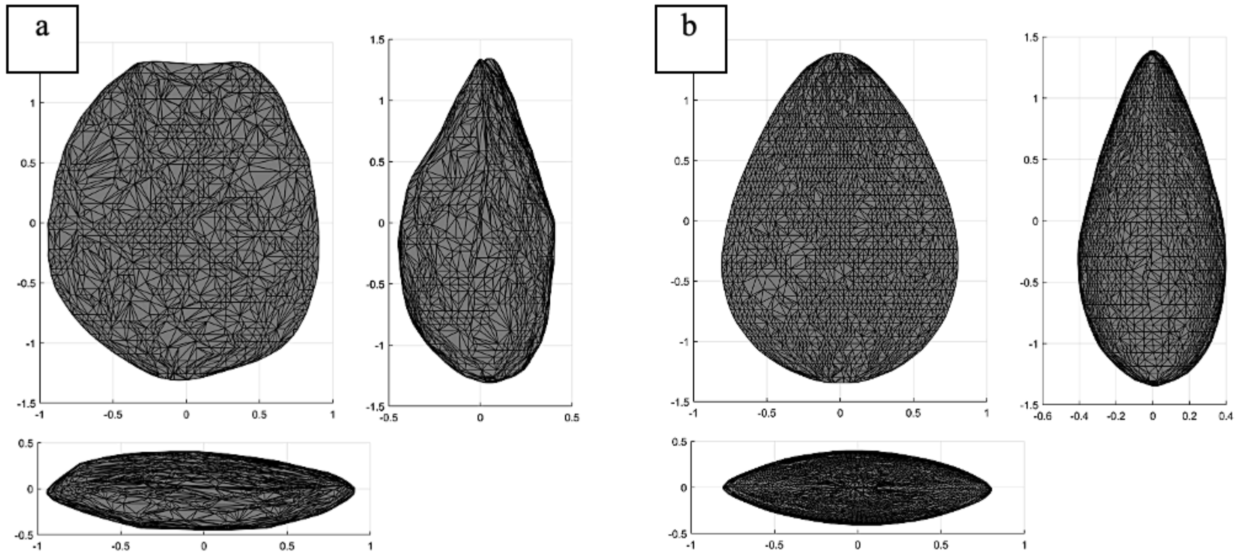

Figure 28: Mean shapes of a) cleavers and b) handaxes.

2.2 Geometric morphometric by raw material

The scatterplot obtained by organizing the groups by raw materials is depicted in Figure 29. According to the plot, LCTs from Galería-GIIa (those made on Neogene chert, quartzite and sandstone) have oval and pick-like shapes, while the ones from Guado San Nicola-USc (those made on limestone, aphanitic and microbrecciated flint) and La Noira-*stratum* c have quite variated morphologies.

Summary statistic applied on Attribute 2 values, which refers to the raw material, indicate variability, deviation from bilateral and bifacial symmetry, left and right edge curvature, left and right planform irregularity, and left and right section irregularity. For Attribute 2, the sample was organized in 9 groups according to the raw materials. Aphanitic flint (n.16) is the group with higher variability (~9,42) followed by Limestone (n.3), Microbrecciated flint (n.7), and Millstone (n.37) that have a variability between ~8,95 and ~8,46. Then, "Chaille" Jurassic flint (n.9), Cretaceous flint (n.4), Neogene chert (n.3), and Quartzite (n.7) have a variability ranging from ~7,02 to ~7,92. Sandstone (n.3) is the group with the lower variability (~6,25).

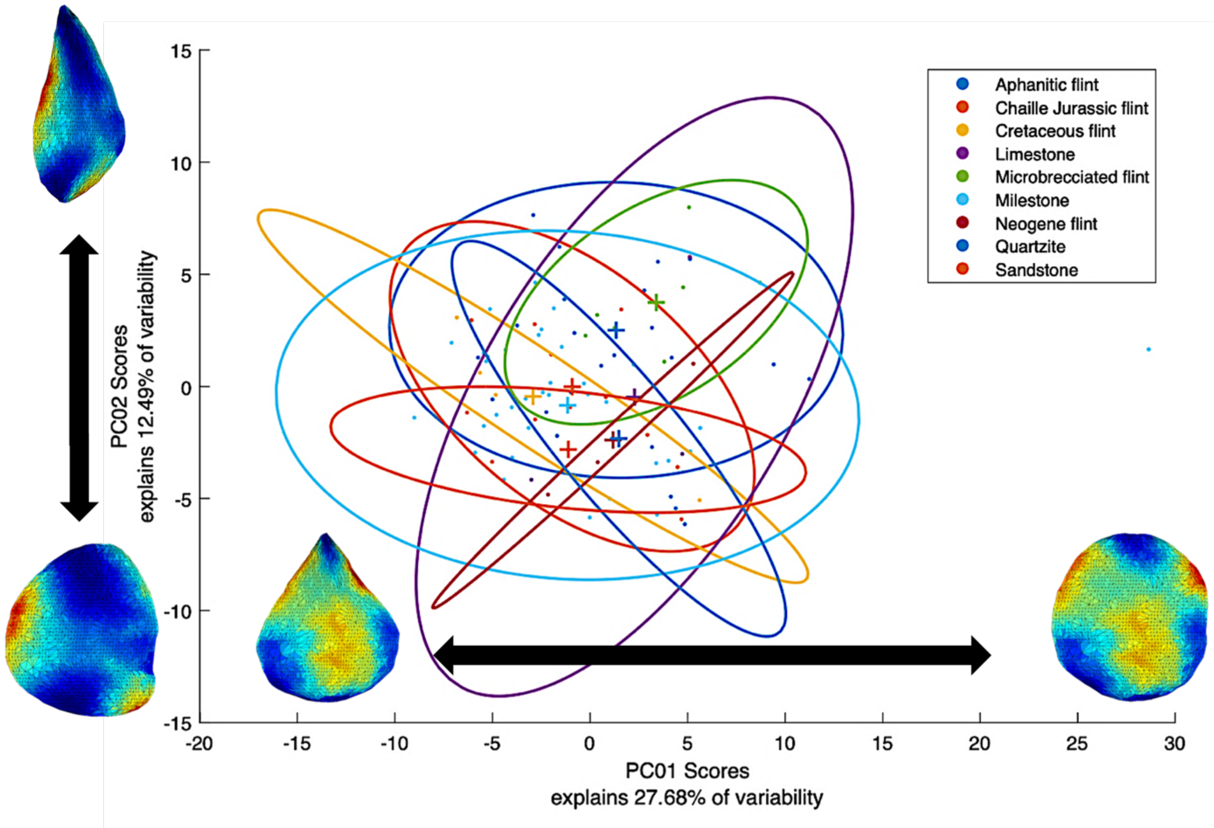

Figure 29: PC scatterplot according to raw material.

Group name	Items	Variability	Deviation from bilateral symmetry	Deviation from bifacial symmetry	Left edge curvature	Right edge curvature
Aphanitic flint	16	9,415383	5,217948	3,899835	0,979423	1,171273
Chaille Jurassic flint	9	7,915966	9,764671	11,91291	0,764448	0,892288
Cretaceous flint	4	7,859964	6,957392	5,562488	0,639597	0,722445
Limestone	3	8,464282	5,495408	3,433724	1,241912	0,846172
Microbrecciated flint	7	8,760845	4,386731	6,856765	0,846444	0,99559
Millstone	37	8,950039	9,225548	7,305799	0,865918	0,856805
Neogene chert	3	7,023275	5,057307	6,631611	1,143939	0,809396
Quartzite	7	7,776731	5,557966	5,431257	0,911681	0,79079
Sandstone	3	6,249157	3,377485	4,133867	1,000634	1,128944

Table 15: Results from summary statistic for Attribute 2.

According to the Wilcoxon Rank-Sum Test, the only shape variability difference between the groups of Attribute 2 that results statistically significant is the one between Aphanitic flint and Sandstone (Rank-Sum = 179; p-value = 0.03). All the other group distances are above the threshold of 0.05.

The groups with higher deviation from bilateral symmetry are "Chaille" Jurassic flint (~9,76) and Millstone (~9,23). Cretaceous flint has a deviation equal to ~6,96, while Quartzite, Limestone, Aphanitic, Neogene chert have values between ~5,06 and ~5,56. The groups with the lower deviation from bilateral symmetry are Microbrecciated flint (~4,39) and Sandstone (~3,38). The results of the summary statistic for the deviation from bifacial symmetry are comparable to the ones obtained from the deviation from bilateral symmetry. "Chaille" Jurassic flint has the higher value (~11,91) together with Millstone (~7,31), even if the difference between the two values is significant. Microbrecciated flint, differently from the results for bilateral symmetry, is also one of the groups with higher deviation from bifacial symmetry with a value (~6,86) very close to the one of Neogene chert (~6,63). The latter are followed by Cretaceous flint and Quartzite, which have respectively a deviation value of ~5,56 and ~5,43. The groups with lower deviation are Sandstone (~4,13), Aphanitic flint (~3,90), and Limestone (~3,43). As for Attribute 1, the deviation from both bilateral and bifacial perfect symmetry is not statistically relevant for any combination of groups.

The groups with a more enhanced left edge curvature are Limestone (~1,24), Neogene (~1,14), and Sandstone (~1,00) followed by Aphanitic flint (~0,98), Quartzite (~0,91), Millstone (~0,87), and Microbrecciated flint (~0,85). "Chaille" Jurassic flint (~0,76) and Cretaceous flint (~0,64) are the groups with the lower values for left edge curvature. Also for the right edge curvature Sandstone (~1,13) has one of the highest values together with Aphanitic flint (~1,17). Then, Microbrecciated flint, "Chaille" Jurassic flint, Millstone, Limestone, and Neogene chert have all values ranging from ~0,99 and ~0,81. Likely to the left edge curvature, Cretaceous flint (~0,72) has one of the lower values, this time together with Quartzite (~0,79).

Still based on Attribute 2, a cluster showing the distance between the raw material groups was obtained (Fig.30). As depicted in the image, sub-dividing the sample by raw materials it is not possible to distinguish groups with significant differences. Exactly for this reason, in the discussions' chapter all the comparisons will be made according to the archaeological site.

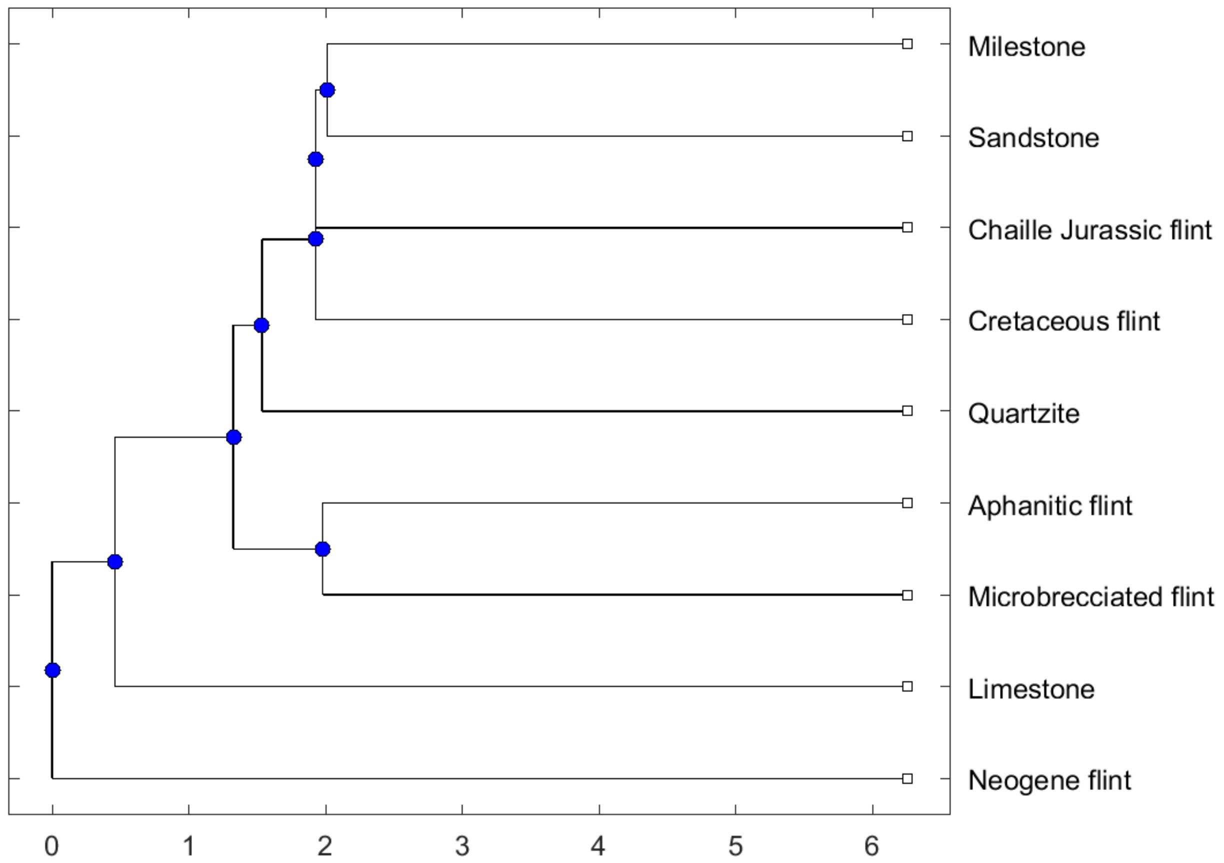

Figure 30: Cluster showing mean distances between the groups of Attribute 2.

Discussion

Once the variability of MIS11 assemblages has been explored through the type of instrument produced and the raw material used, it becomes necessary to explore the variability of these materials depending on their geographical provenance. On this regard, a PCA scatterplot obtained by organizing the tools from the sample according to the archaeological site of provenience has been realized to compare the technological features characterizing the different knapping strategies. The resulting graph is depicted in Figure 31. All the data used to realize the latter Principal Component Analysis are showed in Annex 3.

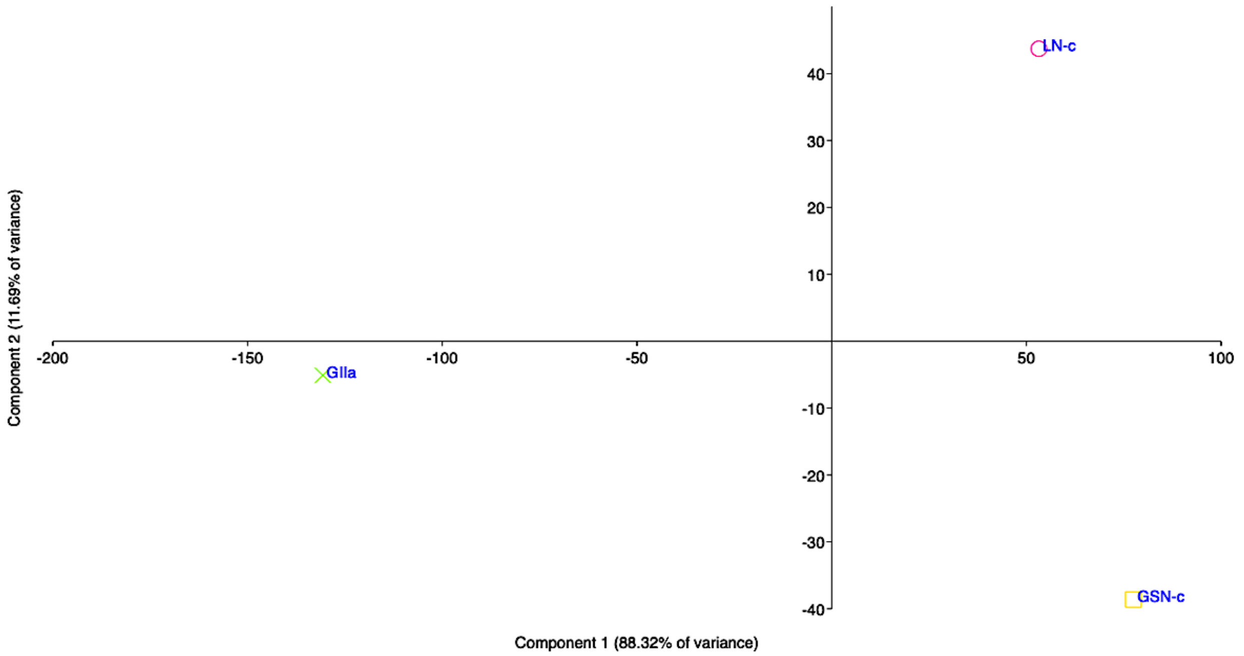

Figure 31: Scatterplot resulting from PCA applied on all technological features of each archaeological site. (GIIa = Galéria-GIIa; LN-c = La Noira-*stratum* c; GSN-c = Guado San Nicola-USc)

In the scatterplot, PC1 represents more than 88% of the variance describing a variability from shorter and more simple shaping strategies (negative values) to longer and more elaborated ones (positive values). In fact, the technological features. According to the loadings of PC1 (Fig. 32), the groups with positive values (La Noira-*stratum* and Guado San Nicola-USc) are mainly characterized by an elevated number of handaxes shaped on slabs or unknown blanks by using soft organic hammer to perform one or two reduction sequences combined with final retouch. Galería-GIIa, which is the only group located in the negative side of the axis, is characterized by a significant presence of both handaxes and cleavers mainly shaped on quartzite cobbles by using hard hammer. The biggest difference from the other two assemblages is the total absence of final retouch within the reduction process.

On the other hand, PC2 represents ~ 11.7% of the variance describing a variability from more standardized features (positive values) to more variable features (negative values). According to PC2 (Fig.33), the only group with positive value is La Noira-*stratum* c which is characterized by very standardized technological features.: large shaped tools worked on flint flakes through two reduction sequences or only one reduction sequence but combined with final retouch. the final products have straight or curved edge-profile and preserve cortex residues in the mid-proximal section of the tools. The groups located on the negative values (Galería-GIIa and Guado San Nicola-USc), instead, show a higher variability in the reduction strategies. The tools included in these groups are shaped on slabs through one reduction sequence without any retouch or two reduction sequences combined with final retouch to obtain tools characterized by a sinuous edge-profile. The percentage and localization of the cortex can be very variated, but the majority of the tools are non-cortical or they preserve cortex in their proximal section.

Considering the results of Principal Component Analysis and the cluster analysis (Fig. 34) applied on the sub-division of the sample according to archaeological site, we can stand that La Noira-*stratum* c and Guado San Nicola-USc are sharing a number of technological features, while Galería-GIIa has more different shaping strategies.

An additional Geometric Morphometric Analysis was performed to represent shape variability according to the archaeological site of provenance. The scatterplot resulting from the latter (Fig.35) explains ~35% of variability (21.10% expressed by PC01 and 13.96% expressed by PC02). With the firsts 87 PCs, 100% of the variability is explained.

As for the previous cases, summary statistics indicate variability, deviation from bilateral and bifacial symmetry, left and right edge curvature, left and right planform irregularity, and left and right section irregularity (Tab. 16). Hence, the sample was organized in 3 groups: Galería-GIIa, Guado San Nicola-USc, and La Noira-*stratum* c.

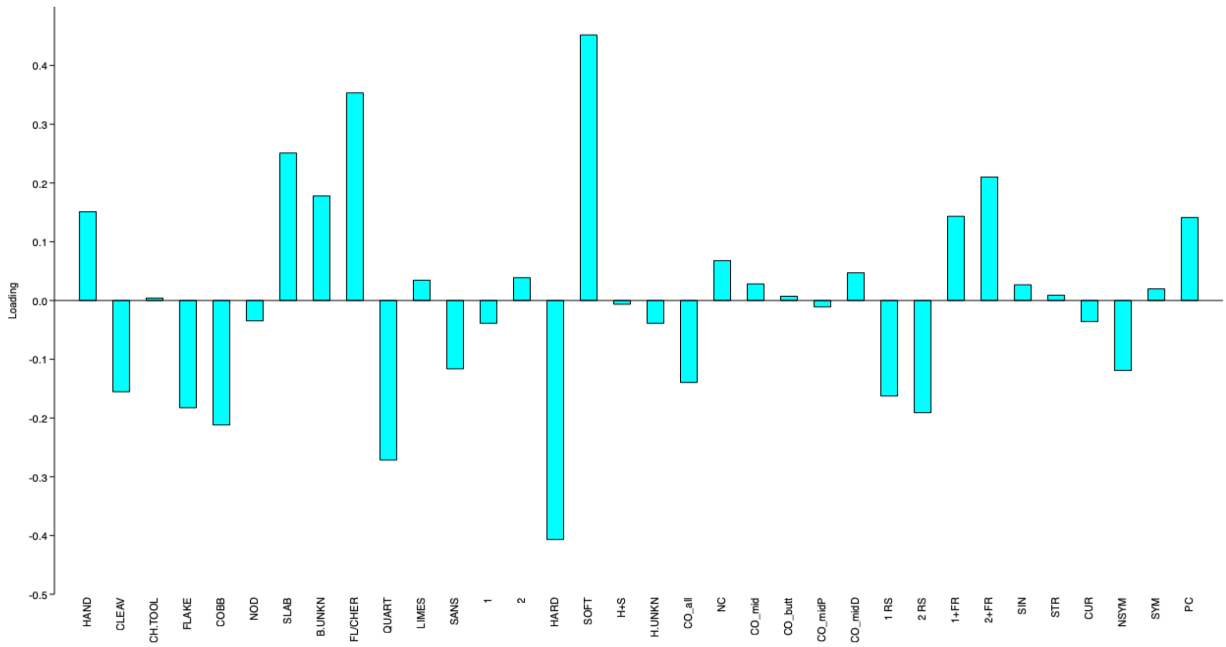

Figure 32: Loadings for PC1.

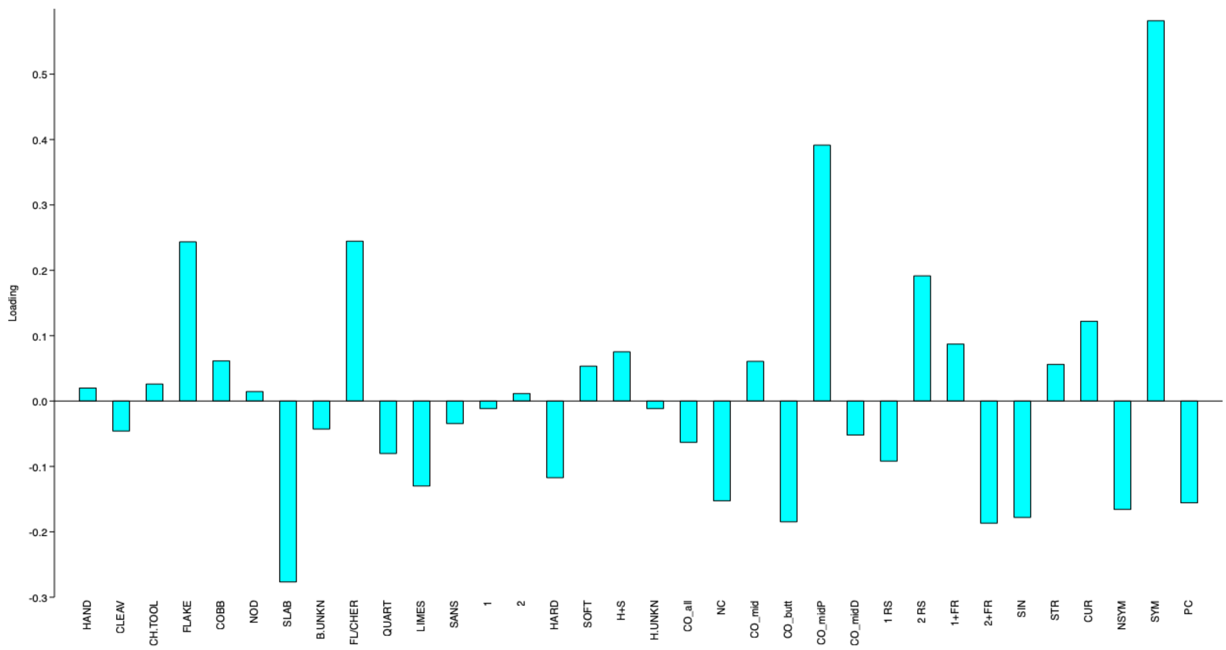

Figure 33: Loadings for PC2.

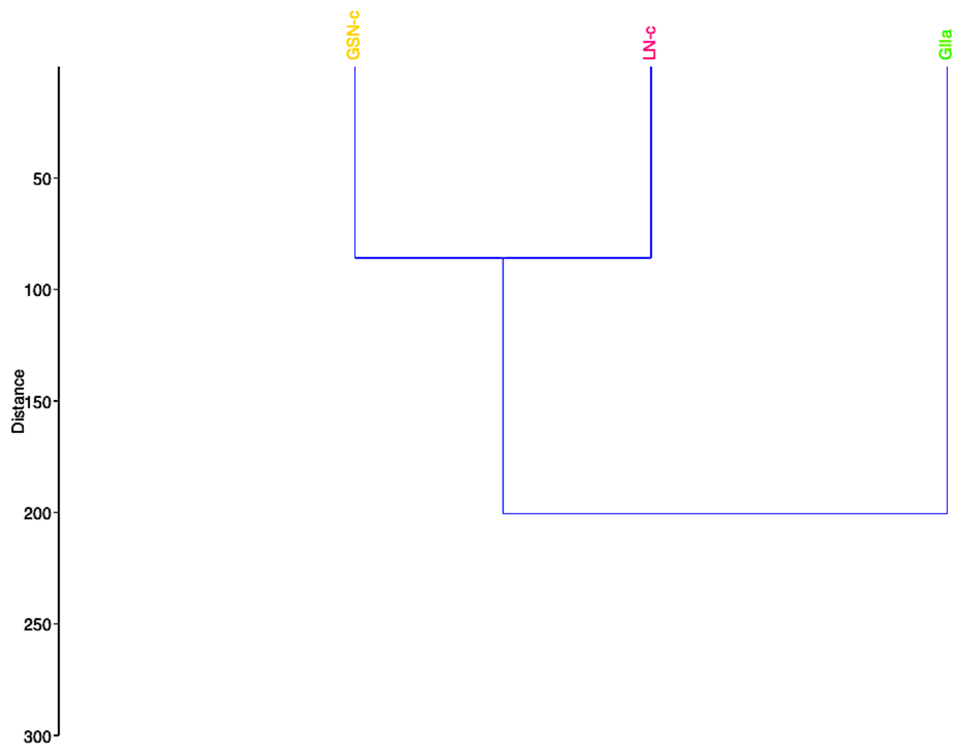

Figure 34: Dendrogram resulting from cluster analysis. (GIIa = Galéria-GIIa; LN-c = La Noira-*stratum* c; GSN-c = Guado San Nicola USc)

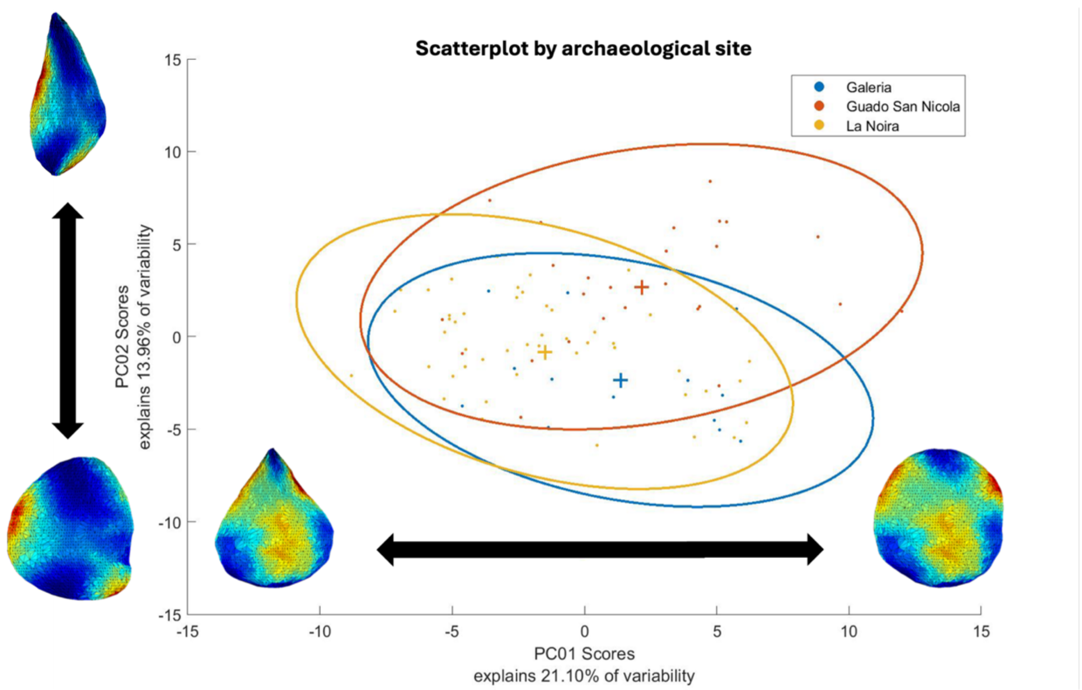

Figure 35: PC scatterplot according to archaeological site.

Guado San Nicola-USc is the group with higher variability while the one with less variability is Galería-GIIa.

For the deviation from perfect bilateral symmetry, Galería-GIIa is the group with the lower value, followed by Guado San Nicola-USc and La Noira-*stratum* c; while for the deviation from perfect bifacial symmetry Guado San Nicola-USc has a slightly lower deviation than Galería-GIIa but La Noira-*stratum* c reconfirms the higher value within the sample. According to these results, it is possible to stand that the large shaped tools from Galería-GIIa and Guado San Nicola-USc are less symmetrical than those from La Noira-*stratum* c. Coherently, La Noira-*stratum* c has the lower difference for both left and right edge curvature.

Group name	**Items**	**Variability**	**Deviation from bilateral symmetry**	**Deviation from bifacial symmetry**	**Left edge curvature**	**Right edge curvature**
Galería-GIIa	13	8,03	4,94	5,41	0,99	0,87
Guado San Nicola-USc	26	9,51	5,03	4,67	0,97	1,09
La Noira-stratum c	49	8,41	9,18	7,99	0,80	0,83

Table 16: Results from summary statistic for each archaeological site.

			Variability caused by (%)		
	n.	Shape variability	Length (x)	Width (y)	Thickness (z)
GIIa	13	8.03	47.37	3.45	49.18
GSNc	26	9.51	33.34	1.98	64.68
LNc	49	8.41	44.60	3.51	51.89

Table 17: Intra-assemblage shape variability and influence (expressed as percentage) on it due each dimension (length, width, and thickness) for each archaeological site (GIIa: Galería-GIIa; GSNc: Guado San Nicola-USc; LNc: La Noira-*stratum* c).

Guado San Nicola-USc's shape variability is statistically different from the ones of both Galería-GIIa and La Noira-*stratum* c at 0.5 level. In fact, the Wilcoxon Rank Sum test results in p-values equal to 0.01 with the other two sites. For all three sites, the dimension that most affects shape variability at a intra-assemblage level is the thickness (z) and length (x) as showed in Table 17. Wideness (y) results the less relevant dimension for shape variability.

Considering inter-assemblage shape variability for each pairwise of sites, it is possible to detect how thickness is the dimension that most influence the shape difference between the couple composed by Galería-GIIa and Guado San Nicola-USc as well as the one that includes Guado San Nicola-USc and La Noira-*stratum* c. Differently, the difference between Galería-GIIa and La Noira-*stratum* c is mainly dependent on length. As for intra-assemblage shape variability, the width is the dimension that less affects shape variability.

				Variability caused by (%)		
	Distance between group means	Shape variability group I	Shape variability group II	Length (x)	Width (y)	Thickness (z)
GIIa/GSNc	5.90	8.03	9.51	46.08	2.76	51.16
GIIa/LNc	4.25	8.03	8.41	57.01	6.46	36.53
GSNc/LNc	5.45	9.51	8.41	14.78	2.37	82.85

Table 18: Inter-assemblage shape variability and influence (expressed as percentage) on it due each dimension (length, width, and thickness) for each pairwise of archaeological sites (GIIa: Galería-GIIa; GSNc: Guado San Nicola-USc; LNc: La Noira-*stratum* c).

1. Guado San Nicola – USc

The sampled assemblage of Guado San Nicola-USc is composed by only handaxes (n.26) made on flint (aphanitic and microbrecciated types) and, in a minority of cases, on limestone. Both from a technological and morphological perspective, there are no significant differences in the exploitation of the two raw materials. Generally, those tools are made on slabs, with frequent recalcified tectonical fractures, worked through two reduction sequences by using soft organic hammer and combined with final retouch. Always from a technological point of view, the invasiveness of the façonnage represent a supportive information to the preferential use of soft hammer which is validate by the presence of fossil antlers within the faunal assemblage of the same stratigraphic unit. As a matter of fact, both the first and the second reduction sequences are commonly defined invasive as the scars are extended on more than 50% of the total surface of the tool. Nevertheless, it should be noted that the high percentage of soft hammer use is certainly also increased by the difficult identification of the early shaping stages, which, according to the literature, are executed by using hard hammer. In fact, the initial preparation of the blank could have been erased by the subsequent phases. The latter hypothesis is also supported by the Scars Density Index (SDI), which shows the higher value exactly for the sample from Guado San Nicola-USc. The percentage of non-cortical final products and unknown blanks also remark the intensity of processing that characterizes the assemblage. Although the handaxes of Guado San Nicola are intensively worked, this is the only assemblage within the whole sample studied for this thesis that does not show any distal refinement.

According to geometric morphometric analysis, Guado San Nicola-USc is the group showing the highest intra-assemblage variability. The latter is mainly caused by thickness (z) and length (x) variations that are concentrated in the basal section of the tool, particularly in the right margin (Fig.36). The high value that this group shows for intra-assemblage variability does not seem to be so related to the typology and morphology of the blank, as this group shows an almost totality of slabs as initial support, but to the presence of numerous fractures and impurities within them. Hence, the morphological variability in the large shaped tools from Guado San Nicola could be explained with the difficult prediction of flint physical behavior during knapping activity because of the pre-existing fracture planes within the blank. Considering the mean shape generated on Euclidean distances within the group, the handaxes from Guado San Nicola-USc have teardrop (or amygdaloid) shapes and are the ones showing the worst bifacial symmetry (Fig.37). The latter information is indicated by the result of deviation from perfect bifacial symmetry analysis, for which this assemblage has the lower value across the whole sample studied. Despite this, the assembly presents a good average symmetry that could be explained by the technological characterization of the group. As a matter of fact, Guado San Nicola-USc is the assemblage with the higher Scar Density Index (SDI) which indicates an intense shaping activity carried out through two reduction sequences combined with final retouch. The SDI value, which quantifies shaping intensiveness, can be complemented with the quantities and distribution of cortex on the final tools. With regard to this, a large majority of the assemblage either do not have cortex presence, pointing to a completely worked surface, or presents less than 50% of cortex localized in the mid-proximal section of the handaxes. This suggests that the proximal section is more variable because it has been less involved in the workmanship, often probably due to the presence of inclusions or imperfections already present in the blank. the extension and intensity of the initial support would have enhanced the obtaining of more bifacially symmetric products.

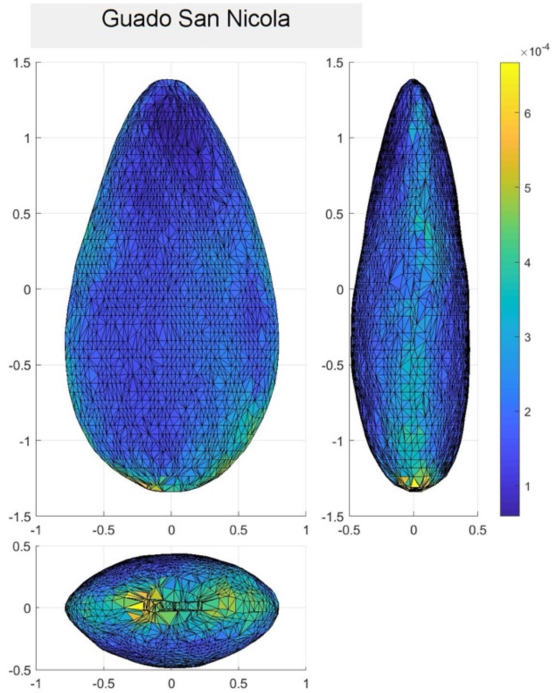

Figure 36: Warp tool showing the localization and the intensity of intra-assemblage shape variability for Guado San Nicola-USc sample.

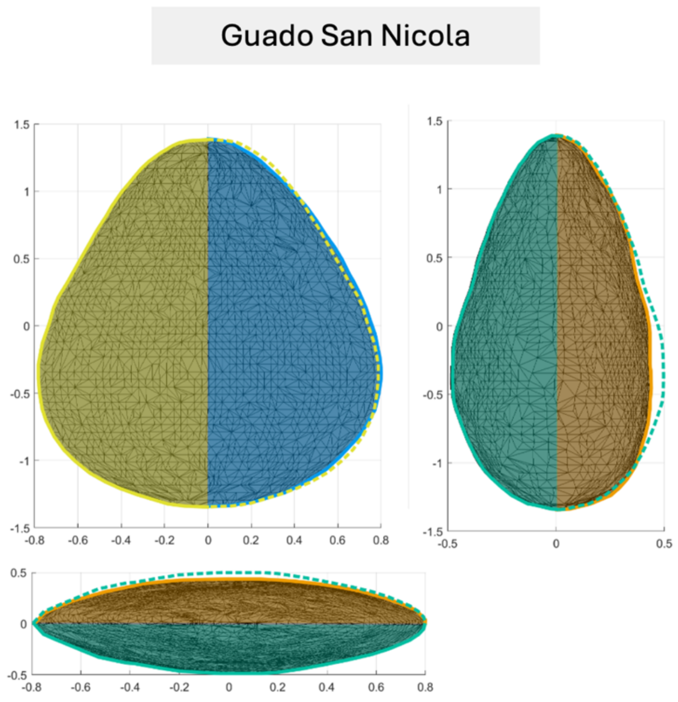

Figure 37: Mean shape of Guado San Nicola-USc and deviation from perfect symmetry. The deviation from perfect bilateral symmetry is depicted on the frontal view of the model by reflecting the profile of left edge (yellow) on the opposite edge (light blue). The deviation from perfect bifacial symmetry is depicted on the sagittal and transversal views of the model by reflecting the profile of ventral face (green) on the opposite face (orange).

2. La Noira – *stratum* c

The assemblage of La Noira-*stratum* c is composed by handaxes (n.47) and one only chopping-tool which is also the only one within the whole sample studied for this work. All of the large shaped tools from the assemblage are made on flint and three different varieties of it have been identified: Millstone (n.36), Cretaceous (n.4), and "Chaille" Jurassic (n.9). Tools made on Millstone show technological features very close to those of Guado San Nicola-USc.Proof of this, handaxes and the chopping-tool realized on the latter material are mainly worked on slabs by using soft organic hammer but, in contrast with the assemblage of Guado San Nicola-USc, La Noira's tools shows higher variability across the shaping strategies. There is a prevalence of tools resulting from one reduction sequence combined with final retouch but also two reduction sequences with or without final retouch are common within the sample. This heterogeneity gets reflected into the variety of cortex distribution which, however, is almost always less than 50 per cent of the total surface area. On the other hand, "Chaille" Jurassic and Cretaceous flint have a precise technological characterization as these raw materials are used to realize only handaxes shaped through two reduction sequences combined with final retouch by using soft organic hammer. Regarding the shaping strategies, the first reduction sequence is always invasive while the second one is more commonly defined as *non-invasive* and it appears to be aimed at edges' regularization. Coherently, "Chaille" and Cretaceous flint handaxes show the lowest values for edge curvature, suggesting a tendency to straight profiles.

The poor representation of tools in the "Chaille" and Cretaceous flint combined with the compatibility of the technological characteristics of the latter with those describing the Millstone group, allow the similarity with Guado San Nicola-USc to be extended to the entire La Noira-*stratum* c assemblage. Additionally, the similarities are evident also from a morphological point of view. Hence, large shaped tools from La Noira-*stratum* c show high value for intra-assemblage variability resulting in heterogeneous shapes ranging from oval (mainly related to the use of cobbles or pebbles as blanks) to pick-like and with occasional sub-triangular morphologies. As Guado San Nicola-USc, morphological variabilities are mainly concentrated in the basal section (Fig. 38) of the tools and are mainly caused by variation in thickness (z) and length (x).

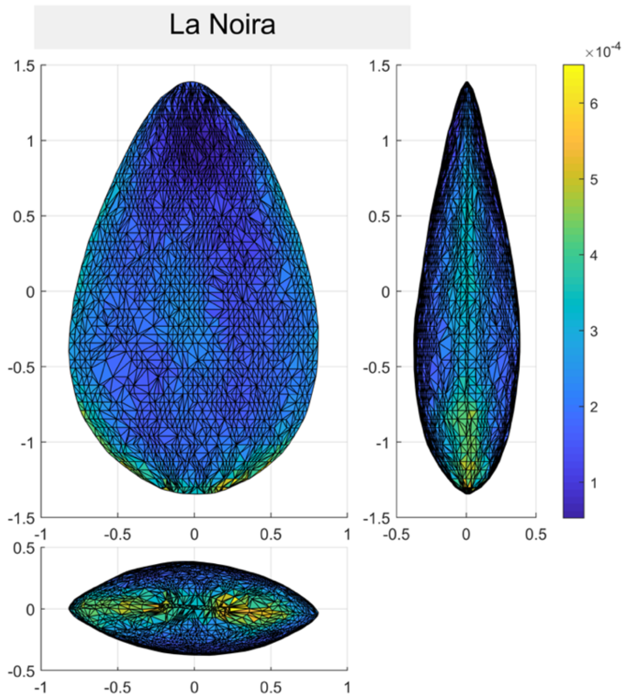

Figure 38: Warp tool showing the localization and the intensity of intra-assemblage shape variability for La Noira-*stratum* c sample.

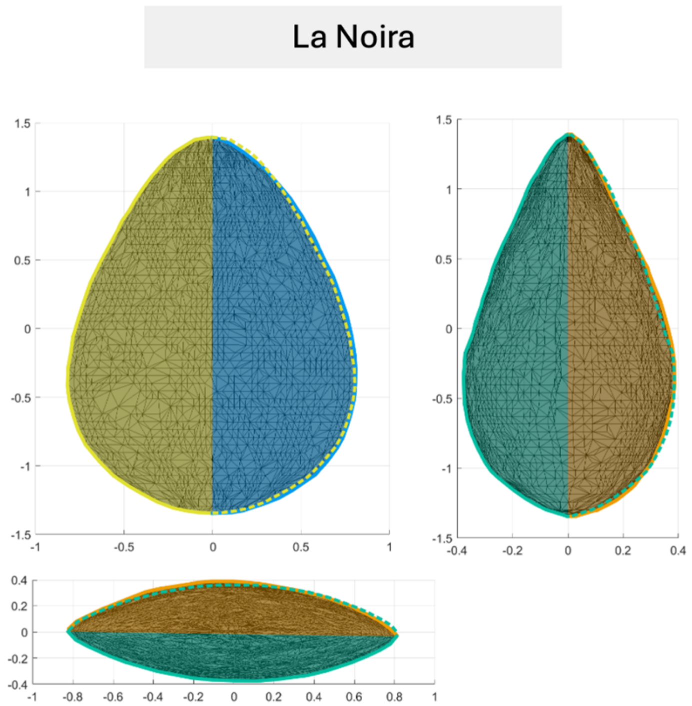

Figure 39: Mean shape of La Noira-*stratum* c assemblage and deviation from perfect symmetry. The deviation from perfect bilateral symmetry is depicted on the frontal view of the model by reflecting the profile of left edge (yellow) on the opposite edge (light blue). The deviation from perfect bifacial symmetry is depicted on the sagittal and transversal views of the model by reflecting the profile of ventral face (green) on the opposite face (orange).

As for the other sites, also for La Noira the deviation from both perfect bilateral and bifacial symmetry is not statistically significant. The mean shape generated on Euclidean distances within the group is depicted by Figure 39 and indicates the best level of both bifacial and bilateral symmetry (already suggested by the cross-section determination) that, as for Guado San Nicola-USc, could be explained by a series of technological features. The most common strategy used to shape La Noira-*stratum* c tools consists of two reduction sequences by using soft organic hammer and which led to a significant reduction in volume as highlighted by Scar Density Index (SDI). Then, ca. an 80% of the sample present final retouch suggesting a particular attention to the final stage of manufacturing, which is mainly focused on the distal section as confirmed by the distal refinement index. The intensiveness resulting from the shaping strategy described above is further supported by cortex information, in fact more than 70% of the assemblage do not present cortex at all or has less than 50% of cortical surface. When cortex residuals are still present in the final tool, those are localized in the mid-proximal section remarking the attention to distal section shaping.

3. Galería – GIIa

The assemblage of Galería-GIIa is composed by two types of tools: cleavers (n.4) and handaxes (n.9). Cleavers are exclusively made on quartzite while handaxes are made also on Neogene chert and sandstone. From the results obtained during this specific study, it could be assumed that quartzite was selected as the preferred raw material to realize cleavers in this Subunit. Nevertheless, along the Galería sequence and in Atapuerca in general, this type of tools is shaped in different raw materials (García-Medrano et al., 2015). Likewise, also for handaxes there seems to have been no selection of a specific raw material. From a technological point of view handaxes and cleavers do not show any difference, the sample is mainly characterized by a large use of hard hammer and absence of final retouch, technological feature that result in asymmetrical cross-section due to deep scars on edge. The shaping process is mainly concentrated in the mid-distal section while the proximal one is usually left intact showing the original morphology of the blank (especially when the blank is a cobble).

Shaping is intensive during the first reduction sequence while the second one, when existing, is always non-invasive. All these data are compatible with the value obtained for the Scars Density Index (SDI), which is not as elevate as Guado San Nicola-USc although higher than La Noira-*stratum* c. In fact, Galería-GIIa has the higher mean number of total scars, and these were detached with hard hammer, which is on average less invasive in terms of the extent of the negatives on the instrument surface but removes more raw material resulting in a greater reduction in volume.

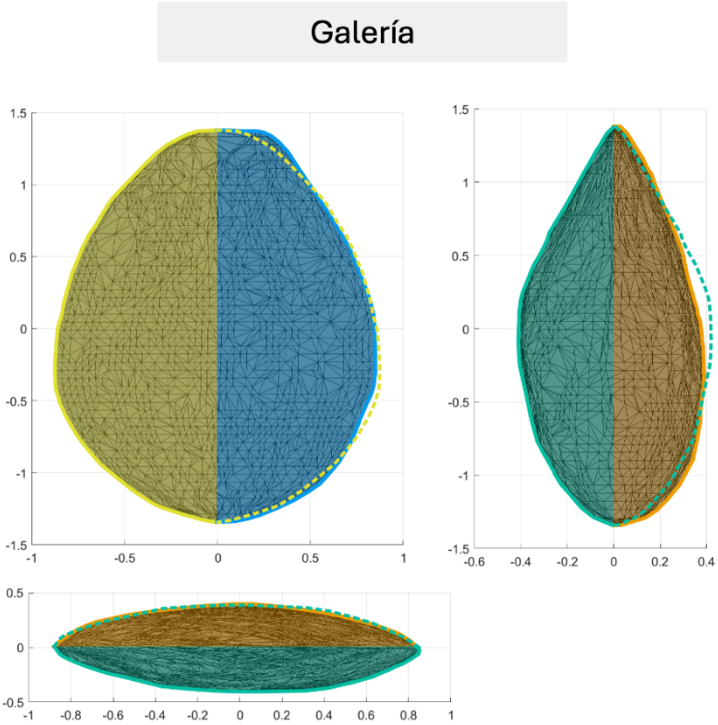

Figure 40: Mean shape of Galería-GIIs assemblage and deviation from perfect symmetry. The deviation from perfect bilateral symmetry is depicted on the frontal view of the model by reflecting the profile of left edge (yellow) on the opposite edge (light blue). The deviation from perfect bifacial symmetry is depicted on the sagittal and transversal views of the model by reflecting the profile of ventral face (green) on the opposite face (orange).

According to geometric morphometric analysis, Galería-GIIa has general oval shaped large shaped tools (Fig.40) and shape variability is concentrated in the point and the butt of the tools (Fig.41). Some differences can be noted between handaxes and cleavers has they are statistically different. The mean shape variability for handaxes is caused by thickness (z), being coherent with the handaxes from the other two sites, while for cleavers the metric value that influence the most the shape variation is the length (x). As a matter of fact, cleavers are more standardize in their morphologies and the area showing higher variability is the tranchet in the distal section of the tool (Fig. 42a) while for handaxes the variability is mainly concentrated in the mid and basal sections (which are strongly related to variation in thickness) (Fig. 42b). Consequently, cleavers correspond to oval shapes and handaxes to both oval and teardrop (or amygdaloid) ones.

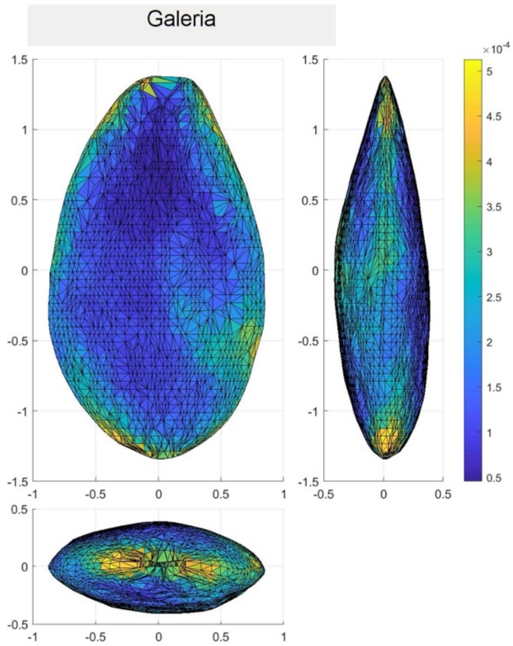

Figure 41: Warp tool showing the localization and the intensity of intra-assemblage shape variability for Galería-GIIa sample.

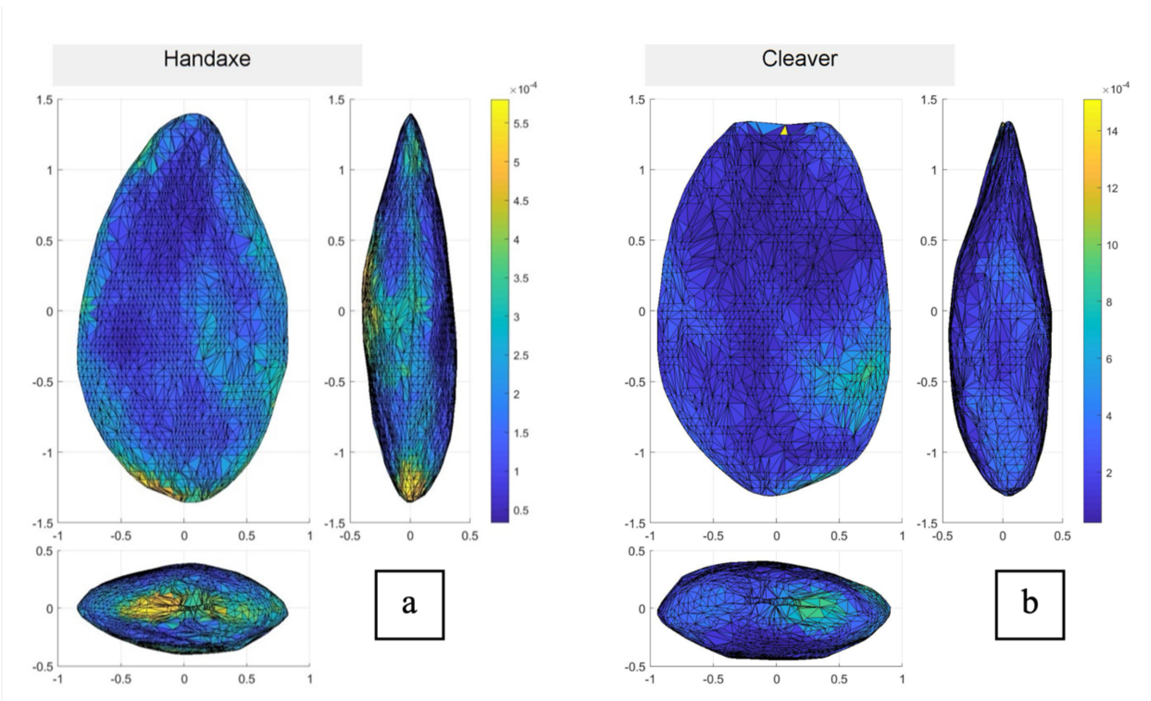

Figure 42: Warp tool showing the localization and the intensity of intra-assemblage shape variability for a) handaxes and b) cleavers from Galería-GIIa sample.

The variability within the assemblage is the lowest across the whole sample analyzed for this study despite having the greatest variability of instruments. This could be due to the low number of specimens composing the assemblage. The mean shape generated for Galería-GIIa shows how the two faces of the hypothetical tool are depicting an asymmetrical cross-section already suggested by technological analysis, also confirmed by the value obtained for deviation from bifacial symmetry. The value for deviation from perfect bilateral symmetry, instead is the lower within the whole sample analyzed suggesting that Galería-GIIa has the less symmetrical tools from a frontal view. For this site, the symmetry seems to be related to the nature of the reduction sequencies: the first one is invasive and aimed to shape intensively the blank by removing significant quantities of raw material, the second one is non-invasive and aimed to the refinement of the distal section as confirmed by the total absence of cortex and the distal refinement index. The presence of a significant percentage of cleavers, which are characterized by a typical distal morphology that does not end in a convergent point, seems to be the most probably explanation for the low bilateral symmetry.

4. Contextualization within MIS11 in Europe

Within the context of this thesis, three assemblages from as many Lower Palaeolithic sites with chronology referable to Marine Isotope Stage (MIS) 11 in Europe were analyzed through technological and morphometric analysis. Each site is located in a different region of the continent to provide a broad representation of the Acheulean framework and of its large shaped tools during the long interglacial stage.

The Galería site (Atapuerca, Burgos, Spain), represented by GIIa assemblage, bears witness to the Iberian record within the whole sample studied. Galería site fits well in the large shaped tools technological context of Iberian Peninsula during MIS11. In fact, handaxes and cleavers from Galería-GIIa are perfectly coherent with those from other sites located in the Sierra de Atapuerca (i.e. Grad Dolina-TD10 and Sima de los Huesos) but also with Ambrona site (Soria, Spain) which is the other main source of documentation for this region and time frame (MIS11). According to these sites, the large cutting tools – mainly handaxes and cleavers – from Iberian Peninsula are mainly realized on flakes or cobbles of different types of raw materials as chert, limestone, quartzite, and quartz. Even if the raw materials used are quite heterogenic, these are always locally available. In all the three sites there is particular attention to the final stages of shaping, or by applying final retouch to regularize the overall shape or using the second reduction sequence to achieve the convex distal convergence (García-Medrano et al., 2020; Ollé et al., 2013; Santonja et al., 2018). The results obtained for the assemblage of Galería-GIIa match with this general framework of large shaped tools from Iberian Peninsula during MIS11: both production of handaxes and cleavers (albeit a predominance of handaxes can be noted) on flakes or cobbles of chert, quartzite or sandstone is attested; the shaping process consists of a first reduction sequences, invasive, aimed to rough out the peripherical shape and a second one, less invasive, to seek the convexity necessary to obtain a converging tip in the distal section of the instrument.

The site of Guado San Nicola, represented by USc assemblage, bears witness to the Italian record within the whole sample studied. In the Italian peninsula, as for many regions of southern Europe, the number of Acheulian sites with handaxes is extremely limited. Due to the presence/absence of handaxes within sites' assemblages, two facies have been defined for Italian Acheulean: 'non-handaxes sites' (i.e. Isernia-La Pineta, Monte Poggiolo) and 'handaxes sites' (i.e. Notarchirico, Guado San Nicola, Castel di Guido, etc.). The latter distinction has been explained in the bibliography through the hypothesis of two migrations that would have happened in different moments: a first movement of human groups that were still using a Mode 1 technology (as the one characterizing the assemblages of Isernia-La Pineta and Monte Poggiolo), and a second movement that finally brought the Mode 2 technology characterized by large cutting tools (Barsky et al., 2021; Santonja & Villa, 2006). A second theory, however, has been advanced considering the alternation of levels with the presence of handaxes and levels without large cutting tools within the stratigraphy of Notarchirico (Venosa, Italy). This last consideration should demonstrate how the presence/absence of handaxes is not a constant throughout the lifetime of a site and, more importantly, Mode 1 and Mode 2 technologies are not mutually exclusive, indeed they can coexist within the same assemblage as demonstrated by numerous sites not only in Europe, but also in Africa and Asia. During MIS 11 the number of sites preserving large cutting tools shows a slight increasement, but the numbers are still scarce. In fact, apart from Guado San Nicola, the only sites with a chronology relatable to MIS 11 are located in the Lazio region as the Frosinone-Ceprano basin complex (i.e. Campogrande, Isoletta, Selvotta and Lademagna), Fontana Ranuccio (Anagni, Italy), and Castel di Guido (Roma, Italy) (Moncel et al., 2020; Santonja & Villa, 2006). Those sites, being in the same geographical area and relating to the same contour conditions provide a very homogeneous term of comparison specifically referring to what happened in this period in southern Lazio. Considering this information, Guado San Nicola-USc differs from the other assemblages for the raw material used (there is a clear predominance of flint within the sample), the type of blank (which are slabs in all the identifiable cases), the recurrent presence of final retouch and a non-prevalent presence of plano-convex tools. Features as the type of blank or the raw materials used to manufact the handaxes are most probably related to availability conditions but divergences in knapping and shaping processes could be an interesting topic to be further investigate.

La Noira site, represented in this work by *stratum*-c assemblage, bears witness to the French record within the whole sample studied. The French framework for Acheulean Large Cutting Tools between Marine Isotope Stage 12 and 11 is characterized by a prevalence of handaxes over cleavers and chopping-tools realized on local raw materials under form of pebbles, nodules or, more rarely, slabs (Barsky, 2013; Lamotte & Tuffreau, 2016; Santonja & Villa, 2006; Tuffreau & Lamotte, 2010). These tools are made through long and elaborated knapping strategies performed by using both hard and soft type of hammers leading to heterogeneous morphologies ranging from lanceolate and amygdalate to oval and sub-triangular shapes (Barsky, 2013; Lamotte & Tuffreau, 2016). La Noira-*stratum* c sample consists almost entirely of handaxes made from locally available flint under form of slabs, which have been worked through two reduction sequences, often followed by final retouch to regularize edges' curvature. This knapping strategy results in intensively worked and symmetrical final products with amygdaloid morphology.

The results obtained within this work express a strong technological and morphological proximity between La Noira-*stratum* c sample and Guado San Nicola-USc sample, while Galería-GIIa remains more isolated due to a greater diversity in both the strategies occupied and the characteristics of the finished products. The diversity between La Noira and Galería complex is not unprecedented; on the contrary, it has been noted in previously published studies that have shown how Galería is characterized by more diversified strategies than La Noira, just as greater diversity is present among the raw materials used in the production of large cutting tools (García-Medrano et al., 2023). A scenario coherent with that indicated by the bibliography can also be argued according to this work. In fact, La Noira-*stratum* c and Guado San Nicola-USc show more standardised technological strategies leading to well-processed large cutting tools with a good level of symmetry. This standardization, however, does not cancel out the significant cultural differences that distinguish the two assemblages and that fit well with the dynamics of regional diversification occurring in Europe at the end of the glacial period during MIS 12 (Moncel et al., 2016). Considering the common elements of the two occupations of La Noira-*stratum* c and Guado San Nicola-USc, it can be inferred that they both occur in open-air sites in a fluvial context and with very close chronologies, ~450 ka for La Noira-*stratum* c (Moncel et al., 2015a) and ~400 ka for Guado San Nicola (Nomade & Pereira, 2014; Peretto et al., 2016), that are temporally placed right at the transition time between the end of the glacial maximum of MIS 12 and the beginning of the long interglacial that is MIS 11 (Sassoon et al., 2023). Taking into account the previous temporal setting during the initial phase of that marine isotopic stage (MIS 11c), the occupations to which we refer occurred during the climatic optimum of the stage characterized by the warmer temperatures recorded during MIS11 and which allowed the glacial melting of MIS12 (*ibid*). Consequently, the standardization recorded in the analyzed sample reflects human adaptation to the new environmental conditions – maximum forest expansion and warm climate – extremely favorable for both geographic and demographic expansion. Such factors seem to foster relatively short occupations interrupted by group movements across the surrounding territory (García-Medrano et al., 2023; Moncel et al., 2015b, 2020). These movements across the continent would have facilitated the development of a shared technological model, particularly in the production of handaxes, while still preserving regional cultural differences (García-Medrano et al., 2023). Galería-GIIa, on the other hand, has a more recent chronology of ~360 ka, lying in the sub-stage MIS 11c. The latter stage is still characterized by warm temperatures, even if not as warm as the ones of sub-stage a, and by significant millennial-scale oscillations alternating arid and temperate climates throughout Europe but affecting the south of the continent to a lesser extent (Sassoon et al., 2023). This phenomenon originates in the development of niches in southern Europe where human groups retreat in search of more favorable conditions, and one of these niches is indeed the Iberian Peninsula. The nature of Galería-GIIa site does not simplify the interpretation of the data, as the site attests repeated but very short-lasting occupations as it was a "complementary site" where humans exclusively went to supply animal resources, such as meat. However, when considered alongside information from the other sites in the Atapuerca complex, it also suggests that the human groups established in the Sierra de Atapuerca during this period had a stable and lasting presence, supporting the ecological niche hypothesis. The isolation and slightly less favorable conditions that characterize MIS 11c in the Iberian Peninsula would therefore have led to greater regional differentiation due to the limited movement of human groups, especially across natural barriers (e.g. the Pyrenean Mountain chain), which resulted in an apparent technological regression suggested by shorter and shaping processes, also less curated in their final stages.

5. Limitations of the study

All these considerations are based on the results obtained from the present study and their comparison with the bibliography on the topic. Therefore, it should be borne in mind the small numerical size of the sites and materials analyzed, which, given the aforementioned scarcity, represent only a sample of the European framework during MIS11. The hypotheses presented above certainly need further analysis that can expand the sample studied from a geographical point of view.

The same issue arises in the analyses conducted on symmetry as, within the context of this thesis, the limited number of sites did not allow for statistical significance in the variation from perfect bifacial and bilateral symmetry. Applying the same methodology to a larger sample with greater variability, the symmetry analysis, through the complementarity of statistical results obtained via Geometric Morphometrics Analysis with data from technological analysis, could reveal interesting regional or temporal patterns that did not emerged in this specific study.

Furthermore, by expanding the sample with a wider number of large shaped tools from the categories underrepresented in this study (cleavers and chopping-tools), it would be possible to analyze symmetry by subdividing the artifacts by techno-typological categories. This would result in better resolution of the results as symmetry has different meanings for the different types of large shaped tools.

Conclusions

This thesis investigated large shaped tools from three European sites—La Galería (Spain), La Noira (France), and Guado San Nicola (Italy)—to explore morphometric variations, particularly in bifacial and bilateral symmetry, during Marine Isotope Stage 11 in Southwestern Europe. The study combined technological analysis of the artifacts and geometric morphometric analysis of their 3D representations, utilizing statistical methods such as Principal Component Analysis (PCA) and cluster analysis to reveal patterns of similarity and divergence among the sites. Thanks to the results obtained, new morphometric data for Guado San Nicola have been introduced, enhances comparative studies of Acheulean technologies after the MIS 12 glaciation, and offers a novel, quantitative approach to analyzing symmetry, aiming to minimize researcher bias and increase the precision of the findings.

According to the outcoming of the study, each site analyzed fits well with the technological context of its own geographical region, indicating that each of the three sites is representative of both area and chronology in which it is located.

La Noira-*stratum* c and Guado San Nicola-USc exhibit strong technological and morphological similarities, indicating a close relationship in their manufacturing strategies. These two sites show a trend towards standardized technological strategies and well-processed tools, which likely represents an adaptation to the more stable climatic conditions of the MIS 11 climatic optimum. However, despite this standardization, notable cultural differences persist, aligning with the broader pattern of regional diversification in Europe following the MIS 12 glaciation. The latter similarities, therefore, suggest a shared technological model, particularly in the production of handaxes, which could have been facilitated by the movement of groups across the continent during this period. In contrast, Galería-GIIa, with its more recent chronology of around 360,000 years ago during MIS 11c appears more distinct, showing greater diversity in both the methods employed and the final products. This diversity may reflect its unique environmental and cultural context. The relative isolation of Galería-GIIa, combined with the less favorable environmental conditions in the Iberian Peninsula during MIS 11c, seems to have led to greater regional differentiation due to a more limited human movement.

Regarding the topic of symmetry, the mean shapes of each sample showed a general good balance for both bifacial and bilateral symmetry corresponding to the introduction of recurrent symmetry starting from the end of MIS 12. On the other hand, no significant difference has been noted between the values obtained for deviation from perfect symmetry for each assemblage suggesting that the symmetry is not a discriminant feature within this specific context.

Considering the limitations of this study, particularly the small sample size and the narrow geographic area, there is a clear necessity of further research to gain a more comprehensive understanding of Europe during MIS11. Hence, there are several improvements that can be done to this work within a future perspective.

In a first place, it is necessary to enlarge the sample size and broad the geographic area. The sites and materials analyzed here represent only a small fraction of the broader archaeological record from MIS11 across Europe. By including a greater number of sites located in different regions, it would be possible to achieve a more representative framework and identify regional variations in material culture, technological practices, and adaptation strategies. Therefore, the comparisons could suggest how different populations across Europe responded to the specific challenges of MIS11. The issue of sample size also affects the analysis of symmetry. As mentioned above, due to the limited number of sites and artifacts in this study, it was not possible to achieve statistical significance in examining variations in bifacial and bilateral symmetry. Symmetry in large shaped tools is a significant indicator of cognitive and with a more extended dataset, we could explore the relationship between symmetry and other technological variables, potentially revealing how shaping strategies evolved over time or differed across regions by highlighting broader cultural trends that were not detectable in the present study.

Secondly, it would be useful to integrate more insights from fields such as paleoenvironmental studies, genetics, and climatology to enhance the understanding of MIS11. For instance, analyzing climatic conditions during this period could provide context for the material culture and technological practices observed. Similarly, genetic research could trace population movements and interactions, offering a more dynamic view of human adaptation across Europe.

Furthermore, a more detailed temporal analysis is warranted. The current study offers a snapshot of MIS11, but a more nuanced chronological framework could reveal how material culture and technology evolved throughout this period. Longitudinal studies, focusing on finer stratigraphic layers corresponding to shorter respective chronologies, could track these changes over time.

In summary, this thesis analyzed how climate change during MIS11 influenced the adaptive strategies of European populations, shedding light on cultural and technological dynamics. The results suggest that climatic variations played a decisive role in the adaptive responses of human groups occupying southwestern Europe during this period. However, the limited sample of sites and materials analyzed is a significant limitation, and future studies should seek to broaden the field of research by integrating more extensive data and interdisciplinary methodologies. Nevertheless, the implications of this research not only enrich our understanding of the technological and morphological dynamics occurring after the end of MIS12, but also offer useful perspectives for future studies of human adaptation processes in contexts of environmental change.

Bibliography

Aguirre, E. (2001). Dépôts fossiliferes du karst de Atapuerca, premiers 20 ans. In L'Anthropologie (Vol. 105).

Arsuaga, J. L., Martínez, I., Arnold, L. J., Aranburu, A., Gracia-Téllez, A., Sharp, W. D., Quam, R. M., Falguères, C., Pantoja-Pérez, A., Bischoff, J., Poza-Rey, E., Parés, J. M., Carretero, J. M., Demuro, M., Lorenzo, C., Sala, N., Martinón-Torres, M., García, N., Alcázar De Velasco, A., … Carbonell, E. (2014). Neandertal roots: Cranial and chronological evidence from Sima de los Huesos. Science, 344(6190), 1358–1363.

Author, A., Alimen, H., & Vignal, A. (1952). Etude statistique de bifaces acheuléens. Essai d'Archéométrie. https://about.jstor.org/terms

Berger, G. W., Pérez-González, A., Carbonell, E., Arsuaga, J. L., Bermúdez de Castro, J. M., & Ku, T. L. (2008). Luminescence chronology of cave sediments at the Atapuerca paleoanthropological site, Spain. Journal of Human Evolution, 55(2), 300–311. https://doi.org/10.1016/j.jhevol.2008.02.012

Bermtidez, M., Castro Atapuerca Trench Burgos, de, & Rosas, A. (n.d.). A human mandibular fragment from the.

Beyene, Y., Katoh, S., Woldegabriel, G., Hart, W. K., Uto, K., Sudo, M., Kondo, M., Hyodo, M., Renne, P. R., Suwa, G., & Asfaw, B. (2013). The characteristics and chronology of the earliest Acheulean at Konso, Ethiopia. Proceedings of the National Academy of Sciences of the United States of America, 110(5), 1584–1591. https://doi.org/10.1073/pnas.1221285110

Bordes, F. (1961). Typologie du Paléolithique Ancien et Moyen.

Cáceres, I. (2002). Tafonomía de yacimientos antrópicos en karst. Complejo Galería (Sierra de Atapuerca, Burgos), Vanguard Cave (Gibraltar) y Abric Romaní (Capellades, Barcelona). Universitat Rovira i Virgili.

Cáceres, I., Pàmies, R. H., Ardèvol, J. R., Nadal, M. E., i Ballesté, P. S., Fernández-Lomana, J. C. D., & Medrano, P. G. (2010). El yacimiento de Galería (Sierra de Atapuerca, Burgos, España): un enclave para la obtención de recursos cárnicos en el Pleistoceno Medio. Zona Arqueológica, 13, 186–196.

Cassoli, P. F., Lefevre, D., Piperno, M., Raynal, J. P., & Tagliacozzo, A. (1993). Una paleosuperficie con resti di Elephas (Palaeoloxodon) antiquus e industria acheuleana nel sito di Notarchirico (Venosa, Basilicata). https://www.researchgate.net/publication/276027752

Cole, J. (2015). Examining the Presence of Symmetry within Acheulean Handaxes: A Case Study in the British Palaeolithic. Cambridge Archaeological Journal, 25(4). https://doi.org/10.1017/S0959774315000141

Despriee, J., Courcimault, G., Moncel, M. H., Voinchet, P., Tissoux, H., Puaud, S., Gallet, X., Bahain, J. J., Moreno, D., & Falgueres, C. (2016a). The Acheulean site of la Noira (Centre region, France): Characterization of materials and alterations, choice of lacustrine millstone and evidence of anthropogenic behaviour. Quaternary International, 411, 144–159. https://doi.org/10.1016/j.quaint.2015.12.101

Despriee, J., Courcimault, G., Moncel, M. H., Voinchet, P., Tissoux, H., Puaud, S., Gallet, X., Bahain, J. J., Moreno, D., & Falgueres, C. (2016b). The Acheulean site of la Noira (Centre region, France): Characterization of materials and alterations, choice of lacustrine millstone and evidence of anthropogenic behaviour. Quaternary International, 411, 144–159. https://doi.org/10.1016/j.quaint.2015.12.101

Dominguez- Rodrigo, M., Serrallonga, J., Juan-Tresserras, J., Alcala, L., & Luque, L. (2001). Woodworking activities by early humans: A plant residue analysis on Acheulian stone tools from Peninj (Tanzania). Journal of Human Evolution, 40(4). https://doi.org/10.1006/jhev.2000.0466

Falguères, C., Bahain, J. J., Bischoff, J. L., Pérez-González, A., Ortega, A. I., Ollé, A., Quiles, A., Ghaleb, B., Moreno, D., Dolo, J. M., Shao, Q., Vallverdú, J., Carbonell, E., Bermúdez de Castro, J. M., & Arsuaga, J. L. (2013). Combined ESR/U-series chronology of Acheulian hominid-bearing layers at Trinchera Galería site, Atapuerca, Spain. Journal of Human Evolution, 65(2), 168–184. https://doi.org/10.1016/J.JHEVOL.2013.05.005

Falguères, C., Barkai, R., Tombret, O., & Gopher, A. (2022). New ESR/U-series dates of the lowest Acheuleo-Yabrudian levels of Qesem cave. Quaternary Geochronology, 69. https://doi.org/10.1016/j.quageo.2022.101266

Feizi, N., Vahdati Nasab, H., & Wynn, T. (2018). Consider the third dimension: A new approach for measuring the symmetry of the middle Paleolithic points of the Mirak Site. Comptes Rendus - Palevol, 17(6), 388–398. https://doi.org/10.1016/j.crpv.2017.11.004

Gamble, C., Gowlett, J., & Dunbar, R. (2011). The social brain and the shape of the palaeolithic. In Cambridge Archaeological Journal (Vol. 21, Issue 1, pp. 115–135). https://doi.org/10.1017/S0959774311000072

García-Medrano, P. (2021). Western European Acheulean: 3D models of handaxes and cleavers. In ZENODO.

García-Medrano, P., Ashton, N., Moncel, M.-H., & Ollé, A. (2020). The WEAP Method: a New Age in the Analysis of the Acheulean Handaxes. Journal of Paleolithic Archaeology, 3(4), 756–793. https://doi.org/10.1007/s41982-020-00054-5

García-Medrano, P., Cáceres, I., Ollé, A., & Carbonell, E. (2017). The occupational pattern of the Galería site (Atapuerca, Spain): A technological perspective. Quaternary International, 433, 363–378. https://doi.org/10.1016/j.quaint.2015.11.013

García-Medrano, P., Despriée, J., & Moncel, M.-H. (2022). Innovations in Acheulean biface production at la Noira (France) during Middle Pleistocene in Western Europe. Archaeological and Anthropological Sciences, 14(4). https://doi.org/10.1007/s12520-022-01506-5

García-Medrano, P., Moncel, M. H., Maldonado-Garrido, E., Ollé, A., & Ashton, N. (2023). The Western European Acheulean: Reading variability at a regional scale. Journal of Human Evolution, 179. https://doi.org/10.1016/j.jhevol.2023.103357

García-Medrano, P., Ollé, A., Mosquera, M., Cáceres, I., & Carbonell, E. (2015). The nature of technological changes: The Middle Pleistocene stone tool assemblages from Galería and Gran

Dolina-subunit TD10.1 (Atapuerca, Spain). Quaternary International, 368, 92–111. https://doi.org/10.1016/j.quaint.2015.03.006

García-Medrano, P., Ollé, A., Mosquera, M., Cáceres, I., Díez, C., & Carbonell, E. (2014). The earliest Acheulean technology at Atapuerca (Burgos, Spain): Oldest levels of the Galería site (GII Unit). Quaternary International, 353, 170–194. https://doi.org/10.1016/j.quaint.2014.03.053

Giannouli, V. (2013). Visual Symmetry Perception. Encephalos.

Grosman, L., Goldsmith, Y., & Smilansky, U. (2011). Morphological Analysis of Nahal Zihor Handaxes: A Chronological Perspective. https://doi.org/10.4207/PA.2011.ART53

Hammer, Ø., Harper, D. A. T., & Ryan, P. D. (2001). PAST: Paleontological statistic software package for education and data analysis. In Paleontologia Electorica (Vol. 4, Issue 1, p. 9).

Hardy, B. L., Moncel, M. H., Despriée, J., Courcimault, G., & Voinchet, P. (2018). Middle Pleistocene hominin behavior at the 700ka Acheulean site of la Noira (France). Quaternary Science Reviews, 199, 60–82. https://doi.org/10.1016/j.quascirev.2018.09.013

Herzlinger, G., & Grosman, L. (2018). AGMT3-D: A software for 3-D landmarks-based geometric morphometric shape analysis of archaeological artifacts. PLoS ONE, 13(11). https://doi.org/10.1371/journal.pone.0207890

Hicks, J. M. (2023). A Volumetric Analysis of Handaxe Symmetry Referencing a Known Symmetrical Ideal. https://doi.org/10.21203/rs.3.rs-2551323/v1

Hodgson, D. (2009). Evolution of the visual cortex and the emergence of symmetry in the Acheulean techno-complex. Comptes Rendus - Palevol, 8(1), 93–97. https://doi.org/10.1016/j.crpv.2008.10.009

Hodgson, D. (2011). The first appearance of symmetry in the human lineage: Where perception meets art. In Symmetry (Vol. 3, Issue 1, pp. 37–53). https://doi.org/10.3390/sym3010037

Hodgson, D. (2015). The symmetry of Acheulean handaxes and cognitive evolution. Journal of Archaeological Science: Reports, 2. https://doi.org/10.1016/j.jasrep.2015.02.002

Inizan, M.-Louise., Reduron-Ballinger, M., Roche, H., & Féblot-Augustins, Jehanne. (1999). Technology and terminology of knapped stone : followed by a multilingual vocabulary, Arabic, English, French, German, Greek, Italian, Portuguese, Spanish. Cercle de Recherches et d'Etudes Préhistoriques.

Iovita, R., & McPherron, S. P. (2011). The handaxe reloaded: A morphometric reassessment of Acheulian and Middle Paleolithic handaxes. Journal of Human Evolution, 61(1), 61–74. https://doi.org/10.1016/j.jhevol.2011.02.007

Iovita, R., Tuvi-Arad, I., Moncel, M. H., Desprieae, J., Voinchet, P., & Bahain, J. J. (2017). High handaxe symmetry at the beginning of the European Acheulian: The data from la Noira (France) in context. PLoS ONE, 12(5). https://doi.org/10.1371/journal.pone.0177063

Isaac, G. L. (1977). . In K. W. Butzer & L. G. Freeman (Eds.), Olorgesaile: Archaeological studies of a middle Pleistocene lake basin in Kenya. Chicago and London: The University of Chicago Press.

Kleindienst, M. R. (1962). Components of the East African Acheulian. Actes Du IVeme Congres Panafricain de Préhistoire et de L'étude Du Quaternaire. , 81–105.

Kohn, M., & Mithen, S. (1999). Handaxes: products of sexual selection?

Li, H., Kuman, K., & Li, C. (2016). The symmetry of handaxes from the Danjiangkou Reservoir Region (central China): A methodological consideration. Quaternary International, 400, 65–72. https://doi.org/10.1016/j.quaint.2015.05.033

Limondin-Lozouet, N., Antoine, P., Bahain, J. J., Cliquet, D., Coutard, S., Dabkowski, J., Ghaleb, B., Locht, J. L., Nicoud, E., & Voinchet, P. (2015). North-West European MIS 11 malacological successions: A framework for the timing of Acheulean settlements. Journal of Quaternary Science, 30(7), 702–712. https://doi.org/10.1002/jqs.2798

Liu, Y., Hel-Or, H., Kaplan, C. S., & Van Gool, L. (2010). Computational symmetry in computer vision and computer graphics. Foundations and Trends in Computer Graphics and Vision, 5(1–2), 1–195. https://doi.org/10.1561/0600000008

Lycett, S. J., von Cramon-Taubadel, N., & Foley, R. A. (2006). A crossbeam co-ordinate caliper for the morphometric analysis of lithic nuclei: A description, test and empirical examples of application. Journal of Archaeological Science, 33(6), 847–861. https://doi.org/10.1016/j.jas.2005.10.014

Machin, A. J., Hosfield, R. T., & Mithen, S. J. (2007). Why are some handaxes symmetrical? Testing the influence of handaxe morphology on butchery effectiveness. Journal of Archaeological Science, 34(6), 883–893. https://doi.org/10.1016/j.jas.2006.09.008

Marathe, A. R. (1980). METHOD FOR DISCRIMINATION OF HANDAXE ASSEMBLAGES80) METHOD FOR DISCRIMINATION OF HANDAXE ASSEMBLAGES. In Bulletin of Deccan College Research Institute (Vol. 39).

Márquez, B., Ollé, A., & Sala, R. (2001). Perspectives m thodologiques de ranalyse fonctionnelle des ensembles lithiques du Pleistocene inf rieur et moyen d'Atapuerca (Burgos, Espagne). In L'Anthropologie (Vol. 05).

Meyer, M., Arsuaga, J. L., De Filippo, C., Nagel, S., Aximu-Petri, A., Nickel, B., Martínez, I., Gracia, A., De Castro, J. M. B., Carbonell, E., Viola, B., Kelso, J., Prüfer, K., & Pääbo, S. (2016). Nuclear DNA sequences from the Middle Pleistocene Sima de los Huesos hominins. Nature, 531(7595), 504–507. https://doi.org/10.1038/nature17405

Moncel, M. H., García-Medrano, P., Despriée, J., Arnaud, J., Voinchet, P., & Bahain, J. J. (2021a). Tracking behavioral persistence and innovations during the Middle Pleistocene in Western Europe. Shift in occupations between 700 and 450 ka at la Noira site (Centre, France). Journal of Human Evolution, 156. https://doi.org/10.1016/j.jhevol.2021.103009

Moncel, M. H., García-Medrano, P., Despriée, J., Arnaud, J., Voinchet, P., & Bahain, J. J. (2021b). Tracking behavioral persistence and innovations during the Middle Pleistocene in Western

Europe. Shift in occupations between 700 and 450 ka at la Noira site (Centre, France). Journal of Human Evolution, 156. https://doi.org/10.1016/j.jhevol.2021.103009

Moncel, M.-H., Despriée, J., Courcimaut, G., Voinchet, P., & Bahain, J.-J. (2020). La Noira Site (Centre, France) and the Technological Behaviours and Skills of the Earliest Acheulean in Western Europe Between 700 and 600 ka. Journal of Paleolithic Archaeology, 3(3), 255–301. https://doi.org/10.1007/s41982-020-00049-2

Muttillo, B., Arzarello, M., & Peretto, C. (2014). L'industria litica in selce. In B. Muttillo, G. Lembo, & C. Peretto (Eds.), L'insediamento a Bifacciali Di Guado San Nicola, Monteroduni, Molise.: Vol. 10/1A (pp. 79–142). Annali dell'Università degli Studi di Ferrara, Sez. Museologia Scientifica e Naturalistica.

Muttillo, B., Lembo, G., & Peretto, C. (2014). MUSEOLOGIA SCIENTIFICA E NATURALISTICA L'INSEDIAMENTO A BIFACCIALI DI GUADO SAN NICOLA MONTERODUNI, MOLISE, ITALIA.

Nomade, S., & Pereira, A. (2014b). Datation 40Ar/39Ar du site de Guado San Nicola. In B. Muttillo, G. Lembo, & C. Peretto (Eds.), L'insediamento a bifacciali di Guado San Nicola, Monteroduni, Molise, Italia.: Vol. 10/1A (pp. 49–52). Annali dell'Università degli Studi di Ferrara, Sez. Museologia Scientifica e Naturalistica.

Núñez-Lahuerta, C., Galán, J., Cuenca-Bescós, G., García-Medrano, P., & Cáceres, I. (2022). A bird assemblage across the MIS 9/8 boundary: The Middle Pleistocene of Galería (Atapuerca). Quaternary Science Reviews, 293. https://doi.org/10.1016/j.quascirev.2022.107708

Ollé, A., Cáceres, I., & Vergès, J. M. (2005). HUMAN OCCUPATIONS AT GALERÍA SITE (SIERRA DE ATAPUERCA, BURGOS, SPAIN) AFTER THE TECHNOLOGICAL AND TAPHONOMICAL DATA. In N. Molines, M.-H. Moncel, & L.-L. Monnier (Eds.), Le premiers peuplements en Europe. Colloque international: Données récentes sur le modalités de peuplement et sur le cadre chronostratigraphique, géologique et paléogéographique des industries du Paléolithique ancien et moyen en Europe (pp. 269–280). John and Erika Hedges Ltd.

Ollé, A., Lombao, D., Asryan, L., García-Medrano, P., Arroyo, A., Fernández-Marchena, J. L., Yeşilova, G. C., Cáceres, I., Huguet, R., López-Polín, L., Pineda, A., García-Tabernero, A., Fidalgo, D., Rosas, A., Saladié, P., & Vallverdú, J. (2023). The earliest European Acheulean: new insights into the large shaped tools from the late Early Pleistocene site of Barranc de la Boella (Tarragona, Spain). Frontiers in Earth Science, 11. https://doi.org/10.3389/feart.2023.1188663

Ollé, A., Mosquera, M., Rodríguez, X. P., de Lombera-Hermida, A., García-Antón, M. D., García-Medrano, P., Peña, L., Menéndez, L., Navazo, M., Terradillos, M., Bargalló, A., Márquez, B., Sala, R., & Carbonell, E. (2013). The Early and Middle Pleistocene technological record from Sierra de Atapuerca (Burgos, Spain). Quaternary International, 295, 138–167. https://doi.org/10.1016/j.quaint.2011.11.009

Ollé, A., Mosquera, M., Rodríguez-Álvarez, X. P., García-Medrano, P., Barsky, D., de Lombera-Hermida, A., & Carbonell, E. (2016). The Acheulean from Atapuerca: Three steps forward, one step back. Quaternary International, 411, 316–328. https://doi.org/10.1016/j.quaint.2016.01.042

Ollé, A., Vergès, J. M., Peña, L., Aranda, V., Canals, A., & Carbonell, E. (2014). A Microwear Analysis Of Handaxes From Santa Ana Cave (Cáceres, Extremadura, Spain). International Conference on Use-Wear Analysis.

Ollé Cañellas, A. (2005). Variabilitat i patrons funcionals en els sistemes tècnics de mode 2. Anàlisi de les deformacions d'ús en els conjunts lítics del riparo esterno de Grotta Paglicci (Rignano Garganico, Foggia), Áridos (Arganda, Madrid) i galería-TN (Sierra de Atapuerta, Burgos) [P.h.D. thesis]. Universitat Rovira i Virgili.

Pereira, A., Nomade, S., Shao, Q., Bahain, J. J., Arzarello, M., Douville, E., Falguères, C., Frank, N., Garcia, T., Lembo, G., Muttillo, B., Scao, V., & Peretto, C. (2016). 40Ar/39Ar and ESR/U-series dates for Guado San Nicola, Middle Pleistocene key site at the Lower/Middle Palaeolithic transition in Italy. Quaternary Geochronology, 36, 67–75. https://doi.org/10.1016/j.quageo.2016.08.005

Peresani, M. (2011). Le materie prime: fratturazione, natura e provenienza. In M. Arzarello, F. Fontana, & M. Peresani (Eds.), Manuale di tecnologia preistorica. Concetti, metodi e tecniche (pp. 53–109). Carocci editore.

Peretto, C., Arzarello, M., Bahain, J. J., Boulbes, N., Dolo, J. M., Douville, E., Falguères, C., Frank, N., Garcia, T., Lembo, G., Moigne, A. M., Muttillo, B., Nomade, S., Pereira, A., Rufo, M. A., Sala, B., Shao, Q., Thun Hohenstein, U., Tessari, U., … Vaccaro, C. (2016). The Middle Pleistocene site of Guado San Nicola (Monteroduni, Central Italy) on the Lower/Middle Palaeolithic transition. Quaternary International, 411, 301–315. https://doi.org/10.1016/j.quaint.2015.11.056

Roe, D. A. (1964). The British Lower and Middle Palaeolithic: Some Problems, Methods of Study and Preliminary Results.

Roe, D. A. (1969). British Lower and Middle Palaeolithic Handaxe Groups.

Rosas, A., Carbonell', E., & Cuenca, G. (1998). Cronología, Bioestratigrafía Y Paleoecología Del Pleistoceno Medio De Galería (Sierra De Atapuerca, España).

Rots, V., & Van Peer, P. (2006). Early evidence of complexity in lithic economy: Core-axe production, hafting and use at late Middle Pleistocene site 8-B-11, Sai Island (Sudan). Journal of Archaeological Science, 33(3). https://doi.org/10.1016/j.jas.2005.08.002

Rufo, M. A. (2014). L'industria litica in calcare. In B. Muttillo, G. Lembo, & C. Peretto (Eds.), ANNUALI DELL'UNIVERSITÀ DI FERRARA: Vol. 10/1A (pp. 143–146).

Sackett, J. R. (1982). Approaches to Style in Lithic Archaeology. In JOURNAL OF ANTHROPOLOGICAL ARCHAEOLOGY (Vol. 1).

Sala, B., Boulbes, N., Moigne, A.-M., & Thun Hohenstein, U. (2014b). L'insieme faunistico del giacimento. In B. Muttillo, G. Lembo, & C. Peretto (Eds.), L'insediamento A Bifacciali Di Guado San Nicola Monteroduni, Molise, Italia: Vol. 10/1a (Pp. 59–78). Annali Dell'università Di Ferrara, Sez. Museologia Scientifica e Naturalistica.

Saragusti, I., Karasik, A., Sharon, I., & Smilansky, U. (2005). Quantitative analysis of shape attributes based on contours and section profiles in artifact analysis. Journal of Archaeological Science, 32(6), 841–853. https://doi.org/10.1016/j.jas.2005.01.002

Saragusti, I., Sharon, I., Katzenelson, O., & Avnir, D. (1998). Quantitative Analysis of the Symmetry of Artefacts: Lower Paleolithic Handaxes Background: The Near Symmetry of Handaxes. In Journal of Archaeological Science (Vol. 25).

Savriama, Y., & Klingenberg, C. (2011). Beyond bilateral symmetry: Geometric morphometric methods for any type of symmetry. BMC Evolutionary Biology, 11(1). https://doi.org/10.1186/1471-2148-11-280

Shen, G., Michel, V., Despriée, J., Han, F., & Granger, D. E. (2012). Datation d'enfouissement par. Anthropologie, 116(1), 1–11. https://doi.org/10.1016/j.anthro.2011.12.007

Shipton, C., & Clarkson, C. (2015). Flake scar density and handaxe reduction intensity. Journal of Archaeological Science: Reports, 2, 169–175. https://doi.org/10.1016/j.jasrep.2015.01.013

Simão Jorge. (2002). Tools evolve: The artificial selection and evolution of Paleolithic stone tools. Behavioral and Brain Science, 25, 419.

Solodenko, N., Zupancich, A., Cesaro, S. N., Marder, O., Lemorini, C., & Barkai, R. (2015). Fat residue use-wear found on Acheulian biface scraper associated with butchered elephant remains at the site of Revadim, Israel. PLoS ONE, 10(3). https://doi.org/10.1371/journal.pone.0118572

Terradillos-Bernal, M., & Rodríguez, X. P. (2012). The Lower Palaeolithic on the northern plateau of the Iberian Peninsula (Sierra de Atapuerca, Ambrona and La Maya I): A technological analysis of the cutting edge and weight of artefacts. Developing an hypothetical model. Journal of Archaeological Science, 39(5), 1467–1479. https://doi.org/10.1016/j.jas.2011.12.037

Treder, M. S. (2010). Behind the looking-glass: A review on human symmetry perception. In Symmetry (Vol. 2, Issue 3, pp. 1510–1543). https://doi.org/10.3390/sym2031510

Tumler, D., Basell, L., Coward, F., Tumler, D., Basell, L., & Coward, F. (2017). Human perception of symmetry, raw material and size in Paleolithic handaxes.

Turrini, M. C., Lembo, G., Peretto, C., Tessari, U., & Vaccaro, C. (2014a). La serie stratigrafica. In B. Muttillo, G. Lembo, & C. Peretto (Eds.), L'insediamento A Bifacciali Di Guado San Nicola Monteroduni, Molise, Italia: Vol. 10/1A (pp. 25–42). Annali dell'Università di Ferrara.

Turrini, M. C., Lembo, G., Peretto, C., Tessari, U., & Vaccaro, C. (2014b). La serie stratigrafica. In B. Muttillo, G. Lembo, & C. Peretto (Eds.), L'insediamento a bifacciali di Guado San Nicola, Monteroduni, Molise, Italia.: Vol. 10/1A (pp. 25–48). Annali dell'Università degli Studi di Ferrara.

Viallet, C. (2016). Bifaces used for percussion? Experimental approach to percussion marks and functional analysis of the bifaces from Terra Amata (Nice, France). Quaternary International, 409. https://doi.org/10.1016/j.quaint.2015.08.068

Villa, P. (1990). Torralba and Aridos: elephant exploitation in middle Pleistocene Spain. Journal of Human Evolution, 19(3), 299–309.

Wynn, T., & Tierson, F. (1990). Regional Comparison of the Shapes of Later Acheulean Handaxes. American Anthropologist, 92(1), 73–84. https://doi.org/10.1525/aa.1990.92.1.02a00050

Zupancich, A., Shemer, M., & Barkai, R. (2021). Biface use in the Lower Paleolithic Levant: First insights from late Acheulean Revadim and Jaljulia (Israel). Journal of Archaeological Science: Reports, 36. https://doi.org/10.1016/j.jasrep.2021.102877

Annex 1

Photogrammetry protocol

The handaxes from Guado San Nicola have been digitalized using photogrammetry.

Photogrammetry is surveying technique that enables the creation of 3D models from digitized data (2D images). The images are overlapped with the aim of reconstruct the volume and the texture of an object rendering back the three-dimensionality of the latter (Lauria et al., 2022). To obtain the photos necessary to digitalize each handaxe the following items have been used:

- *Rotating base*
  The base was used to facilitate the rotation of the object without having to change its position in relation to the camera lens.
- *Polyurethane foam structure*
  The polyurethane foam structure was used to maintain the object in a fixed and stable position while moving the rotating base.
- *Black background*
  The background was covered with a black velvet drape to have a better focus on the object and, in this way, to ensure easier recognition of the same by the software with which the digitization would be carried out.

The setting of the equipment for the acquisition of photos has been arranged with reference to the protocol presented by Lauria and colleagues (Lauria et al., 2022). The latter theorised the protocol to perform photogrammetry of human artefacts and, for this reason, in the context of this work the protocol was modified to suits the different exigencies that arose when digitizing lithic tools.

According to the above-mentioned protocol, the camera should be placed in a fixed position at a distance of 30cm from the specimen which is located on the rotating base that will be moved at 20° intervals until it completes a 360° turn. At each interval, the photographs were taken at three different inclinations: 0°, 30°, and 45°.

In the present study, the camera has been placed in a fixed position, but the distance has been changed from 30 to 50 cm from the object. This adjustment was necessary to obtain images that were in focus and in which the entire area of interest was visible. Furthermore, it was deemed sufficient to take the photos at a single inclination of the camera (positioned with an angle between 30 and 40 degrees) that was able to document in detail both the two faces of the instruments and the ends. In this way, the final number of photos is reduced, and the editing process will be faster without compromising on quality.

Another necessary adjustment was due to the use of the polyurethane foam structure to keep the handaxes upright. In fact, as it is inserted into the polyurethane foam structure to maintain its stability, the object cannot be documented in its entirety without being moved and change its distance from the camera lens. The latter modification would have caused problems in the software's alignment of the photos, so it was decided to make two sets of photos for both the mid-proximal and the mid-distal section. Each set was composed by a minimum of 20 photos, number that results from repeating one photo each time the base is rotated by 20° plus two additional photos to capture details in the tip or base of the tool (Lauria et al., 2022), and each photo should be realized considering an overlap of ca. 60% of the surface present in the previous and following ones (Gargari et al., 2023). The number may be higher depending on the specific characteristics (e.g. raw material, morphology, size) of the item being digitised. Once all the photos for each handaxe have been collected, the images are processed on the Agisoft Metashape Professional software v. 1.6.3 build 10723 (64 bit).

Once the necessary photographs were collected for each archaeological find, the images were processed using the software Agisoft Metashape Professional software v. 1.6.3 build 10723 (64 bit) developed by the Agisoft LLC (St. Petersburg, Russia).

Agisoft Metashape is a stand-alone software that enables the photogrammetric processing of digital images to realise 3D models. This software is able to process different types of images: aerial, satellite or, as in the case of this study, close-range photographs. A four-steps photogrammetry workflow on the latter software has been followed to obtain the 3D models of Guado San Nicola’s archaeological artefact. The latter fundamental steps are:

1) Alignment and generation of sparse cloud
2) Dense cloud construction
3) Mesh construction
4) Texture construction

Within the context of this thesis, the four steps have been applied following the methodology proposed by Lauria and colleagues (Lauria et al., 2022) , which was slightly modified through the choice of different options from those presented in the software's user manual.

The tools digitized through photogrammetry for this work were partially inserted into a polyurethane structure to stabilize them during the acquisition of the photographs. This caused the need to perform two sets of photographs (subsequently grouped into two different chunks on the software) for each instrument: the first set documented the mid-distal section of the object, while the second documented the mid-proximal section. For this reason, as suggested by Lauria and colleagues (Lauria et al., 2022), the two sets of photos have been uploaded and managed separately until the generation of the dense cloud. Before proceeding with the phase of mesh building, the two chunks were merged as described in the Section 3 of this annex.

A last section has been included to explain how the 3D models have been exported and scaled on the opensource software MeshLab v.2022.02 before to be modified to respect the requirement of the software Artifact Geo-Morph Toolbox 3-D that will be used to proceed with Geometric Morphometric Analysis.

1. Photo alignment and sparse cloud generation

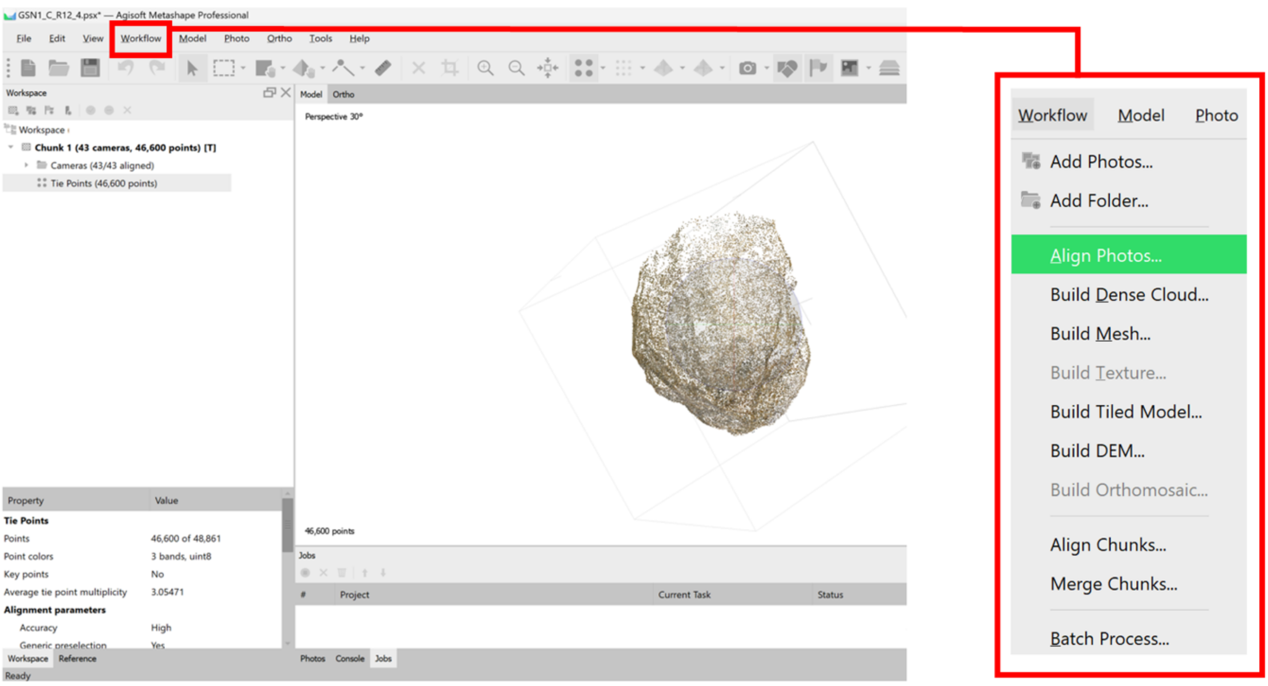

Figure 1: Result of align photos on Chunk 1.

The first step to be done on Metashape is to upload the photos of the object we want to digitalize using the option *Add photos* in the *Workflow* section. In order to avoid problems related to the zoom and the distance between the artefact and the camera's lens, the different sets of photos have been separately uploaded into different chunks (Lauria et al., 2022). Using again the *Workflow* section, for each chunk it will be necessary to proceed with the option *Align photos* which is a fundamental step to create a cloud of points that the software identifies directly from the photos and organizes in the virtual space recreating a first rendering of the volume (sparse cloud) thanks to the overlap between the photos (Fig.1). If the photos upload have a poor quality, physical markers can be placed on the individual photos of a chunk to realign the tie-points and improve the alignment result (Jones & Church, 2020).

2. Dense cloud construction

Maintaining an individual chunk level, it is possible to proceed by selecting the *Build dense cloud* option to increase the number of points that make up the cloud (Fig.2). This is achieved by a calculation of depth information that the software performs based on the positions of individual photographs (Jones & Church, 2020).

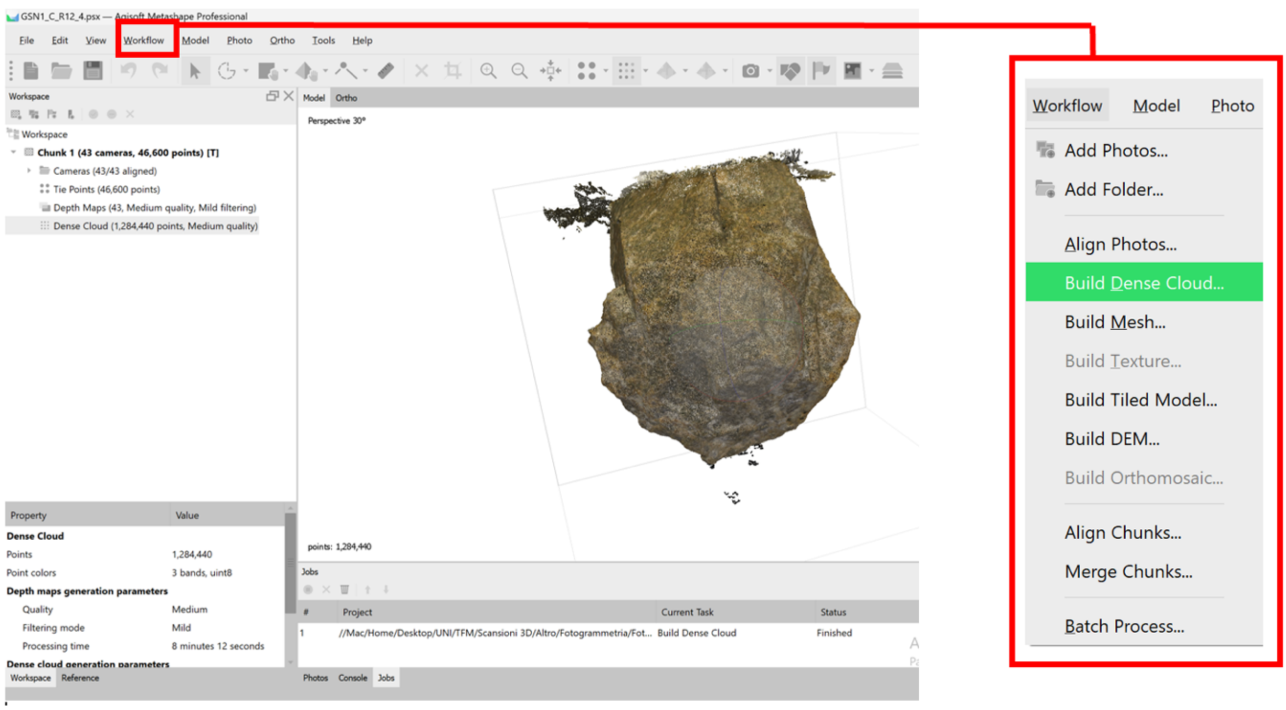

Figure 2: Result of build dense cloud on Chunk 1.

Before continuing, it is extremely important to clean the virtual item by deleting all points of the dense cloud that do not belong to the object that is being digitized by using a selection tool. It is possible to choose the selection mode you prefer, in this case free-form selection was used (Fig.3) (Lauria et al., 2022).

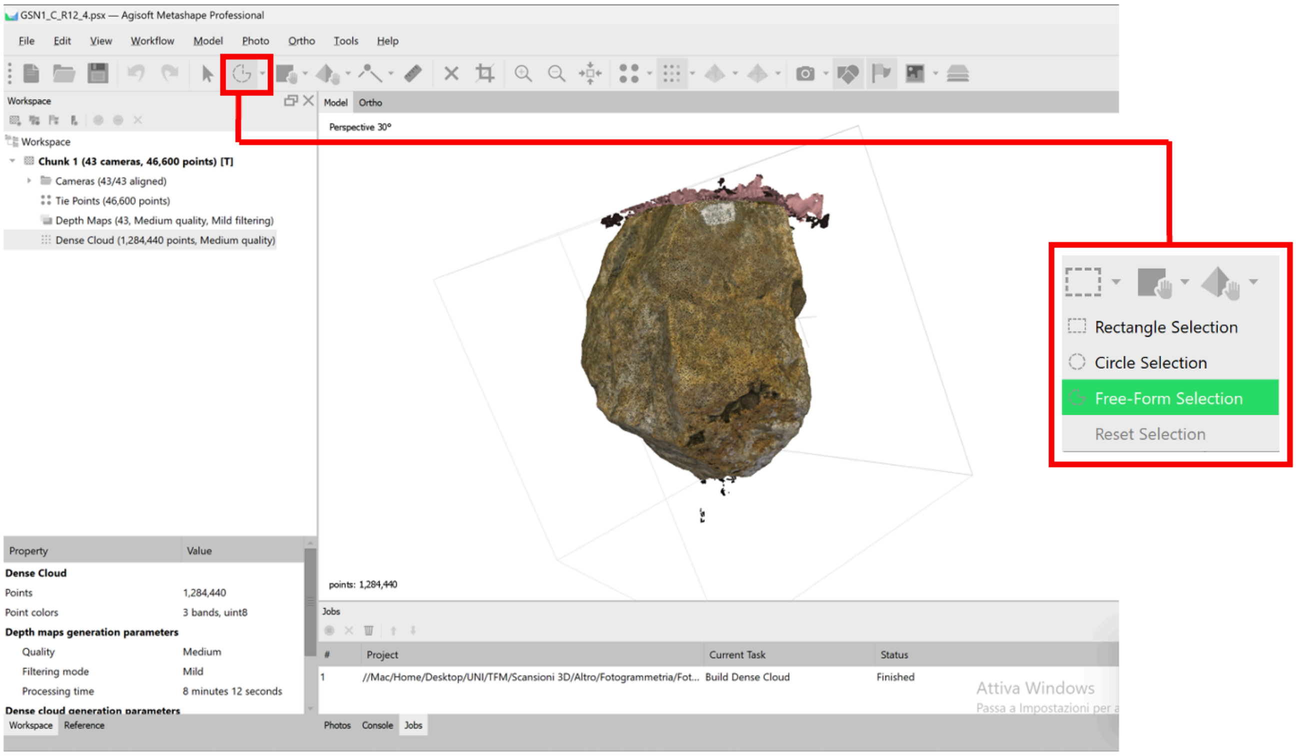

Figure 3: Selecting option to delete the points which don't belongs to the object (in light red).

3. Chunks alignment and merging

Once the dense clouds of each chunk have been construed, it is possible to proceed with aligning the different chunks selecting the option *Align chunks* in the *Workflow* section. The alignment con be done by using two different methods depending on the needs that arise at this stage of the process.

The first option, which can be choose if the points of the dense cloud are tightly organized, consist in selecting the chunks we want to merge and setting the *Point base alignment* (Fig.4). In this case the software will automatically align the chunks using the point of the dense cloud as reference.

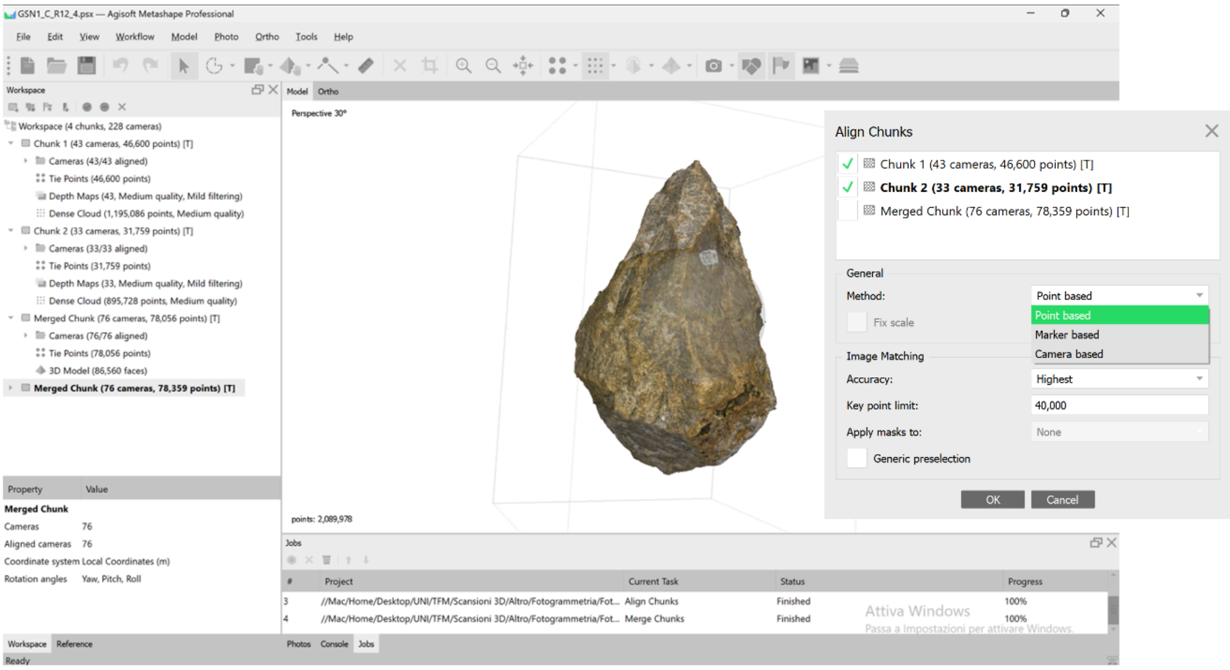

Figure 4: Dense cloud resulting from align (point based) and mesh chunks.

The second option consist in selecting the *Marker based alignment*: by choosing this command, it will be necessary to manually place the same reference points (with a minimum of three points) on both chunks in order to mark the points of junction between them and thus suggest to the software that they overlap. Once that the markers have been placed, it is possible to proceed with aligning and merging the two chunks (Lauria et al., 2022).

4. Mesh construction

From this step all the actions will be applied directly on the *Merged chunk* that will appear in the *Workspace* area once the merge process will be conclude. The construction of the mesh allows to generate a continuous exterior surface of the artifact. Mesh construction is based on the polygonization of the combined point cloud information (both sparse and dense) (Jones & Church, 2020; Lauria et al., 2022).

5. Texture construction

The model can now be texturized by choosing the option *Build texture* in the *Workflow* section. As suggested by the methodology of Lauria and colleagues (Lauria et al., 2022), the texturing process was left at default settings with the mosaic merging mode, the generic mapping mode and the 4096 × 1 texture size/count option selected.

Once the texture has been generated, in the section *Model view* it will be possible to select different mode of view of the 3D. By selecting the *model wireframe* mode, it is possible to show the grid of triangles composing the 3D model to verify the accuracy of the mesh. The tighter the grid of triangle is, the higher the accuracy and homogeneity of the final result.

Figure 5: a) Merged chunks after build mesh; b) Merged chunks after build texture; c) Merged chunks with model wireframe filter.

The 3D model can be exported in the mode of your choice among those listed in the *Model view section* according to the requirements of the analyses that will be applied on the model itself or its purpose.

6. Model export and scaling

Finally, the 3D models have been exported as .ply (which save the 3D model with his tecture) and .stl (which save the 3D model without texture) file and scaled on MeshLab software (v. 2022.02). To scale the items, I proceeded opening each single file, selecting the option *Normals, Curvatures and Orientation* in the *Filter* section and then choosing *Transform: scale, normalize*. The last command will open a window where the ratio of the maximum length of the real artefact to the maximum length measured on the 3D model must be entered for x, y and z before to apply the filter. Here it is necessary to save again the model which will show the real dimensions of the original handaxe.

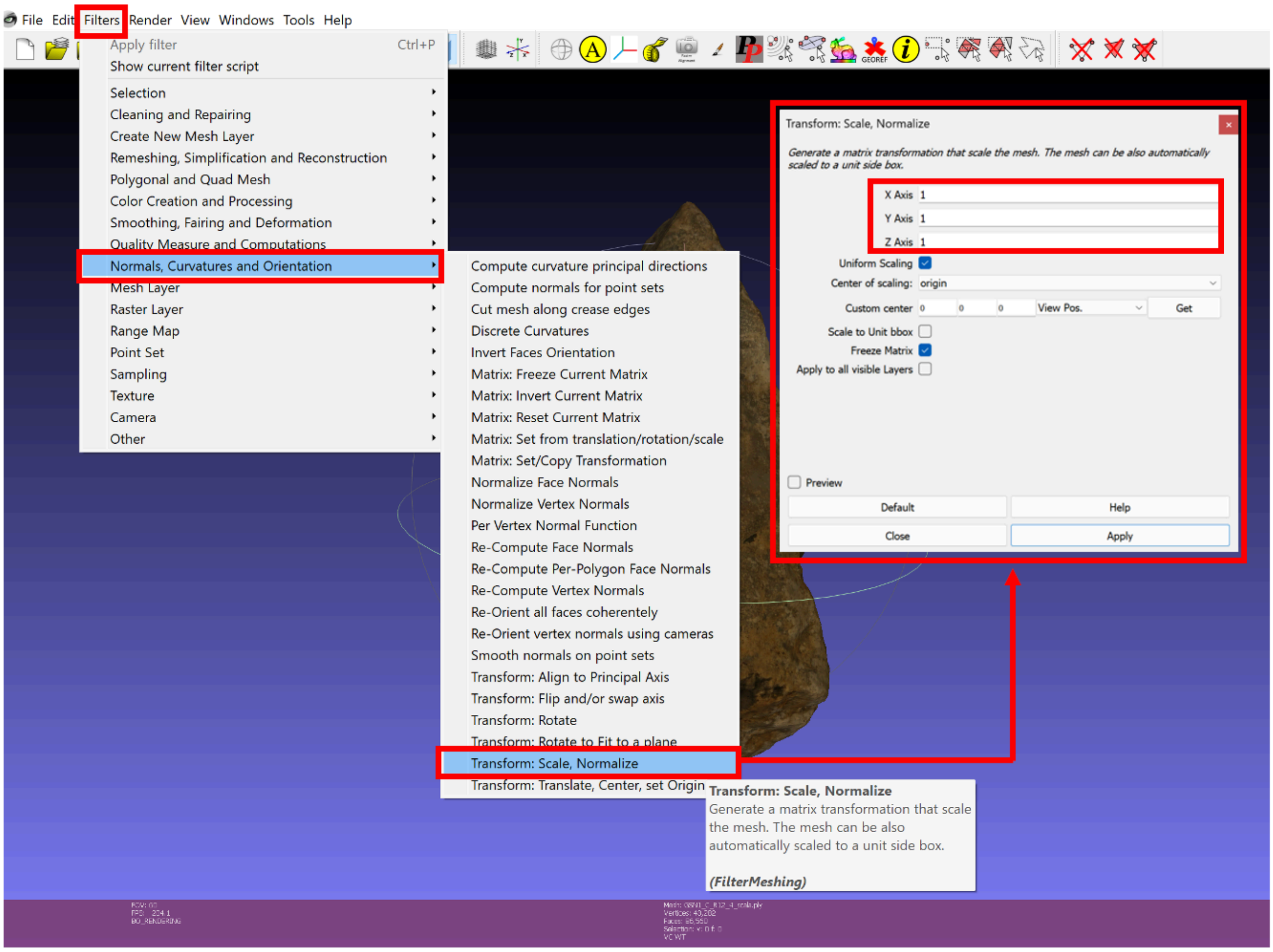

Figure 6: Workflow followed to set the scale on each 3D model on MeshLab.

Bibliography

Gargari, A. M., Ebadi, H., Esmaeili, F., & Latifzadeh, S. (2023). Dynamic 3D network design for UAV-based photogrammetry in mountainous terrain. Environmental Earth Sciences, 82(7). https://doi.org/10.1007/s12665-023-10864-9

Jones, C. A., & Church, E. (2020). Photogrammetry is for everyone: Structure-from-motion software user experiences in archaeology. Journal of Archaeological Science: Reports, 30. https://doi.org/10.1016/j.jasrep.2020.102261

Lauria, G., Sineo, L., & Ficarra, S. (2022). A detailed method for creating digital 3D models of human crania: an example of close-range photogrammetry based on the use of Structure-from-Motion (SfM) in virtual anthropology. Archaeological and Anthropological Sciences, 14(3). https://doi.org/10.1007/s12520-022-01502-9

Annex 2

Metric information

	Statistic	n.	L	m	e	n	a	L-a	B1
GIIa	Mean	13	106,09	69,02	34,30	65,56	48,42	57,36	44,96
	SD		25,34	15,19	9,17	14,84	18,10	14,26	12,77
	CV		23,88	22,01	26,74	22,63	37,37	24,86	28,41
GSN-Usc	Mean	26	81,24	49,12	32,49	43,85	27,73	52,90	27,76
	SD		17,21	10,61	9,52	9,20	7,49	14,57	7,67
	CV		21,19	21,60	29,30	20,99	27,02	27,55	27,61
LN-stratum c	Mean	49	112,33	73,52	39,93	64,97	41,68	70,65	39,52
	SD		28,49	20,36	14,46	17,60	19,00	20,74	12,52
	CV		25,36	27,70	36,21	27,09	45,59	29,36	31,69

	Statistic	n.	B2	T1	E.I.	R.I.	D-R.I.	Vol.	S.A.
GIIa	Mean	13	54,49	18,16	1,54	2,07	2,53	106735,7	5432,51
	SD		9,36	4,39	0,19	0,43	0,65	70278,38	2233,26
	CV		17,17	24,17	12,28	20,77	25,53	65,84	41,11
GSN-Usc	Mean	26	41,97	17,92	1,66	1,55	1,62	48713,70	2870,36
	SD		10,32	6,40	0,18	0,37	0,37	34943,73	1185,60
	CV		24,59	35,70	10,68	23,81	22,99	71,73	41,30
LN-stratum c	Mean	49	60,24	16,77	1,56	1,97	2,57	110501,8	5627,69
	SD		15,27	8,10	0,26	0,53	0,83	92640,88	2685,93
	CV		25,35	48,30	16,72	27,01	32,44	83,84	47,73

Table 1: Mean values of metric data obtained for each site from the sample studied.

Abbreviations used in the table:

L = Maximum length
m = Maximum width
e = Maximum thickness
n = Width at middle length
a = Distal length
L-a = Base length
B1 = Distal width

B2 = Proximal width
T1 = Distal thickness
E.I. = Elongation index
R.I. = Refinement index
D-R.I. = Distal refinement index
Vol. = Volume
S.A. = Surface area

Annex 3

Technological features

In this Annex all the data for each technological feature used to perform Principal Component Analysis are reported.

Abbreviations used in the following tables:

Chop. Tool = Chopping-tool
Peb/Cob = Pebble or cobble
Indet = Unknown blank-type
Flint/Che = Flint or chert
H+S = Combined hammer (hard hammer + soft hammer)
CO_all = Cortex all over the tool
NC = Non-cortical
CO_mid = Cortex on the mid section of the tool
CO_butt = Cortex on the butt of the tool
CO_midP = Cortex on the mid-proximal section of the tool
CO_midD = Cortex on the mid-distal section of the tool
1 R.S. = One reduction sequence
2 R.S. = Two reductions sequences
1+FR = One reduction sequence combined with final retouch
2+FR = Two reduction sequences combined with final retouch

	TOOL-TYPE						BLANK-TYPE					
	Handaxe		**Cleaver**		**Chop.Tool**		**Flake**		**Peb/Cob**		**Nodule**	
	n.	**%**	**n.**	**%**	**n.**	**%**	**n.**	**%**	**n.**	**%**	**n.**	**%**
Galería - GIIa	9	69,2	4,0	30,8	0,0	0,0	6,0	46,2	6,0	46,2	1,0	7,7
Guado San Nicola - USc	26	100	0,0	0,0	0,0	0,0	0,0	0,0	0,0	0,0	0,0	0,0
La Noira – stratum c	48	98	0,0	0,0	1,0	2,0	12,0	24,5	5,0	10,2	1,0	2,0

	BLANK-TYPE				RAW MATERIAL							
	Slab		**Indet**		**Flint/Che**		**Quartzite**		**Limestone**		**Sandstone**	
	n.	**%**	**n.**	**%**	n.	%	n.	%	n.	%	n.	%
Galería - GIIa	0,0	0,0	0,0	0,0	3,0	23,1	7,0	53,8	0,0	0,0	3,0	23,1
Guado San Nicola - USc	16,0	61,5	10,0	38,5	23,0	88,5	0,0	0,0	3,0	11,5	0,0	0,0
La Noira – stratum c	16,0	32,7	15,0	30,6	49,0	100,0	0,0	0,0	0,0	0,0	0,0	0,0

	Nº OF WORKED FACES				TYPE OF HAMMER							
	1		**2**		**Hard**		**Soft**		**H+S**		**Unknow**	
	n.	%	n.	%	n.	%	n.	%	n.	%	n.	%
Galería - GIIa	1	7,7	12	92	11	84,6	0	0,0	1	7,7	1	7,7
Guado San Nicola - USc	0	0	26	100	1	3,8	24	92,3	1	3,8	0	0,0
La Noira – stratum c	0	0	49	100	2	4,1	42	85,7	5	10,2	0	0,0

LOCALIZATION OF THE CORTEX

	CO_all		**NC**		**CO_mid**		**CO_butt**		**CO_midP**		**CO_midD**	
	n.	%	n.	%	n.	%	n.	%	n.	%	n.	%
Galería - GIIa	4,0	30,8	2,0	15,4	0,0	0,0	1,0	7,7	6,0	46,2	0,0	0,0
Guado San Nicola - USc	1,0	3,8	9,0	34,6	1,0	3,8	4,0	15,4	8,0	30,8	3,0	11,5
La Noira – stratum c	1,0	2,0	10,0	20,4	4,0	8,2	0,0	0,0	31,0	63,3	3,0	6,1

	REDUCTION SEQUENCES								EDGE-PROFILE					
	1 R.S.		**2 R.S.**		**1+FR**		**2+FR**		**Sinuous**		**Straight**		**Curved**	
	n.	%	n.	%	n.	%	n.	%	n.	%	n.	%	n.	%
Galería - GIIa	5,0	38,5	6,0	46,2	0,0	0,0	2,0	15,4	5,0	38,5	5,0	38,5	3,0	23,1
Guado San Nicola - USc	2,0	7,7	0,0	0,0	7,0	26,9	17,0	65,4	13,0	50,0	10,0	38,5	3,0	11,5
La Noira – stratum c	2,0	4,1	10,0	20,4	15,0	30,6	22,0	44,9	17,0	34,7	21,0	42,9	11,0	22,4

CROSS-SECTION

	Asymmetrical		**Symmetrical**		**Plano-convex**		**TOT**
	n.	%	n.	%	n.	%	n.
Galería - GIIa	10,0	76,9	3,0	23,1	0,0	0,0	13
Guado San Nicola - USc	15,0	57,7	2,0	7,7	9,0	34,6	26
La Noira – stratum c	23,0	46,9	27,0	55,1	9,0	18,4	49